

**RELIABILITY AND AVAILABILITY OF PV POWER SYSTEM
APPLYING DECENTRALIZED INVERTER CONCEPT**



**A Thesis Submitted to the Graduate School of Naresuan University
in Partial Fulfillment of the Requirements
for the Doctor of Philosophy in Renewable Energy**

July 2015

Copyright 2015 by Naresuan University


Thesis entitled "Reliability and availability of PV power system applying decentralized inverter concept"

by Mr. Panu Tanomvorsin

has been approved by the Graduate School as partial fulfillment of the requirements for the Doctor of Philosophy in Renewable Energy of Naresuan University

Oral Defense Committee


.....Chair
(Assistant Professor Boonyang Plangklang, Dr.-Ing.)


.....Advisor
(Assistant Professor Prapita Thanarak, Ph.D.)


..... Co-Advisor
(Associate Professor Wattanapong Rakwichian, Ph.D.)


..... Internal Examiner
(Assistant Professor Nipon Ketjoy, Ph.D.)

Approved


.....
(Panu Putthawong, Ph.D.)

Associate Dean for Administration and Planning
for Dean of the Graduate School

24 JUL 2015

ACKNOWLEDGEMENT

I would like to express my sincere thanks to my thesis advisor, Assistant Professor Dr.Prapita Thanarak, Assistant Professor Dr.Wattanapong Rakwichian and Assistant Professor Dr.Nipon Ketjoy for their invaluable support of my Ph.D. study and research. Their guidance helped me in all the time of research, writing of this thesis, encouragement, insightful comments, and their hard questions.

My sincere thank also goes to staffs at SERT; school of renewable energy technology, of Naresuan University for help on this program.

In addition, I specially thank my classmate, Ms.Una Tontakulchanchai for the stimulating and motivation.

Unforgettably, I would like to thank Ms.Pimnipa Khuntiausaha for kindness, friendship, and great support.

Finally, I most gratefully thank to my family especially my parents Mr.Somsak Tanomvorsin and Mrs.Sasithorn Tanomvorsin for supporting me spiritually throughout my life.

Panu Tanomvorsin

| | |
|-----------------------|--|
| Title | RELIABILITY AND AVAILABILITY OF PV POWER SYSTEM APPLYING DECENTRALIZED INVERTER CONCEPT |
| Author | Panu tanomvorsin |
| Advisor | Assistant Professor Prapita Thanarak, Ph.D. |
| Co-Advisor | Associate Professor Wattanapong Rakwichian, Ph.D. Assistant Professor Nipon Ketjoy, Ph.D. |
| Academic Paper | Thesis Doctor of Philosophy in Renewable Energy, Naresuan University, 2014 |
| Keywords | Decentralized inverter, PV power system |

ABSTRACT

This dissertation studies the availability and reliability of PV power plant applying centralized and decentralized inverter concept in Thailand. In addition, the economics analysis with the availability and reliability result is also included in this thesis. The dissertation methodology is separated to 5 steps that are literature reviewing, PV power plant samples and data measuring, efficiency and performance evaluation, availability and reliability evaluation, and economic analysis.

Two 5 MW PV power plant that are Decentralized Inverter PV Power Plant (DIPVP) that constructed with the decentralized inverter concept with string inverter and Centralized Inverter PV Power Plant (CIPVP) that constructed with the centralized inverter concept are selected as the PV power plant samples. These PV power plant are located in the same area in the central region of Thailand that is a good representative for the centralized and decentralized inverter concept, climate, and environment in Thailand. The study period is during May 2013 to October 2014. The efficiency and performance evaluation result presents no significant different except η_{tot} that is the result from PV module technologies. The availability evaluation is separated in 2 cases for higher accurate availability evaluation that are availability with and without grid failure. The average availability with and without grid failure in DIPVP are 99.29 and 99.80 % respectively while CIPVP are 99.65 and 99.80 %

respectively. The total inverter failure probability and the inverter reliability evaluated result of DIPVP are 67.60 and 32.40 % respectively while CIPVP are 10.00 and 90.00 % respectively. For the economics analysis with the availability and reliability result, the availability with grid failure case, Cost per Unit of DIPVP and CIPVP are 2.90 and 2,88 Baht/kWh respectively while LCOE with the actual availability of these PV power plants are 3.72 and 3.70 Baht/kWh respectively. In the availability without grid failure case, Cost per Unit with these availability of DIPVP and CIPVP are 2.88 Baht/kWh while LCOE with the availability without grid failure of these PV power plants are 3.70 Baht/kWh. NPV with the availability with grid failure of DIPVP and CIPVP are 452.58 and 457.30 million Baht respectively while NPV with the availability without grid failure of these PV power plants are 457.25 and 458.63 million Baht respectively. IRR with the availability with and without grid failure of DIPVP are 24.67 and 24.86 % respectively while IRR with the availability with and without grid failure of CIPVP are 24.86 and 24.92 % respectively.

The availability evaluation result clearly indicates that grid failure has the highest effect to availability with grid failure and the PV power system applying decentralized and centralized inverter concepts have not significant different in availability during evaluation period. The reliability evaluation result explicitly mentions that the inverter failure probability of central inverter is far lower than string inverter while reliability is far higher than string inverter. It can signify that the PV power system applying decentralized inverter concepts has far worse reliability than centralized inverter concepts during evaluation period. To evaluate the higher accurate availability and reliability of the PV power system applying decentralized and centralized inverter concepts, the total PV power plant component failure and the life time evaluation period at 25 years is essential for availability and reliability evaluation of the PV power system applying both concepts. From the economic analysis result, all of the indicators point out that the grid failure influence is far higher than the effect from the PV power system applying centralized or decentralized inverter concepts in the economic analysis. For 8.0 Baht/kWh adder for 10 year subsidy case, all of the indicators point out that DIPVP and CIPVP is feasibility in commercial.

LIST OF CONTENTS

| Chapter | Page |
|---|----------|
| I INTRODUCTION | 1 |
| Statement of purpose | 1 |
| Objectives of the Study | 3 |
| Expected outputs of the study | 4 |
| Expected outcomes..... | 4 |
| II THEORETICAL AND RELATED LITERATURE..... | 5 |
| Photovoltaic systems..... | 5 |
| PV power plant..... | 7 |
| Reliability and Availability of PV power plant..... | 11 |
| Reliability and Availability of PVsystem in Springerville, Arizona, U.S.A..... | 11 |
| Reliability of various sizes of PV systems | 13 |
| Performance and Availability of 202 PV systems in Taiwan | 15 |
| Reliability of PV systems focusing on causes..... | 17 |
| Field Reliability Analysis Methods for Photovoltaic Inverters..... | 18 |
| System Availability Analysis for a Multi-megawatt Photovoltaic Power Plant..... | 21 |
| Economical Design of Utility-Scale Photovoltaic Power Plants with Optimum Availability | 24 |
| Reliability Assessment for Components of Large Scale Photovoltaic Systems..... | 26 |

LIST OF CONTENTS (CONT.)

| Chapter | Page |
|--|-----------|
| A design tool to study the impact of mission-profile on the reliability of SiC-based PV-inverter devices | 30 |
| Critical components test and reliability issues for Photovoltaic Inverter..... | 33 |
| Photovoltaic Inverter: Thermal Characterization to Identify Critical Components..... | 34 |
| Assessment of PV system Monitoring Requirement by Consideration of Failure Mode Probability..... | 37 |
| Diagnostic architecture: A procedure based on the analysis of the failure causes applied to photovoltaic plants..... | 43 |
| Reliability Performance Assessment in Modeling Photovoltaic Networks | 46 |
| Information-based reliability weighting for failure mode prioritization in photovoltaic (PV) module design..... | 48 |
| Performance and degradation analysis for long term reliability of solar photovoltaic systems..... | 53 |
| Reliability assessment of photovoltaic power systems: Review of current status and future perspectives | 55 |
| III METHODOLOGY | 58 |
| Literature reviewing | 58 |
| PV power plant samples and data measuring..... | 60 |
| Efficiency and performance evaluation..... | 66 |
| Availability and reliability evaluation..... | 70 |

LIST OF CONTENTS (CONT.)

| Chapter | Page |
|--|------------|
| IV RESULT AND DISCUSSION | 81 |
| Efficiency and performance evaluation result..... | 81 |
| Availability and reliability evaluation result | 88 |
| Economic analysis result | 105 |
| V CONCLUSION AND RECOMMENDATION..... | 111 |
| REFERENCES..... | 114 |
| APPENDIX | 119 |
| BIOGRAPHY | 140 |

LIST OF TABLES

| Table | Page |
|--|------|
| 1 The expected number of failures as predicted by model for each component for 5, 10, and 20 years | 13 |
| 2 Number of components for each PV system | 14 |
| 3 Component adopted failure rates..... | 14 |
| 4 Causes of Maintenance Events by Category | 18 |
| 5 Availability and reliability evaluation criteria..... | 60 |
| 6 The specification of DIPVP and CIPVP | 62 |
| 7 The list of sensors and instruments that used for measuring the significant parameters in both PV power plant | 63 |
| 8 The efficiency and performance evaluation result of DIPVP and CIPVP during May 2013 to October 2014 | 82 |
| 9 The equivalent PV power plant downtime of the inverter, other PV power plant component, grid, and total in DIPVP and CIPVP during May 2013 to October 2014 | 89 |
| 10 The estimated total time and total time without grid failure of DIPVP and CIPVP in each month during May 2013 to October 2014 | 96 |
| 11 The evaluation result of the availability with and without grid failure in DIPVP and CIPVP during May 2013 to October 2014..... | 98 |
| 12 The inverter failure probability and the inverter reliability evaluated result of DIPVP and CIPVP during May 2013 to October 2014 | 102 |

LIST OF FIGURES

| Figure | | Page |
|--------|---|------|
| 1 | The centralized inverter concept | 8 |
| 2 | The decentralized inverter concept with string inverter | 10 |
| 3 | The decentralized inverter concept with micro-inverter | 10 |
| 4 | Springerville PV power plant in Arizona, U.S.A. | 11 |
| 5 | Overview of Reliability Program for PV systems..... | 12 |
| 6 | The variation of PR values for PV systems in Taiwan..... | 15 |
| 7 | Definitions of PV system performance indices..... | 16 |
| 8 | The distribution of PV system availabilities in Taiwan | 16 |
| 9 | Definitions of system availability indices | 17 |
| 10 | Classic bathtub curve..... | 18 |
| 11 | Distribution of warranty downtime hours for a sample population of 30kW inverters | 19 |
| 12 | Warranty downtime for a sample population of 30kW inverters | 20 |
| 13 | Field hours and availability factor (AF) for a sample population of 30kW inverters..... | 20 |
| 14 | Two phases of subsystem (inverter) reliability analysis for a limited case considering only temperature stresses. Blue boxes represent simulation outputs..... | 22 |
| 15 | Arrhenius-Weibull life-stress parameters for the inverter reliability..... | 23 |
| 16 | Example calculation of cumulative failure rates for three inverter failure modes and the overall inverter subsystem and average downtime per year due to inverter failures..... | 23 |
| 17 | Availability of the example inverter based on downtime due to failure | 23 |

LIST OF FIGURES (CONT.)

| Figure | | Page |
|--------|--|------|
| 18 | Average predicted inverter availability and resulting MWh lost annually for a hypothetical 10MW PV power plant | 24 |
| 19 | Basic topologies for PV energy systems: (a) Centralized, (b) string, (c) multistring, and (d) ac modular | 25 |
| 20 | Availability analysis of a 100 kW PV power plant | 25 |
| 21 | (a) NSEE for megawatt-scale PV plants. (b) ELCOE versus the inverter size. (c) Sensitivity of ELCOEi with respect to the inverter size | 26 |
| 22 | Electrical structure of the large scale PV system | 27 |
| 23 | Number of components per each PV system | 27 |
| 24 | Fault tree for the PV system | 28 |
| 25 | Component failure rates | 28 |
| 26 | The all results of reliability for seven PV systems | 29 |
| 27 | Critical component priorities | 30 |
| 28 | Proposed reliability oriented design structure for the new generation of grid connected PV-inverters | 31 |
| 29 | PV-system design ratings | 31 |
| 30 | The realistic PV-inverter loading current (a) and thermal loading estimation (b) of the inverter devices (MOSFET, Diode) for one year operation in USA-Arizona | 32 |
| 31 | Proposed electro-thermal model structure for device junction and case temperature estimation | 32 |
| 32 | MP and device-aging impact in lifetime | 32 |
| 33 | MTBF (Mean Time Between Failure) vs temperature | 33 |

LIST OF FIGURES (CONT.)

| Figure | | Page |
|--------|--|------|
| 34 | DC link capacitor voltage and chamber temperature trends during destructive test session | 34 |
| 35 | Duty cycle vs MTBF | 34 |
| 36 | The MTBF vs temperature and system electrical stress..... | 35 |
| 37 | Measurement set-up | 36 |
| 38 | The temperature of IGBTs and DC capacitors | 36 |
| 39 | Capacitors temperature vs time after installed cooling system | 37 |
| 40 | Summary of failure/loss modes included in the FMEA..... | 39 |
| 41 | Normalised average RPN values for the 31 failure modes presented in descending order of maximum value. The two columns represent the maximum and minimum values obtained for that mode | 40 |
| 42 | Categorization of variations in RPN provided by the respondents to the consultation. The variations result in a change in one or both of the occurrence or severity index assigned and thus the resulting RPN value..... | 41 |
| 43 | Summary of monitoring requirements for 10 modes with the highest derived RPN | 42 |
| 44 | Simplified schematic diagram of photovoltaic plant | 44 |
| 45 | PV smart monitoring system | 44 |
| 46 | Failure modes detection strategies..... | 45 |
| 47 | Results of the measurements performed during the test period | 46 |
| 48 | Reliability Block Diagram for a photovoltaic system..... | 46 |
| 49 | The Weibull parameters values | 47 |

LIST OF FIGURES (CONT.)

| Figure | | Page |
|--------|---|------|
| 50 | The total reliability of the PV system: 1- empiric total reliability; 2 – analytical total reliability..... | 48 |
| 51 | FMEA severity and likelihood classifications used to calculate the RPN. Note that the RPN ranges from 1 to 125 in this application..... | 49 |
| 52 | Simplified photovoltaic system model with the principal components of the BNL's NSERC PV array..... | 50 |
| 53 | FMEA Worksheet excerpt for case study PV modules | 51 |
| 54 | Information score for PV module failure modes | 52 |
| 55 | Comparison of surprise index and risk priority number for PV module sub components..... | 52 |
| 56 | Degradation mechanism, corresponding stress factors and accelerated aging tests | 53 |
| 57 | Ultrasonic inspection methodology..... | 54 |
| 58 | Summary of failure mode analysis techniques..... | 55 |
| 59 | The dissertation methodology | 59 |
| 60 | The single line diagram of data measuring and recording of DIPVP..... | 64 |
| 61 | The single line diagram of data measuring and recording of CIPVP..... | 65 |
| 62 | Graphical method of IRR computation | 79 |
| 63 | Y_r of DIPVP and CIPVP during May 2013 to October 2014 | 83 |
| 64 | Y_f of DIPVP and CIPVP during May 2013 to October 2014 | 84 |
| 65 | L_t of DIPVP and CIPVP during May 2013 to October 2014..... | 85 |
| 66 | PR of DIPVP and CIPVP during May 2013 to October 2014 | 86 |
| 67 | η_{tot} of DIPVP and CIPVP during May 2013 to October 2014 | 87 |

LIST OF FIGURES (CONT.)

| Figure | | Page |
|--------|---|------|
| 68 | The equivalent PV power plant downtime of the inverter in DIPVP and CIPVP during May 2013 to October 2014..... | 90 |
| 69 | The equivalent PV power plant downtime of the other PV power plant component in DIPVP and CIPVP during May 2013 to October 2014 | 91 |
| 70 | The equivalent PV power plant downtime of the grid in DIPVP and CIPVP during May 2013 to October 2014 | 92 |
| 71 | The total equivalent PV power plant downtime in DIPVP and CIPVP during May 2013 to October 2014 | 93 |
| 72 | The estimated total time and total time without grid failure of DIPVP and CIPVP in each month during May 2013 to ctober 2014 | 97 |
| 73 | The evaluation result of the availability with grid failure in DIPVP and CIPVP during May 2013 to October 2014..... | 99 |
| 74 | The evaluation result of the availability without grid failure in DIPVP and CIPVP during May 2013 to October 2014..... | 100 |
| 75 | The inverter failure probability evaluated result of DIPVP and CIPVP during May 2013 to October 2014 | 103 |
| 76 | The inverter reliability evaluated result of DIPVP and CIPVP during May 2013 to October 2014 | 104 |
| 77 | Cost per Unit and LCOE with the both availability case of DIPVP and CIPVP | 107 |
| 78 | NPV with the both availability case of DIPVP and CIPVP PV power plant | 108 |
| 79 | IRR with the both availability case of DIPVP and CIPVP PV power plants..... | 109 |

CHAPTER I

INTRODUCTION

Statement of purpose

Global warming and Carbon mission are the biggest challenges facing our society today. Many parts of the world as more and more nations express their commitment to preserve the nature and seriously start thinking about renewable energy. Solar energy has been a major area of focus worldwide because it is freely available, can be used directly and no harmful emission. In case of Thailand, good amount of funding had been allotted to solar energy especially photovoltaic (PV) power plant.

Since, 2006, Thai government announced an incentive in form of adder, a system when the subsidy applied on top of the base electricity cost, of 8 Baht/kWh for 7 year and extended to 10 year in 2007. As a result, commercial PV power plant has gained popularity dramatically until recent years. In early 2009, 15-year Renewable Energy Development Plan (REDP 2008-2022) was implemented and the solar powered generation capacity target was set at 500 MW. In 2010, the incentive was reduced to 6.5 Baht/kWh for the projects that not approved before 28 June 2010 but the growing rate of installed commercial PV power plant is still higher from the reducing investment cost of commercial PV power plant. In 2012, REDP was updated to Alternative Energy Development Plan (AEDP 2012-2021) and the solar powered generation capacity target was extended to 2 GW. In 2013, Thailand's National Energy Policy Commission (NEPC) increased the solar generation target to 3 GW and approved feed in tariff (FiTs) for rooftop (100 MW for systems smaller than 10kW and 100 MW for systems between 10kW and 1 MW) as well as community-owned ground-mounted solar plants, in addition to the Adder scheme. FiTs were set at 6.96 Baht/kWh for residential size systems (≤ 10 kW), 6.55 Baht/kWh for medium-sized building systems and industrial plants (≤ 250 kW) and 6.16 Baht/kWh for large building and industrial plants (> 250 kW) for 25 year period. In 2015, NEPC increased the solar generation target to 6 GW in 2036 and decrease FiTs to 6.85 Baht/kWh for

residential size systems (≤ 10 kW), 6.40 Baht/kWh for medium-sized building systems and industrial plants (≤ 250 kW), 6.01 Baht/kWh for large building and industrial plants (> 250 kW) and 5.66 Baht/kWh for ground mounted system for 25 year period. In 2011, the accumulated COD commercial solar powered generation capacity was about 75.48 MW and increased to 360 and 824MW in the end of 2012 and 2013 respectively. There are already over 1.28 GW of PV power systems operating today [1, 2, 3, 4, 5, 6]. However, the growing rate in 2014 is slower from PPA limited. It is expected that the growing rate of installed commercial PV power plant will be higher again after Energy Regulatory Commission (ERC) approving the new PPA about 1.6 GW.

As solar PV power system grows commercially, the study of grid connected PV system performance is focused in order to maximize the economic aspects. A lot of grid tied PV system performance has been studied that covering every system type, climate, and environment in every part of the world. It results in the improvement of grid connected PV system performance but still does not reach the maximum level of economical yields. In order that grid tied PV system to achieve the highest level of economical yields, increasing detail of many electrical performances must be taken into consideration because small differences in these performances can translate into significant differences in levelized cost of energy (LCOE). Among them, availability and reliability of the system is the most important in determining the success of the system. The better the availability and reliability of the PV system, the better its yields commercially.

Availability is defined as the probability that equipment will be able to perform its intended function when required [7]. Many refinements of this definition have been made in various industries. In a PV power plant, availability can be defined as the probability that, if enough irradiance exists and all other external conditions are met (e.g. grid voltage within specification), the system will function as intended and produce rated power.

Reliability, it is commonly defined as the probability that a system will operate properly for a specified time period under the design operating conditions without failure [8]. Clearly, for this definition of reliability to be meaningful, the time interval, must be stated. In addition, failure must be clearly defined. For example, in

the case of an inverter, failure may be defined simply as the inability to produce power, or it may include loss of auxiliary functions such as data transmission. With the increasing complexity of remote monitoring and control systems at the inverter level, this distinction is becoming increasingly important.

From many studies, inverter is the main factor and by far the most sensitive one in among all components of the PV power system, therefore, it is worthwhile to study the availability and reliability of the PV power system by focusing on the inverter and its types. The common types of inverter being used in the large scale PV power plant are the centralized inverter concept because it is easier to design and less maintenance due to fewer numbers of inverters are being taken into consideration; however, there is a new concept that applies decentralized inverter where the far higher number of the smaller inverters are used to serve the same purpose. In this concept, string inverter with power capacity about 0.7–25 kW that connected with a few PV string and micro-inverter with power capacity lower than 0.7 kW that connected with 1 or 2 PV modules are the prefer inverter types for decentralized inverter concept PV power plant.

There are many studies already on the availability and reliability of PV power system applying centralized and decentralized inverter concept but almost of these study based on climate and environment in other country. So, the outcome of these study cannot completely use in Thailand. The study of availability and reliability of PV power system applying decentralized inverter concept will focus on central and string inverter, climate, and environment in Thailand. The outcome of the study of availability and reliability of PV power system applying decentralized inverter concept will reveal a very useful knowledge to help improve commercial PV system in Thailand or even worldwide.

Objectives of the study

1. To analyze and compare reliability and availability of PV power system applying decentralized and centralized inverter concepts.
2. To analyze the economics aspects between PV power system applying decentralized and centralized inverter concepts.

Expected outputs of the study

1. To obtain Reliability and Availability of PV power systems applying centralized and decentralized inverter (String inverter) concepts.

Expected outcomes

1. To have the guideline for developing and improving of PV power systems.
2. To obtain useful information for further considering and selecting inverter concept.



CHAPTER II

THEORETICAL AND RELATED LITERATURE

Photovoltaic systems

Solar power is one of the more desirable types of renewable energy. One of the most efficient ways to convert solar power into electrical energy is through the use of solar cells. These devices create a photovoltaic DC current through the photovoltaic effect.

The photovoltaic effect was first observed by Alexandre-Edmond Becquerel, a French experimental physicist, in 1839. When the sunlight or any other light is incident upon a material surface, the electrons present in the valance band of the metallic atom absorbs energy and, being excited, jump to conduction band and become free. Now these free electrons are attracted by a positively charged electrode and thus the circuit completes and the light energy is converted into electric energy.

This occurs in the natural elements in the group of semiconductors including silicon, gallium, germanium, etc. All of them belong to one of two types: P and N. P-type semiconductors tend to pick up a small positive charge, and N-type ones a negative. Inside every solar cell is a sandwich of two of those semiconductors, one layer of P-type and one layer of N-type. The electrons in the N-type start excited by the light, then rush out of their home N-type layer and stream towards the positive charge in the P-type.

An experiments launched by Becquerel had certain characteristics that could not be explained by the theories of that period which saw the light and all other kinds of electromagnetic radiation behave as waves. For example, as the light falling on metal becomes more intense, the wave theory of light suggests that the metal is released electrons with increasing energy. However, the experiments showed that the maximum possible energy of the emitted electrons depends only on the frequency of the incident light, and not of their intensity.

In 1905, an attempt to explain the mechanism of the photoelectric effect, Albert Einstein suggested that light could be seen in some cases behave like a particle, and that the energy of each light particle, or photon, depends only on the frequency of light. To explain the external photoelectric effect, Einstein considered light as a series of “rounds” that hit the metal. When a free electron metal is beaten by a photon, it absorbs the energy of it. If the photon has enough energy, the electron is ejected from the metal.

Einstein’s theory explained many features of the photoelectric effect, such that the maximum energy of the ejected electrons is independent of light intensity. According to Einstein’s theory, the maximum energy depends only on the photon energy that is expelled, which in turn depends only on the frequency of light. Einstein’s theory was verified by further experiments. His explanation of the photoelectric effect, by demonstrating that electromagnetic radiation can behave in some cases as a set of particles, contributed to the development of quantum theory. Photoelectric effect can also refer to three processes: The photo ionization, The photoconduction and Photovoltaic effect

Photo ionization is the ionization of a gas by light or other electromagnetic radiation. For this, photons must possess enough energy to separate one or more outer electrons of atoms of gas. In photoconduction, electrons in crystalline materials absorb energy from photons and thus arrive at the range of energy levels where they can move freely and conduct electricity. In the photovoltaic effect, photons create electron-hole pairs in semiconductor materials. In a transistor, this effect leads to the creation of an electrical potential at the junction between two different semiconductors, which is essential for the generation and use of solar energy.

Solar cells are linked together electrically to make a combination of cells into a solar panel or a photovoltaic (PV) module. PV modules are often connected in series to provide high voltage at a reasonable current.

PV system is made up of one or more PV modules, an AC/DC power converter (also known as an inverter), a tracking system that holds the solar panels, and the interconnections and mounting for the other components. A small PV system may provide energy to a single consumer, or to an isolated device like a lamp or a weather instrument. Grid connected PV system (typically the public electricity grid)

feeds power either directly into a residential or commercial building or back into the grid. Grid connected systems vary in size from residential (2-10kW) to solar power stations (up to GW scale). This is a form of decentralized electricity generation. The feeding of electricity into the grid requires the transformation of DC into AC by a special, grid-controlled solar inverter.

PV power plant

A PV power plant or PV power station, also known as a solar park, solar farms, or solar ranches, is a large-scale photovoltaic system (PV system) designed for the supply of merchant power into the electricity grid. They are differentiated from most building-mounted and other decentralised solar power applications because they supply power at the utility level, rather than to a local user or users. The generic expression utility-scale solar is sometimes used to describe this type of project. Normally, the nameplate capacity of a photovoltaic power stations is rated in megawatt-peak (MW_p or MW_{DC}) and refers to the solar array's DC power output. However, AC output (MW , MW_{AC} , or MVA) is used in many countries. Most solar farms are developed at a scale of at least 1 MW_p . The first 1 MW_p solar farm was built by Arco Solar at Lugo near Hesperia, California at the end of 1982 [9], followed in 1984 by a 5.2 MW_p installation in Carrizo Plain. [10] Both have since been decommissioned. The first multi-megawatt plant in Europe was the 4.2 MW community-owned project at Hemau, Germany that commissioned in 2003 [11]. The next stage followed the 2004 revisions [12] to the feed-in tariffs in Germany when a substantial volume of solar parks were constructed. The first to be completed under this programme was the Leipziger Land solar park developed by Geosol. that commissioned in 2004 [13]. After that, many countries launch the subsidies or incentive programs that result in the wide spread of PV power plant in every region of the world. As of 2015, the world's largest operating photovoltaic power stations have capacities of 550 MW and will be reached 750 MW in next year. In addition, the projects up to 1,000 MW are planned. Most of the existing large-scale PV power plant are owned and operated by independent power producers, but the involvement of community- and utility-owned projects is increasing. In present day, more than 90% have been supported at least in part by regulatory incentives such as adder, feed-in

tariffs or tax credits, but as levelized costs have dropped remarkably in the last decade and grid parity has been reached in an growing number of markets, it is possible that the external incentives cease to exist in the near future.

For the concept of PV power plant, the centralized inverter concept is the general concept for the large scale PV power plant because it is easier to design and less maintenance due to fewer numbers of inverters are being taken into consideration. Moreover, the PV power plant component for this concept is extensively available in the market. For example, the central inverter size in the market is ranging from 25 kW to 2500 kW with input voltage from 100 to 1500 VDC, the other BOS equipment in the market have the variety size and type. From this point, the cost per watt of central inverter and other BOS equipment for the centralized inverter concept are cheapest that result in lowest investment cost. The centralized inverter concept is presented in Figure 1. However, there is a new concept that applies decentralized inverter where the far higher number of the smaller inverters are used to serve the same purpose.

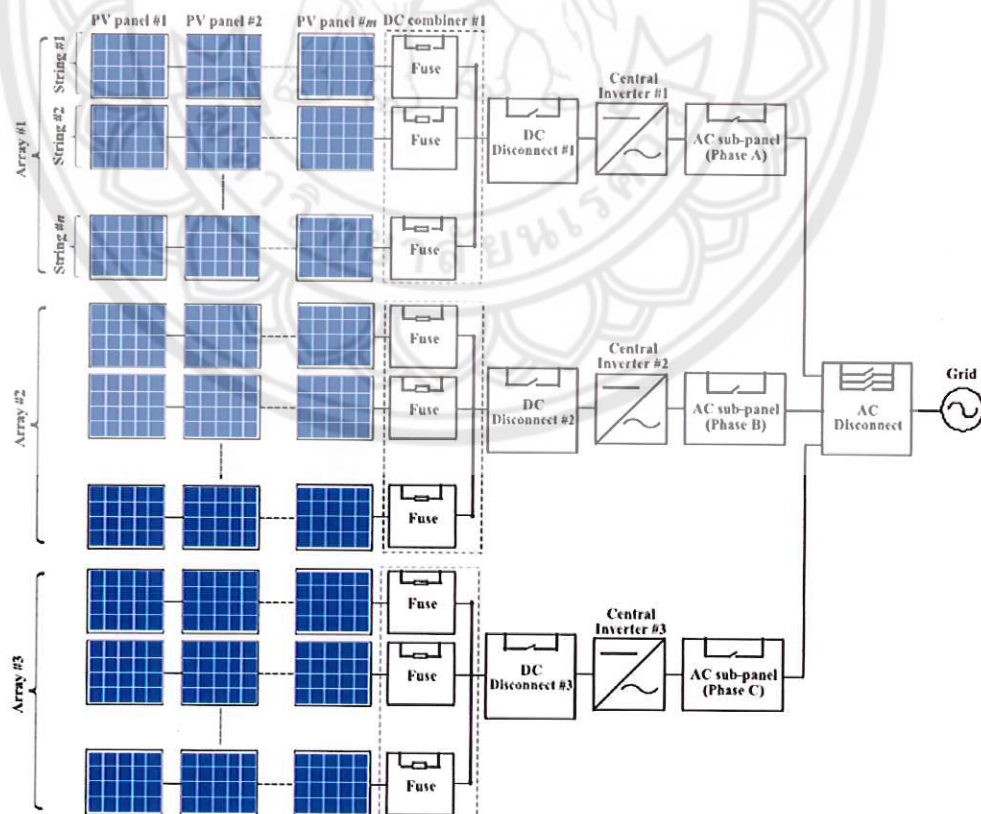


Figure 1 The centralized inverter concept [28]

In this concept, string inverter with power capacity about 0.7–25 kW that connected with a few PV string and micro-inverter with power capacity lower than 0.7 kW that connected with 1 or 2 PV modules are the preferred inverter types for the decentralized inverter concept PV power plant. In case of string inverter, the generated yield is possible higher than the centralized inverter concept when operate in partial shaded condition because it can reduce the mismatch loss when PV array is shaded from the smaller PV array area per inverter. In addition, the PV power plant component for this concept is wide spread available in the market because the string inverter is the main inverter type for residential and commercial market and possible using other BOS equipment of the centralized inverter concept. From these reasons, the decentralized inverter with string inverter has a little bit higher cost per watt of string inverter and other BOS equipment than the centralized inverter concept that result in slightly higher investment cost. The decentralized inverter concept with string inverter is displayed in Figure 2. In case of micro-inverter, the generated yield is possible highest in every condition because it can get rid of the mismatch loss in PV array. Normally, micro-inverter is connected with a PV module and operating at the maximum power output of the PV module. So, every PV module in the PV system operating at maximum power output in every condition. It is possible gain the surplus energy from the plus power tolerance PV module and not losing energy from the minus power tolerance PV module. For the partial shaded condition, the PV system is losing produced energy only in the shaded PV module while other PV modules are still operating at maximum power output. However, the micro-inverter was introduced to the market over past few years that result in the PV power plant component for this concept is limited in the market and only a few other BOS equipment of the centralized inverter concept is possible used. From these reasons, the decentralized inverter with micro-inverter has the highest cost per watt of micro-inverter and other BOS equipment that result in really high investment cost. The decentralized inverter concept with micro-inverter is showed in Figure 3. From these information, each PV power plant concept has different strong and weak point. There are many factors that have to study for selecting the suitable PV power plant concept such as site location, climate, environment, performance, reliability, availability, financial aspect, etc.

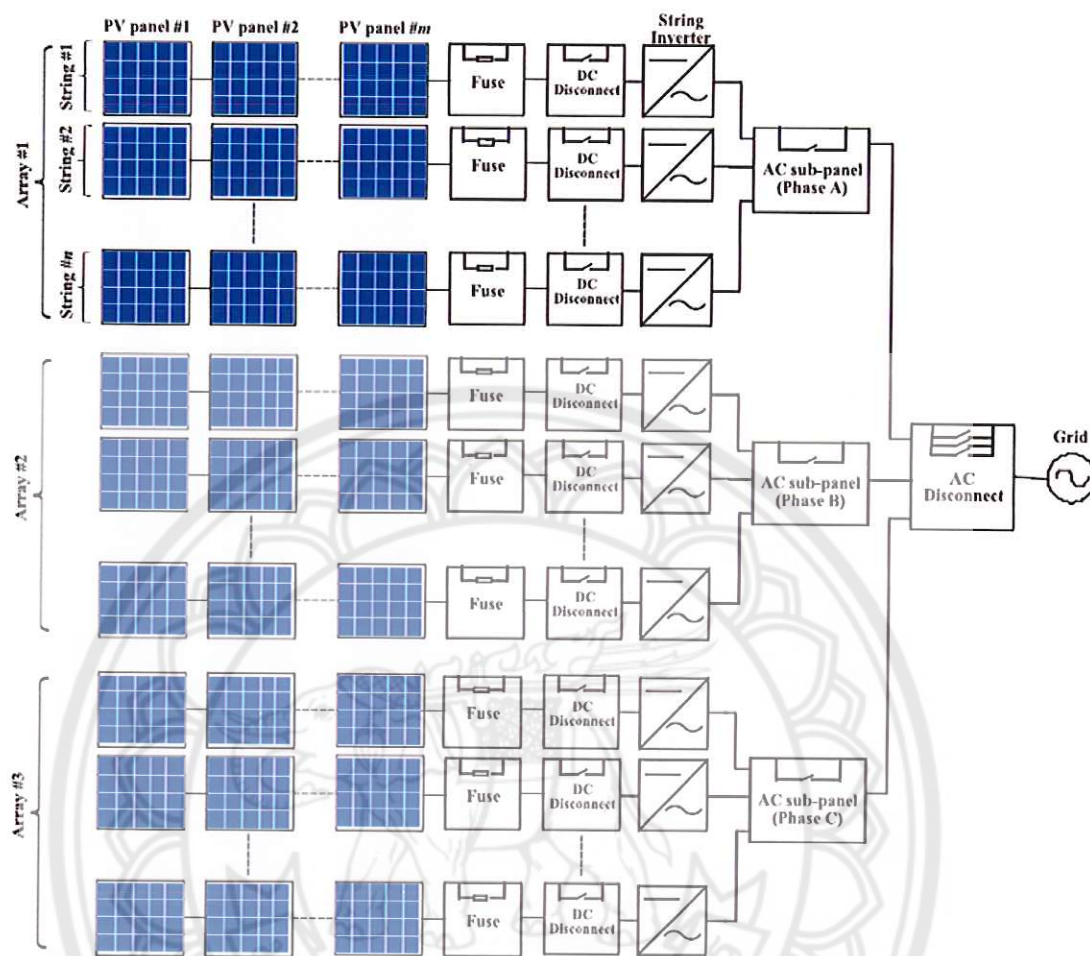


Figure 2 The decentralized inverter concept with string inverter [28]

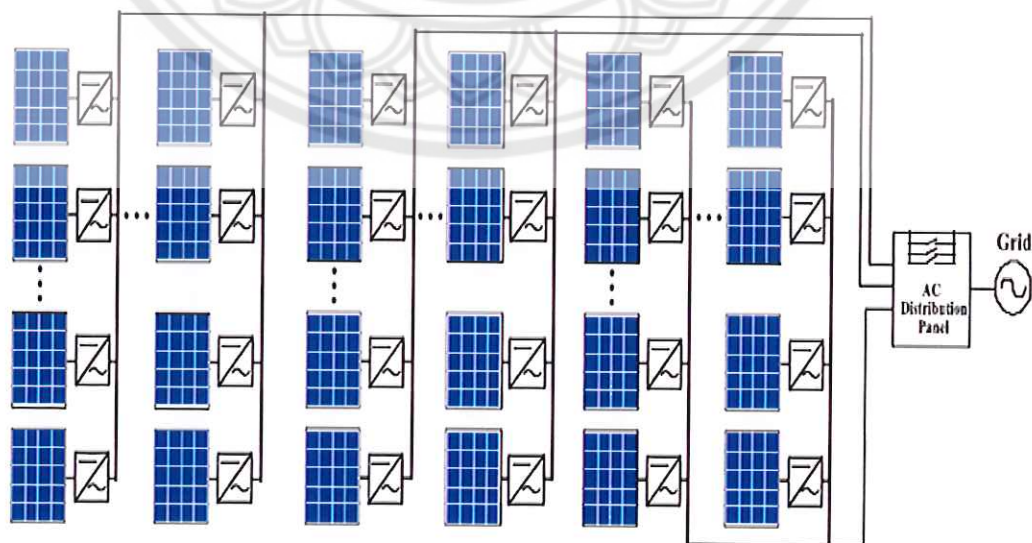


Figure 3 The decentralized inverter concept with micro-inverter [28]

Reliability and Availability of PV power plant

An important issue in grid connected PV systems as their operations rely on business plans developed over periods of time at least twenty years; manufacturers in the PV industry are commonly offering warranties, are reliability and availability. System reliability and availability estimates are required to facilitate cost trade off studies. Estimates of reliability are necessary in developing maintenance cost projections over the system lifetime. Availability estimates provide an input annual energy generation projections. Field data, failure times and repair times, are needed to collect and analyze. The study about reliability and availability is available in many aspects. Over the past years, the study have produced a good development in many ways.

Reliability and Availability of PVsystem in Springerville, Arizona, U.S.A.

The case study of a fielded grid-connected PV power plant in Springerville, Arizona, USA that showed Figure 4 by Elmer Collins, Michael Dvorack, Jeff Mahn, Michael Mundt, and Micheal Quintana [14] present that crystalline silicon PV modules is comprising approximately 80% of PV generating system's capacity. The case study



Figure 4 Springerville PV power plant in Arizona, U.S.A.

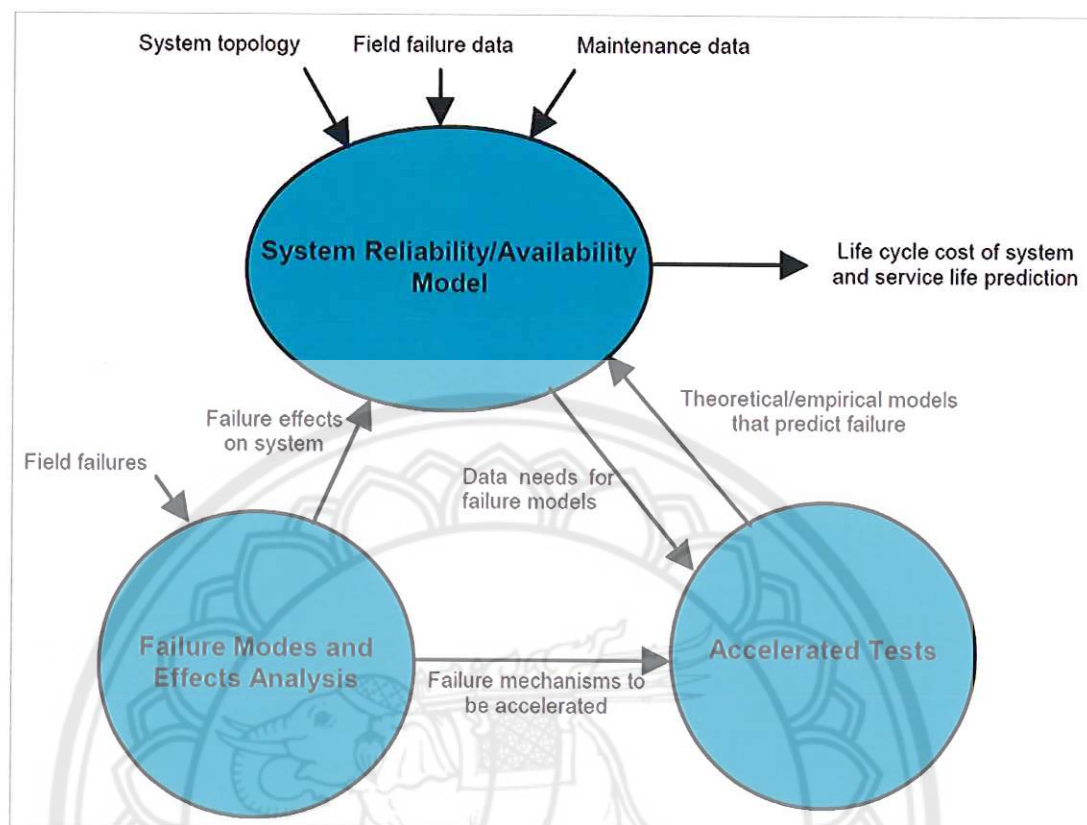


Figure 5 Overview of Reliability Program for PV systems

using three basic activities associated with a reliability and availability program are Failure Modes and Effects Analysis (FMEA), System Reliability/Availability Model, and Accelerated Tests. Overview of Reliability Program for PV systems. FMEA is a technique for systematically identifying, analyzing and documenting the possible failure modes on system performance or safety. System Reliability/Availability Model allows quantification of system reliability and availability using multiple data inputs, such as field data, test data, and accelerated life test data. The expected number of failures as predicted by model for each component for 5, 10, and 20 years are shown in Table 1. For the first five years, the inverter repair rate was 0.96 per inverter per years. For PV modules, the replacement rate was approximately 5 in 10,000 modules per year. Inverters are the most unreliable component in this system. Yet the availability of continuous power delivered to the grid is projected to be very high over life of this system. However, an increase in inverter reliability can still lower corrective maintenance costs over the system life.

Table 1 The expected number of failures as predicted by model for each component for 5, 10, and 20 years

| Component | Actual Number of Failures 5 yr Cum | Expected Number of Failures 5 yr Cum | Expected Number of Failures 10 yr Cum | Expected number of Failures 20 yr Cum |
|-------------------------------------|---|---|--|--|
| PV 150 Inverter (26 cSi arrayes) | 125 | 132 | 231 | 429 |
| PV Module | 29 | 26 | 31 | 38 |
| AC Disconnect | 22 | 17 | 23 | 31 |
| Lightning | 16 | 10 | 20 | 41 |
| 208/480 Transformer | 4 | 3 | 3 | 3 |
| Row Box | 34 | 25 | 35 | 50 |
| Marshalling Box | 2 | 4 | 7 | 11 |
| 480 OVAC/34.5 KV Xformer | 5 | 4 | 5 | 9 |

Reliability of various sizes of PV systems

The another case study done by Gabriele Zini, Christophe Mangeant and Jens Merten [15]. PV systems, with nominal power ranging from 100 kW to 2500 kW are designed in order to evaluate their overall reliability. To compute the total number of components needed for each system, the PV module and inverter with the characteristics shown in the Table 2. The reliability of PV systems over a period of time of twenty years, with an average of 8.5 h operations a day was analyzed. The failure rate units is hence failures/hour. In this study, system failure is intended not only as a complete shut-down, but even as a small loss due to a single cell in a single module being damaged. This consists in a very strong constraint, since a small power loss due to a single module cannot even be spotted in a large-scale PV system. As far as the inverters are concerned, using the failure rate in the Table 3, 23 inverters out of 24 would have a fault over the twenty years period. The energy loss caused by one inverter would be

easily traceable, but for a 2.5 MW PV system, two weeks of lost production per each inverter would entail a loss of more than 4% of overall system production.

Table 2 Number of components for each PV system

| Power (kWp) | 100 | 200 | 500 | 1000 | 1500 | 2000 | 2500 |
|------------------------------|-----|------|------|------|-------|-------|-------|
| PV modules | 437 | 874 | 2166 | 4351 | 6517 | 8702 | 10868 |
| String Protection | 23 | 46 | 114 | 229 | 343 | 458 | 572 |
| DC switch | 3 | 6 | 15 | 27 | 42 | 57 | 72 |
| Inverter | 1 | 2 | 5 | 9 | 14 | 19 | 24 |
| AC circuit breaker | 1 | 2 | 5 | 9 | 14 | 19 | 24 |
| Grid protection | 1 | 1 | 1 | 1 | 1 | 1 | 1 |
| AC switch | 1 | 1 | 1 | 1 | 1 | 1 | 1 |
| Differential circuit breaker | 1 | 1 | 1 | 1 | 1 | 1 | 1 |
| Connector (couple) | 874 | 1748 | 4332 | 8702 | 13034 | 17404 | 21736 |

Table 3 Component adopted failure rates

| Component | Failure Rate (10^{-6} failures/hour) |
|------------------------------|---|
| PV modules | 0.0152 |
| String Protector (Diode) | 0.313 |
| DC switch | 0.2 |
| Inverter | 40.29 |
| AC circuit breaker | 5.712 |
| Grid protector | 5.712 |
| AC switch | 0.034 |
| Differential circuit breaker | 5.712 |
| Connector (couple) | 0.00024 |

Performance and Availability of 202 PV systems in Taiwan

H. S. Huang, J.C. Jao, K. L. Yen and C. T. Tsai [16] concluded in their study that 60% of systems failed by inverters. Only 12% of systems failures caused by modules and over 20% caused by BOS. This information indicates that inverter is the most vital components of solar system. The data were collected for 3 years on 202 PV systems found out that performance ratios (PR) ranged from 0.6-0.9 as seen in the Figure 6.

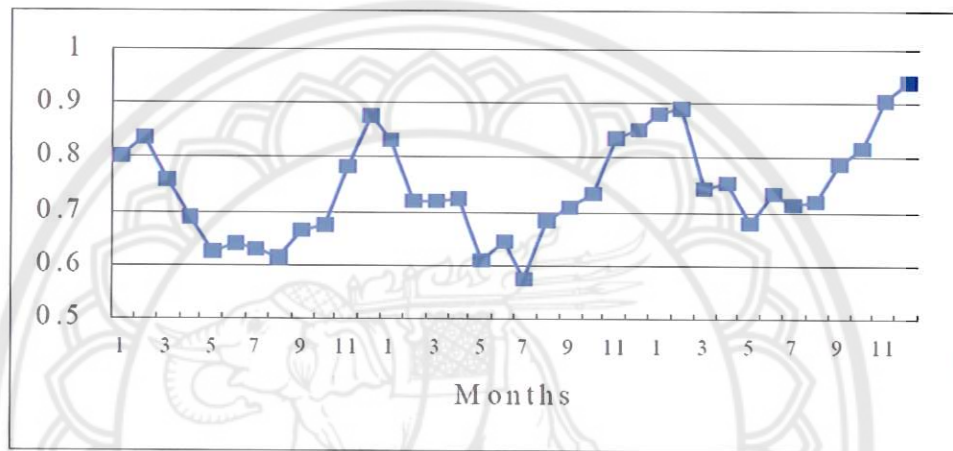


Figure 6 The variation of PR values for PV systems in Taiwan

The performance ratio that presented in Figure 7 were calculated from:

Performance ratio

$$PR = \frac{Y_f}{Y_r}$$

where Y_f is Final System yield (hours/day) and Y_r is Reference yield (hours/day)

Final System Yield

$$Y_f = E_{pv} / P_o$$

where E_{pv} is Energy delivered to the load (kWh) and P_o is Norminal power of PV array at standard test conditions (STC) (kWp)

Reference Yield

$$Y_r = H_i / G_{stc}$$

where H_{iv} is Actual in-plane irradiation (kWh/m^2) and G_{stc} is Reference in-plane irradiation at standard test conditions = 1kW/m^2

Average availability summarized from the study was 95.7% calculated from the following equation:

$$Availability = \frac{m}{m+r} = \frac{m}{T}$$

The distribution of PV system availabilities in Taiwan is illustrated in Figure 8.

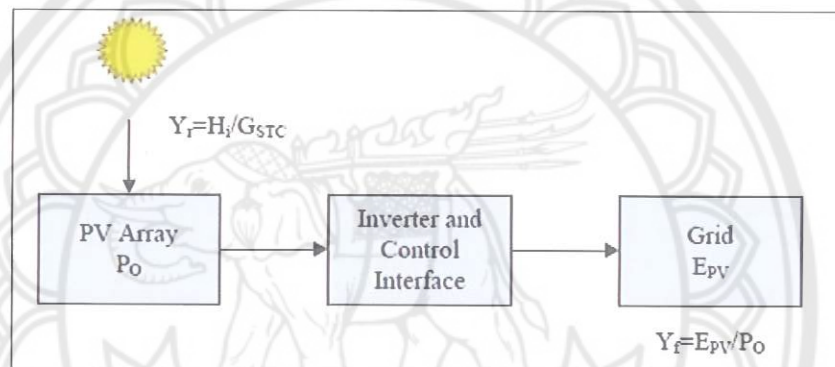


Figure 7 Definitions of PV system performance indices

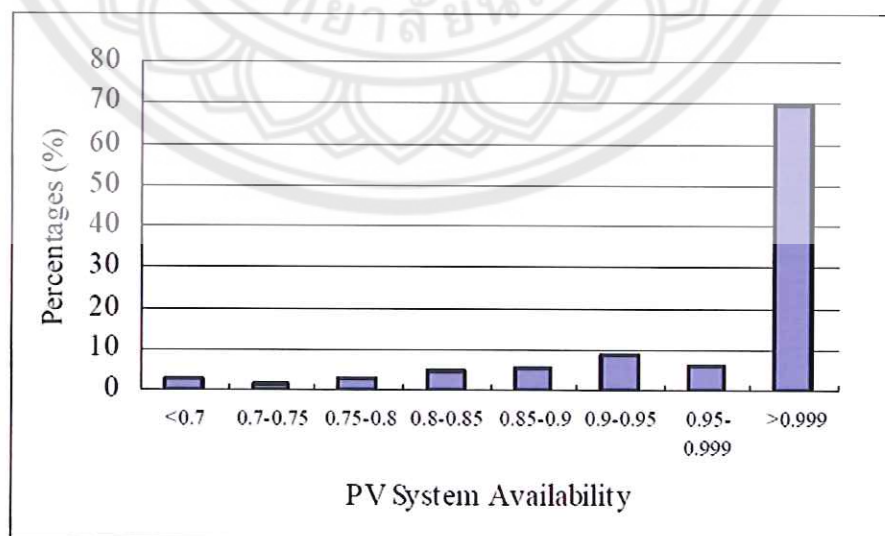


Figure 8 The distribution of PV system availabilities in Taiwan

Where m is mean time to failure (MTTF), r is mean time to repair (MTTR), and T is mean time between failure (MTBF = $m+r$). Definitions of system availability indices is presented in Figure 9.

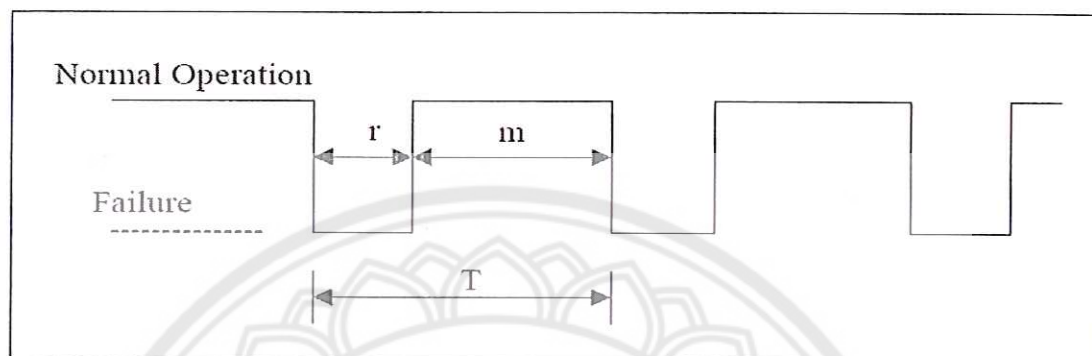


Figure 9 Definitions of system availability indices

Reliability of PV systems focusing on causes

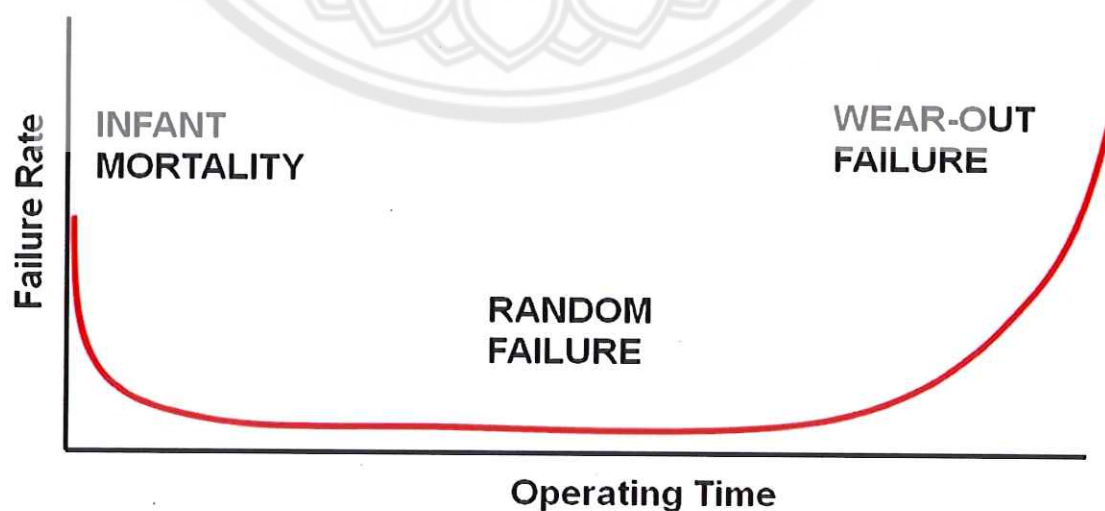
John H. Wohlgemuth [17] from BP Solar International Inc. presented in his study that reliability of PV systems is best described by defining types of failures. There are 3 distinct types of failures. The first type is the total loss of power caused by the problem with inverters and other BOS components. Second type is the slow decaying of output power extended over a period of time mostly caused by the module degradation and other critical components. The third type is failure to meet the required expectation of the system owner. It was found by data collecting that the inverters are the main effects to reliability related to its failure described in Table 4. It can be concluded from the related literatures that reliability and availability plays vital roles in rating the commercial success of PV Power systems. The most critical components that are the main cause of failure in turn effect the reliability and availability the most is inverter.

Table 4 Causes of Maintenance Events by Category

| Category | # of events | Cost | Notes |
|---------------|-------------|------|-----------------------------------|
| Inverter | 37% | 59% | 25% from 1 lightning storm |
| DAS | 7% | 14% | 90% from 1 lightning storm |
| AC Disconnect | 21% | 12% | 50% due to dirt accumulation |
| Module/J Box | 12% | 3% | 60% due to failed blocking diodes |
| PV Array | 15% | 6% | 45% from 1 lightning storm |
| System | 8% | 6% | All utility meters |

Field Reliability Analysis Methods for Photovoltaic Inverters

Fife J. M., Scharf M., Hummel S. G. and Morris, R. W. [8] present the measuring and reporting methods for PV inverters by using a sample population of 30kW commercial-class inverters as an example calculation. Normally, equipment typically goes through three phases during its fielded lifetime: infant mortality, random failure, and wearout. The infant mortality phase is dominated by failures related to out-of-the-box quality and manufacturing defects, and manifests very early in the equipment life. The failure rate typically decreases after a break-in period. In the random failure phase, failures

**Figure 10 Classic bathtub curve**

occur due to random events such as lightning strikes. These failures are typically infrequent and occur at the same rate regardless of inverter age. The final wear-out phase is characterized by an increasing failure rate due to wear-out of specific components. Figure 10 shows a schematic representation of these phases, which are commonly described together as the bathtub curve. Reliability, inverter downtime, and availability are the important indicators in this study. For the example calculation, the sample data set is a population of 373 PV Powered 30kW commercial inverters. In this case, the parameter being considered is warranty downtime, which is defined as unplanned inverter downtime due to inverter defects of any type. Distribution of warranty downtime hours for a sample population of 30kW inverters is showed in Table 5. It is useful to plot downtime as a function of time after inverter commissioning. However, the commissioning is not available for all inverters in the sample population, the downtime will be plotted versus shipment date. Warranty downtime for a sample availability of the sample inverter population can be calculated versus time using the

| Downtime Duration | % of Downtime |
|--------------------------|----------------------|
| < 6 hours | 0.6% |
| 6-24 hours | 0.0% |
| > 24 hours | 99.4% |

Figure 11 Distribution of warranty downtime hours for a sample population of 30kW inverters



Figure 12 Warranty downtime for a sample population of 30kW inverters

availability factor' (AF) metric. Field hours and availability factor (AF) for a sample population of 30kW inverters is illustrated in Figure 12. From the trend toward larger PV power plants and exponential industry growth, reliability is now being viewed with importance equal to electrical conversion efficiency. For that reason, the indicators used to describe inverter reliability are being carefully scrutinized, with focus on the ones that reflect true PV plant operating cost and LCOE such as failure rate and availability.

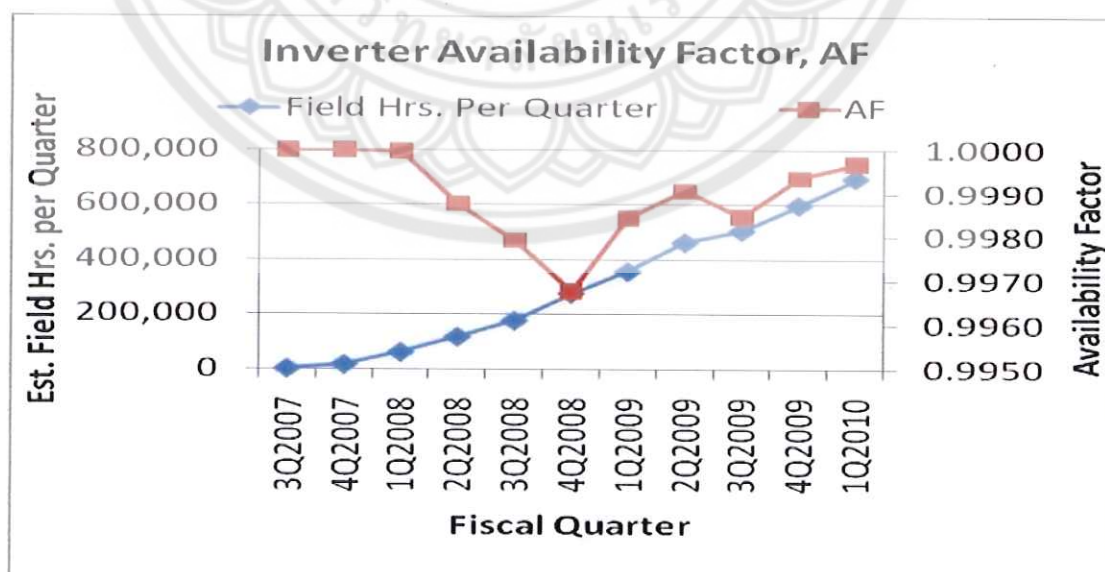


Figure 13 Field hours and availability factor (AF) for a sample population of 30kW inverters

System Availability Analysis for a Multi-megawatt Photovoltaic Power Plant

Fife J. M., and Morris R. W. [7] presents an analytical method for time-dependent modeling of subsystem availability in any geographic location. It can be applied to subsystems such as solar panels, tracking devices, and power inverters. The results for each subsystem can then be combined in a system-level reliability and performance analysis of the complete photovoltaic power plant. This methodology can be useful to help assess a PV plant's financial viability, obtain more realistic estimates of expected downtime, plan preventative maintenance schedules, and budget for spares. The subject PV plant reliability analysis consists of three phases: Time-Dependent Stress (Thermal) Simulation of Each Subsystem that to obtain and understand the environmental stress at a target geographic location, Time-Dependent Probabilistic Reliability Simulation that involves calculating subsystem reliability while taking into account the component stresses by using life-stress relationships to accomplish, this, and System-Level Analysis that classical methods of system-level reliability analysis are may be used to estimate the overall performance of the system taking into account downtime due to failures and other causes of subsystem unavailability. The first two phases dealing with subsystems, such as modules, trackers, junction boxes and inverters, are shown schematically in Figure 13. This example deals with temperature stress, salt, hail, and ice. As an example of this analysis process, a hypothetical solar power inverter with active cooling control will be used. The inverter power profile is based on a fixed mount installation. The geographic location is assumed to be Needles, California. Three failure modes of the inverter are modeled. The failure modes are associated with components 1, 10, and 12. For each failure mode, an Arrhenius-Weibull life-stress model is assumed. The model parameters for each of these are given in Table 6. From the simulation result, example calculation of cumulative failure rates for three inverter failure modes and the overall inverter subsystem and average downtime per year due to inverter failures is presented in Figure 14. Availability is then calculated as a function of time based on the downtime and shown in Figure 15. The method applied above in the inverter example may also be applied to any geographic location where stress (temperature) data is available. By performing the same analysis for two other geographic locations, a comparison of relative inverter availability may be made. As an example, take a 10 MW

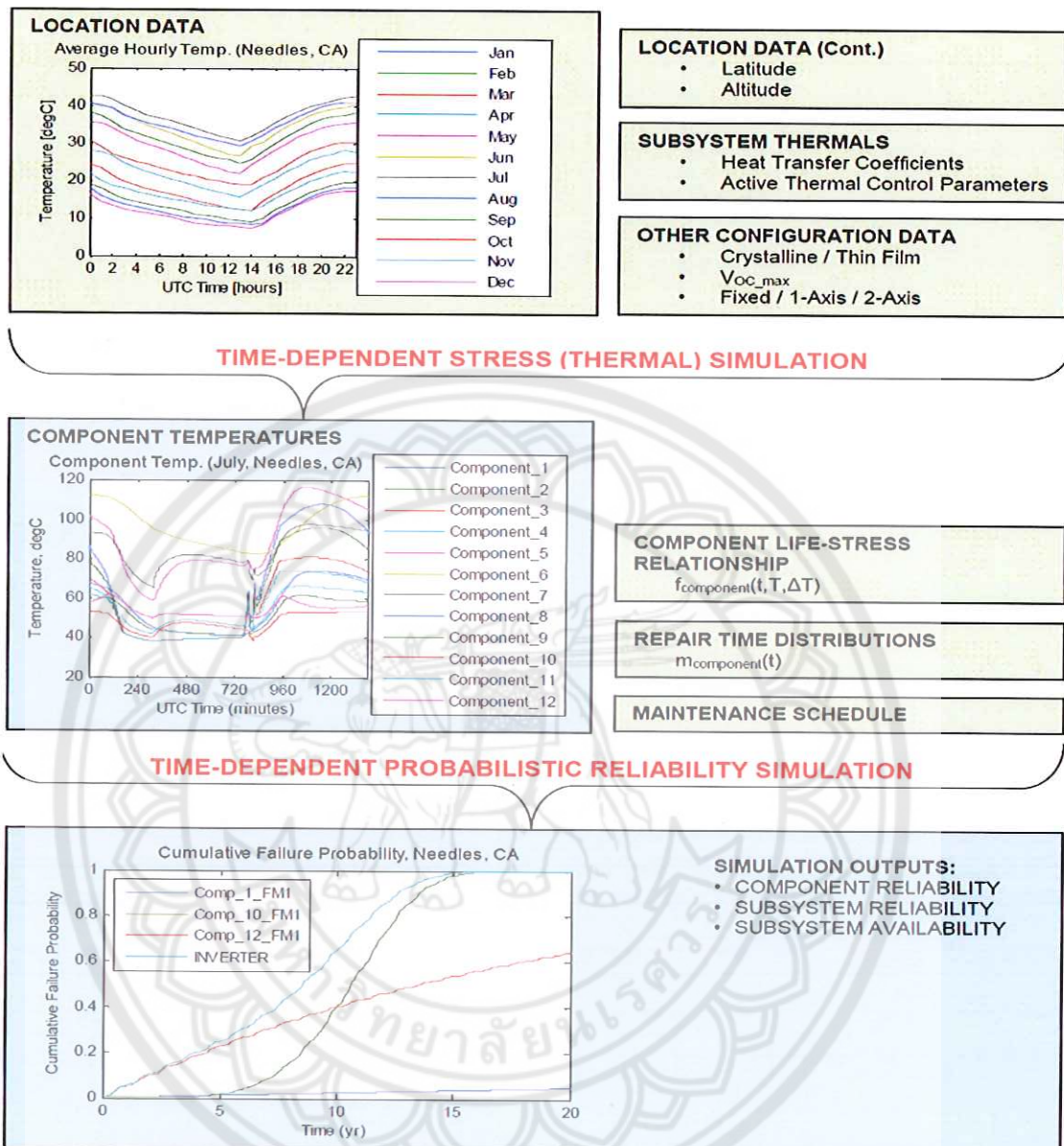


Figure 14 Two phases of subsystem (inverter) reliability analysis for a limited case considering only temperature stresses. Blue boxes represent simulation outputs

peak PV power plant with 5 MW average output and 3500 hours of generating time per year. Assuming the inverter is the dominant failure mode, the annual energy loss is

| Failure Mode | β | $\alpha(T_0)$ (hr) | T_0 (degC) | A_e (eV) |
|--------------|---------|-----------------------|-----------------|---------------|
| Comp_1_FM1 | 1 | 1.0e6 | 100 | 1.0 |
| Comp_10_FM1 | 5 | 1.0e5 | 40 | 0.3 |
| Comp_12_FM1 | 1 | 2.0e5 | 48 | 1.0 |

Figure 15 Arrhenius-Weibull life-stress parameters for the inverter reliability example

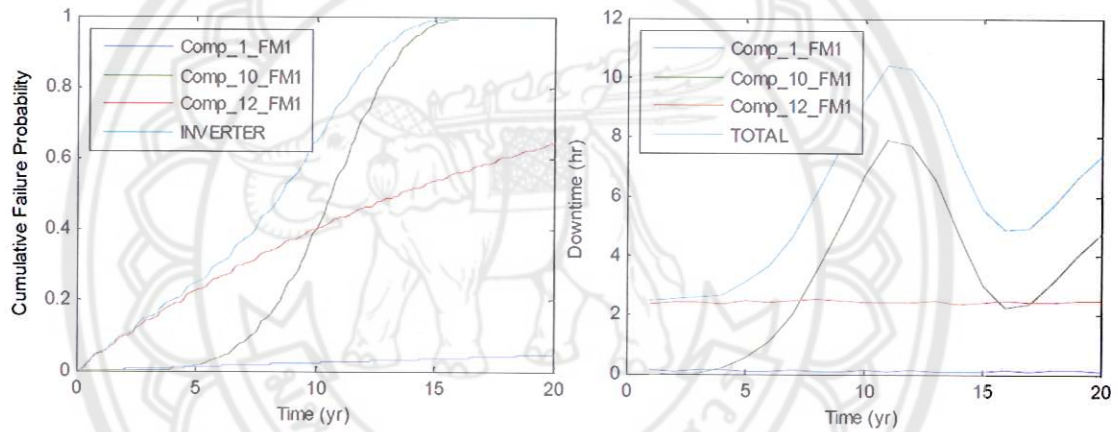


Figure 16 Example calculation of cumulative failure rates for three inverter failure modes and the overall inverter subsystem and average downtime per year due to inverter failures

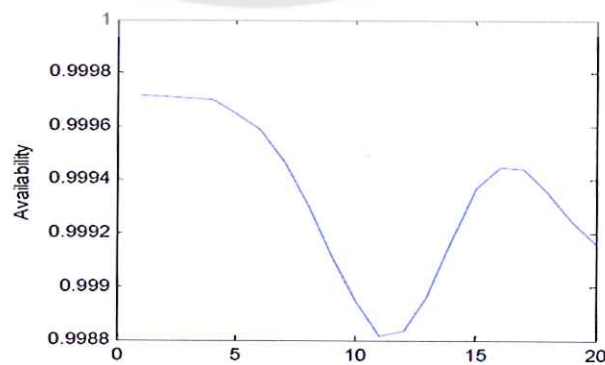


Figure 17 Availability of the example inverter based on downtime due to failure

estimated as the product of the inverter unavailability, average power output, and the number of generating hours per year. Multiplying the energy loss by an average cost of electricity of \$0.05 per kWh yields the annual cost of downtime due to inverter failures. These values are also shown in Table 7.

| Location | Avg. Avail. | MWh Lost Annually | \$ Lost Annually |
|----------------------|-------------|-------------------|------------------|
| Needles, California | 0.9933 | 117 | \$6,000 |
| San Jose, California | 0.9956 | 77 | \$4,000 |
| Bozeman, Montana | 0.9971 | 51 | \$3,000 |

Figure 18 Average predicted inverter availability and resulting MWh lost annually for a hypothetical 10MW PV power plant

Economical Design of Utility-Scale Photovoltaic Power Plants with Optimum Availability

Moradi-Shahrbabak, Z., Tabesh, A. and Yousefi, G. R., [18] presents an algorithm for the economical design of a utility-scale photovoltaic (PV) power plant via compromising between the cost of energy and the availability of the plant. The algorithm inputs are the plant peak power and the price of inverters with respect to their power ratings. The outputs are the optimum inverter ratings and the interconnection topology of PV panels that displayed in Figure 16. This paper introduces the effective levelized cost of energy (LCOE) (ELCOE) index as the core of the proposed design algorithm. ELCOE is an improved index based on the conventional LCOE that includes the availability of a power plant in economical assessments. To investigate the advantages of the introduced ELCOE compared with the conventional LCOE, these two criteria are compared for 100-kW PV power plants using the four aforementioned basic topologies. The investigation results are summarized in Table 8. Comparing the total price of the inverters shows that the excess costs of inverters in modular, string, and multistring topologies are 300%, 70%, and 15% higher than that of the centralized topology, respectively. Given the price of commercially available PV inverters at present, the case studies result in this paper is showed in Figure 17 that, for 0.1–100-MW PV power plants, the economical ratings of

inverters range from 8 to 100 kW. The recently installed PV power plants confirm the feasibility of the calculations based on the suggested algorithm.

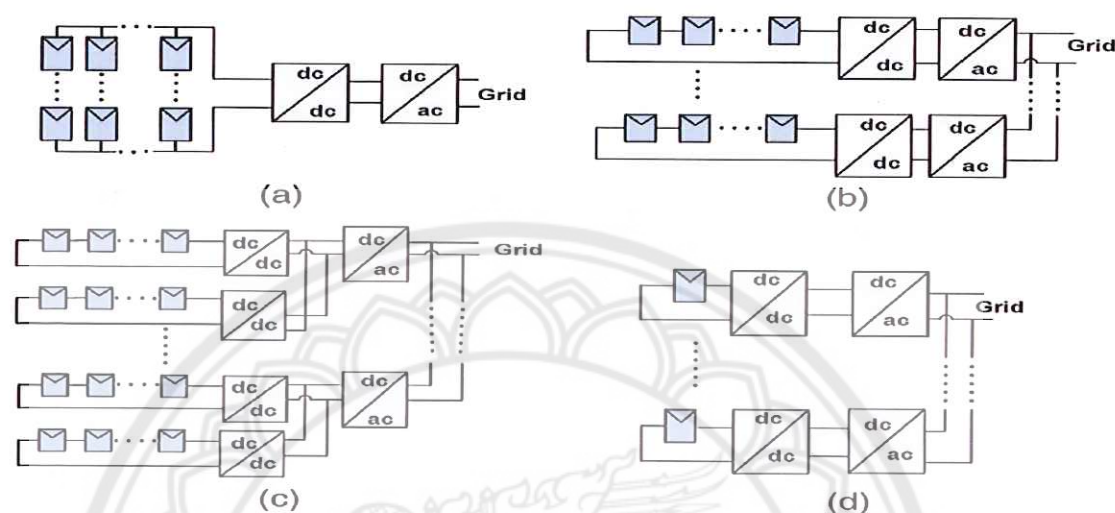


Figure 19 Basic topologies for PV energy systems: (a) Centralized, (b) string, (c) multistring, and (d) ac modular

| | Centralized | Multi-String | String | Modular |
|----------------------------------|-------------|--------------|--------|---------|
| 1- INVERTER: | | | | |
| Size [kW] | 100 | 10 | 3.34 | 0.7 |
| Numbers | 1 | 10 | 30 | 143 |
| Unit Price [\$] | 43.5k | 5k | 2.44k | 1.2k |
| Total Price [\$] | 43.5k | 50k | 73.17k | 171.6k |
| 2- PV PLANT: | | | | |
| Total Cost [\$] | 595k | 603k | 688k | 834k |
| Efficiency [%] | 80 | 82 | 81.6 | 83 |
| 3- AVAILABILITY ANALYSIS: | | | | |
| NSEE [MWh/yr] | 147 | 1.28 | 0.39 | 0.07 |
| LCOE [\$/kWh] | 0.190 | 0.210 | 0.225 | 0.282 |
| ELCOE [\$/kWh] | 0.241 | 0.219 | 0.231 | 0.278 |

Figure 20 Availability analysis of a 100 kW PV power plant

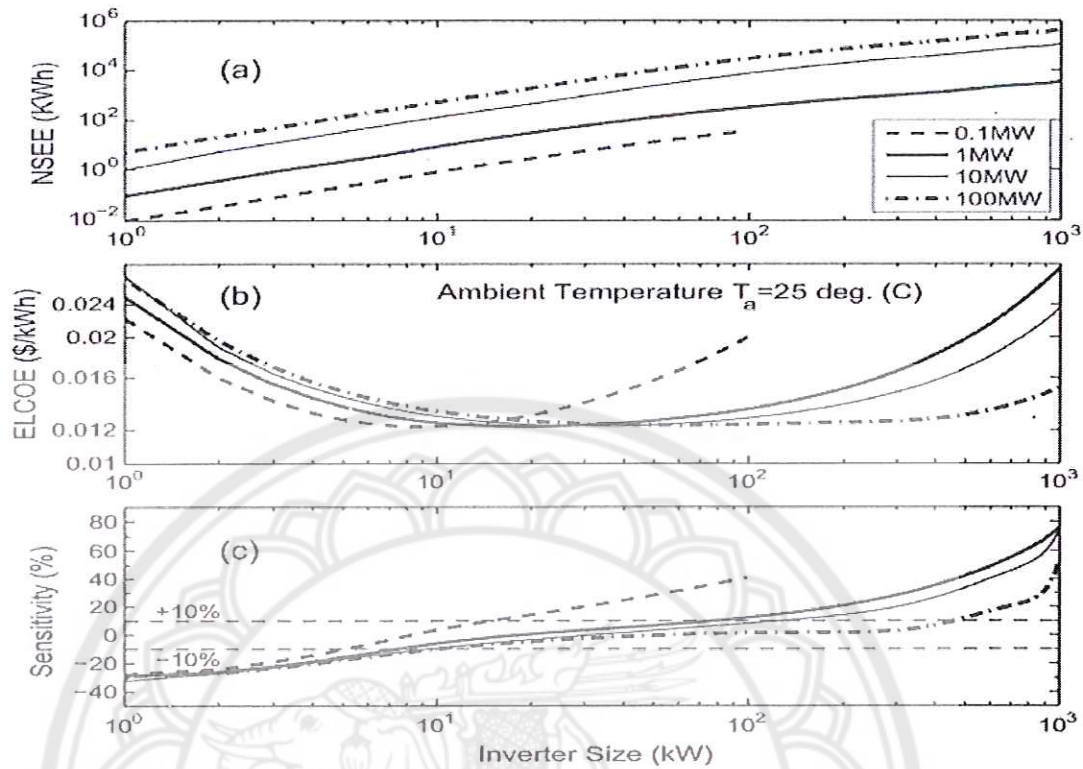


Figure 21 (a) NSEE for megawatt-scale PV plants. (b) ELCOE versus the inverter size. (c) Sensitivity of ELCOEi with respect to the inverter size

Reliability Assessment for Components of Large Scale Photovoltaic Systems

Ahadi, A., Ghadimi, N. and Mirabbasi, D. [19] study an analytical approach to evaluate the reliability of large-scale, grid-connected PV systems. The fault tree method with an exponential probability distribution function is used to analyze the components of large-scale PV systems that their electrical structure is presented in Figure 18 and number of components per each PV system is showed in Table 9. The system is considered in the various sequential and parallel fault combinations in order to find all realistic ways in which the top or undesired events can occur that the fault tree for the PV system is illustrated in Figure 19 and component failure rates is displayed in Table 10. For the total system reliability calculation and the simulation that use FusselleVesely method, there are 7 PV system sizes that are 100, 200, 500, 1,000, 1,500, 2,000 and 2,500 kW and 11 PV system components that are PV module, string protection, DC switch, inverter, AC circuit breaker, grid protection, AC switch, differential circuit breaker, connector,

battery system, and charge controller are the input dataset. The result of the calculation and simulation is presented in Figure 20 and the ranking of the most critical components appears in Table 11. This approach can be used to ensure secure operation of the system by its flexibility in monitoring system applications.

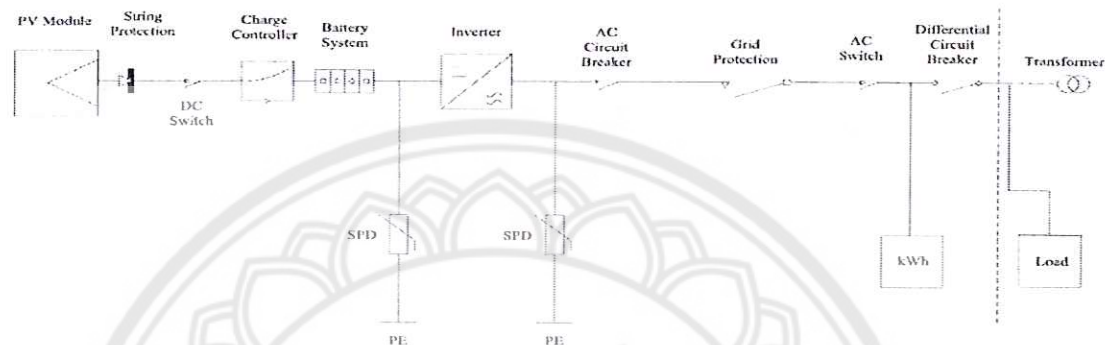


Figure 22 Electrical structure of the large scale PV system

| Power (kW) | 100 | 200 | 500 | 1000 | 1500 | 2000 | 2500 |
|------------------------------|-----|------|------|------|--------|--------|--------|
| PV modules | 437 | 874 | 2166 | 4351 | 6517 | 8702 | 10,868 |
| String protection | 23 | 46 | 114 | 229 | 343 | 458 | 572 |
| DC switch | 3 | 6 | 15 | 27 | 42 | 57 | 72 |
| Inverter | 1 | 2 | 5 | 9 | 14 | 19 | 24 |
| AC circuit breaker | 1 | 2 | 5 | 9 | 14 | 19 | 24 |
| Grid protection | 1 | 1 | 1 | 1 | 1 | 1 | 1 |
| AC switch | 1 | 1 | 1 | 1 | 1 | 1 | 1 |
| Differential circuit breaker | 1 | 1 | 1 | 1 | 1 | 1 | 1 |
| Connector (couple) | 874 | 1748 | 4332 | 8702 | 13,034 | 17,404 | 21,736 |
| Battery system | 16 | 30 | 76 | 150 | 224 | 298 | 372 |
| Charge controller | 1 | 1 | 1 | 1 | 1 | 1 | 1 |

Figure 23 Number of components per each PV system

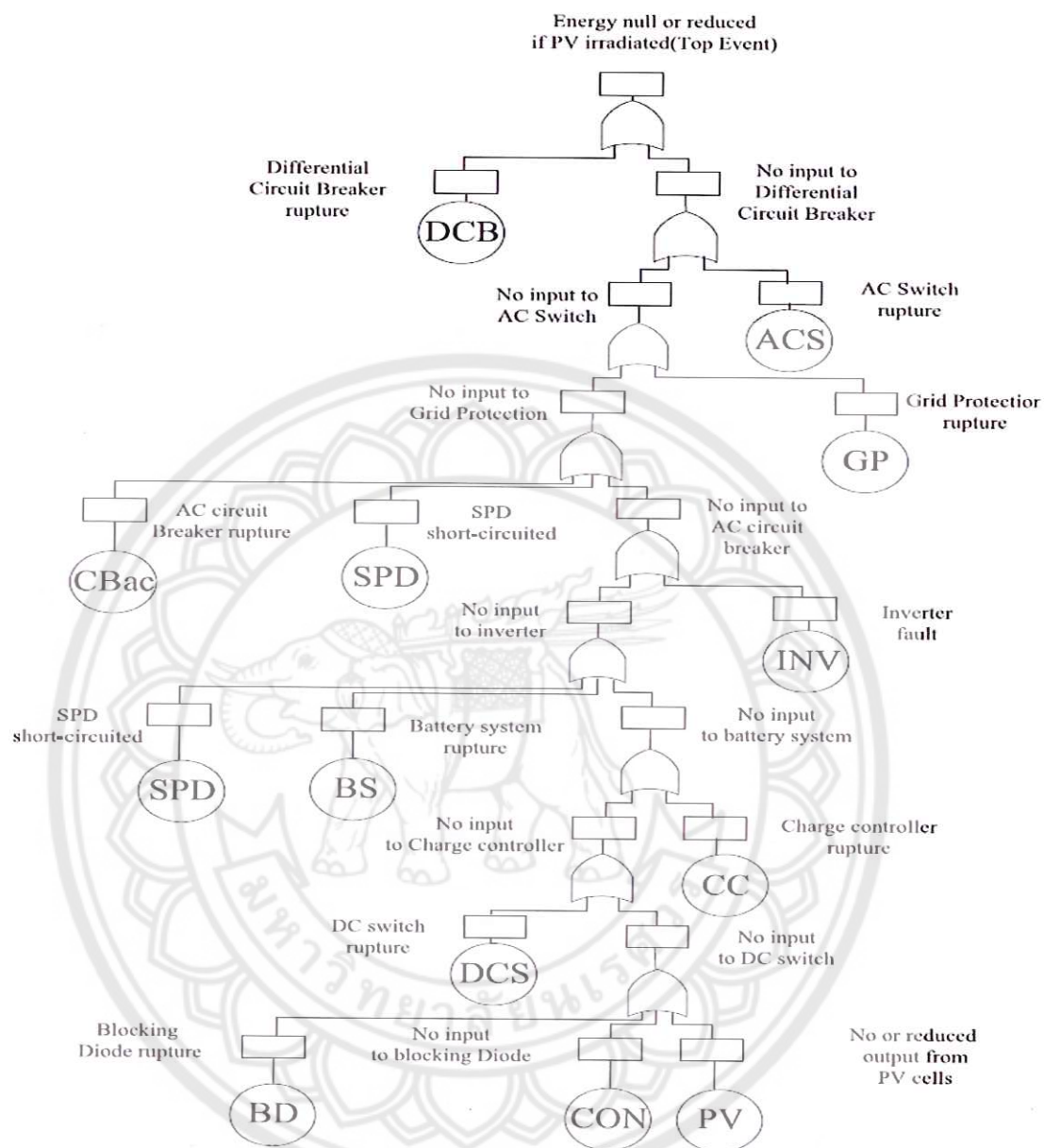


Figure 24 Fault tree for the PV system

| Component | Failure rate (10^{-6} failures h^{-1}) | Reference |
|------------------------------|--|-----------------|
| PV modules | 0.0152 | [18] |
| String protection | 0.313 | [35] Sect. 6-2 |
| DC switch | 0.2 | [35] Sect. 22-1 |
| Inverter | 40.29 | [21] |
| AC circuit breaker | 5.712 | [35] Sect. 14-5 |
| Grid protection | 5.712 | [35] Sect. 14-5 |
| AC switch | 0.034 | [35] Sect. 14-1 |
| Differential circuit breaker | 5.712 | [35] Sect. 14-5 |
| Connector (couple) | 0.00024 | [35] Sect. 17-1 |
| Battery system | 12.89 | [36] |
| Charge controller | 6.44 | [36] |

Figure 25 Component failure rates

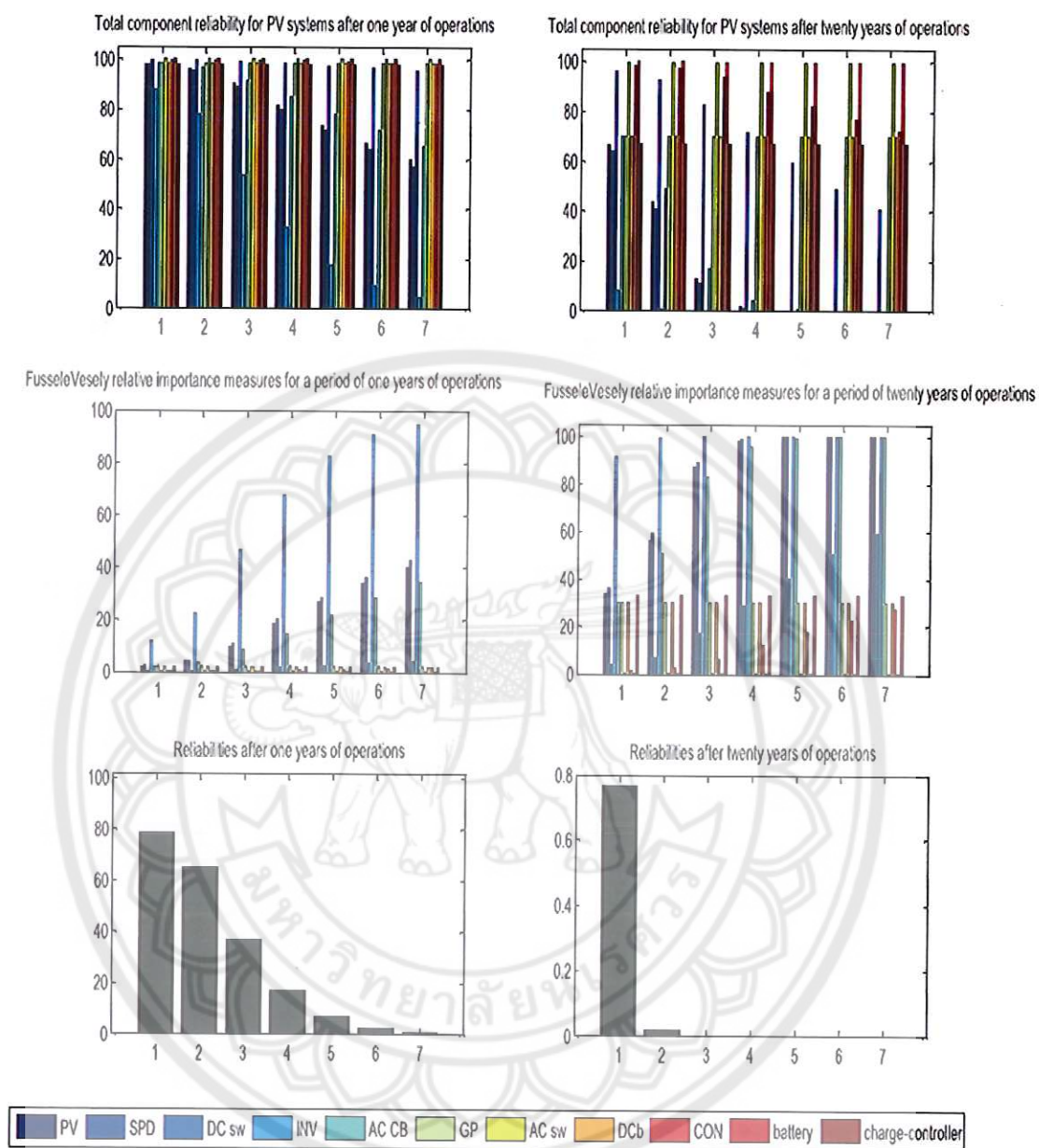


Figure 26 The all results of reliability for seven PV systems

| Priority | Component |
|----------|------------------------------|
| 1 | Inverter |
| 2 | String protection |
| 3 | PV modules |
| 4 | AC circuit breaker |
| 5 | DC switch |
| 6 | Charge controller |
| 7 | Grid protection |
| 7 | Differential circuit breaker |
| 9 | Connector (couple) |
| 10 | AC switch |
| 11 | Battery system |

Figure 27 Critical component priorities

A design tool to study the impact of mission-profile on the reliability of SiC-based PV-inverter devices

Sintamarean, N.C., Wang, H., Blaabjerg, F. and Rimmen, P.de P. [20] introduces a reliability-oriented design tool for a new generation of grid connected PV-inverters that its proposed reliability oriented design structure is presented in Figure 21. The proposed design tool consists of a real field mission profile model (for one year operation in USA-Arizona), a PV-panel model, a grid connected PV-inverter model, an electro-thermal model and the lifetime model of the power semiconductor devices. The PV-system design ratings for simulation model is displayed in Table 12. The simulation model able to consider one year real field operation conditions (solar irradiance and ambient temperature) is developed. Thus, one year estimation of the converter devices thermal loading distribution that illustrated in Figure 22 is achieved and is further used as an input to a lifetime model. The proposed reliability oriented design tool is used to study the impact of MP and device degradation (aging) in the PV-inverter lifetime. In addition, proposed electro-thermal model structure for device junction and case temperature estimation is the key model in device degradation that showed in Figure 23. The obtained results that available in Table 13 indicate that the MP of the field where the PV-inverter is operating has an important impact in the converter lifetime expectation, and it should be considered in the design stage to better optimize the converter design margin. In order to improve the accuracy of the lifetime estimation, it is crucial to consider also the device degradation feedback (in the simulation model) which has an impact of 30% in the precision of the lifetime estimation.

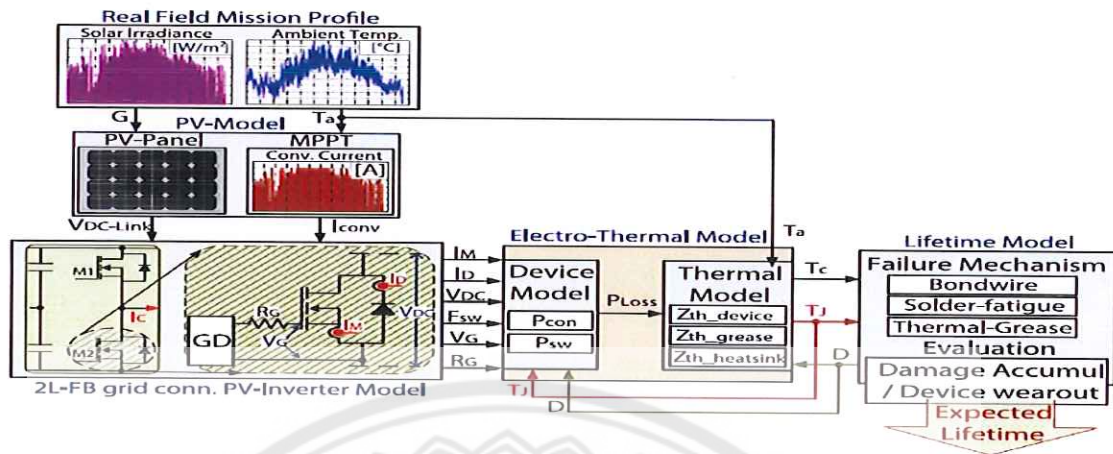


Figure 28 Proposed reliability oriented design structure
for the new generation of grid connected PV-inverters

| | | |
|--------------------------------------|--|---|
| 3L-FB VSI PV-inverter specifications | | |
| Rated power | | $S = 25 \text{ kVA}$ |
| Conv. output phase voltage | | $V_N = 230 \text{ V (RMS) (325 V peak)}$ |
| Max. output current | | $I_{\text{max}} = 37 \text{ A (RMS) (52 A peak)}$ |
| Max. DC-link voltage | | $V_{\text{DC-max}} = 1000 \text{ V}$ |
| Switching frequency | | $f_{\text{sw}} = 50 \text{ kHz}$ |
| Thermal impedance values | | |
| Heatsink | $R_{\text{th}} = 0.13 \text{ (K/W)}$ | $\tau = 570 \text{ (s)}$ |
| Thermal grease | $R_{\text{th}} = 0.0059 \text{ (K/W)}$ | $\tau = 1.3 \text{ (s)}$ |
| LCL-filter parameters | | |
| Parameters | $L_c = 4\text{e-}4 \text{ H}$ | $L_g = 1.5\text{e-}4 \text{ H}$ |
| | | $C_f = 0.4 \text{ }\mu\text{F}$ |
| Device characteristics | | |
| Device type | | CREE MOSFET module (CCS050M12CM2) |
| PV-panel characteristics-connection | | |
| PV-panel type | ET black module (ET-M660250BB) | |
| Conn. type | Series = 24 | Parallel = 3 |

Figure 29 PV-system design ratings

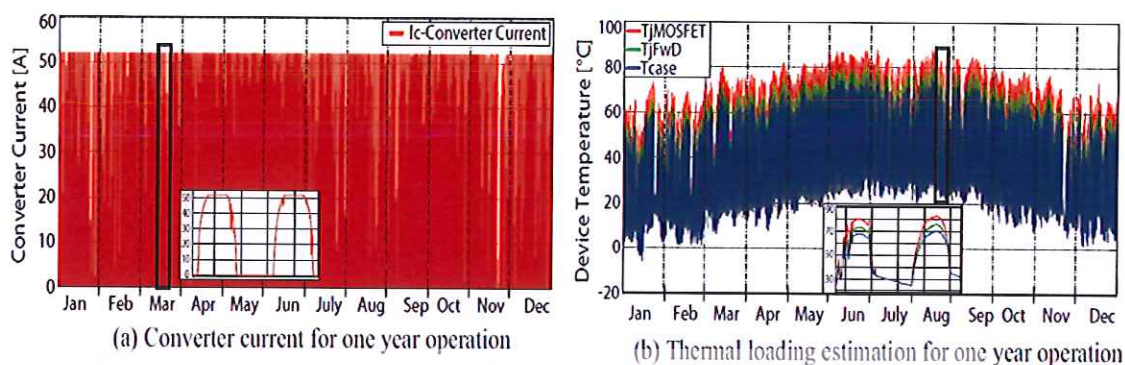


Figure 30 The realistic PV-inverter loading current (a) and thermal loading estimation (b) of the inverter devices (MOSFET, Diode) for one year operation in USA-Arizona.

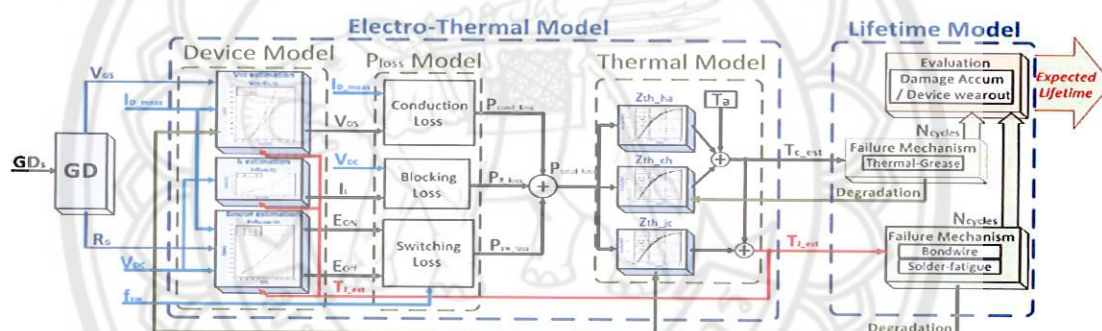


Figure 31 Proposed electro-thermal model structure for device junction and case temperature estimation

| MP | Lifetime | | Degradation impact in lifetime |
|-------------|---------------------|------------------|--------------------------------|
| | Without degradation | With degradation | |
| USA-Arizona | 5.5 (years) | 4.2 (years) | 30% |

Figure 32 MP and device-aging impact in lifetime

Critical components test and reliability issues for Photovoltaic Inverter

Catelani, M., Ciani, L. and Reatti, A. [21] evaluate the behavior of the critical components of a photovoltaic inverter. Normally, the trend of the MTBF (Mean Time Between Failure) vs temperature that presented in Figure 24 is linearly decreased when the temperature increased that confirming the important role in reliability. So, the thermal analysis of the inverter is presented and a series of thermal tests were carried out in order to individuate the most critical components. A 500 kW PV inverter has been subjected to several tests of thermal stress, in a special thermal chamber, to evaluate its operating range in temperature simulating the ventilation conditions of a shelter. From the testes, the first components subject to failure are the DC link capacitors as depicted in Figure 25. To improve the reliability of inverter, derating and redundancy techniques are used and the result of these techniques is showed in Table 14. The example 750 kW power plants with 2 scenarios that are operating 3 of 4 x 250 kW inverter and 14 of 18 x 55 kW inverter are considering for the optimum redundant configuration. It found that MTBF values of the first scenario is 188.395 while the second scenario is 58.912. The scope of such analysis is to optimize the inverter design and therefore its efficiency taking into account the real operative condition that are present when the equipment is installed on the field. Finally, by means of the data obtained with this study correlated with some reliability optimization rules, such as derating and redundancy, it is also possible to improve the maintenance policy of the PV inverter hence its availability and that of the whole PV plant.

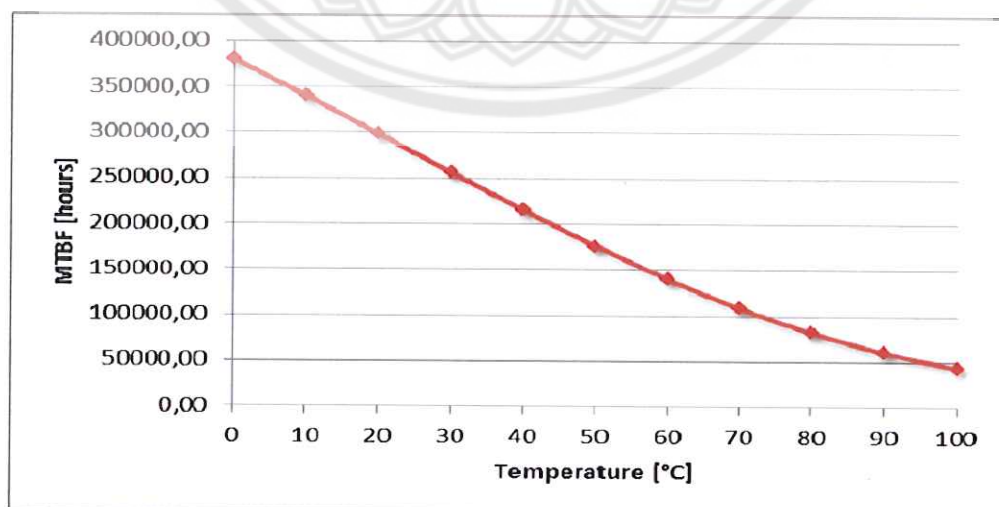


Figure 33 MTBF (Mean Time Between Failure) vs temperature

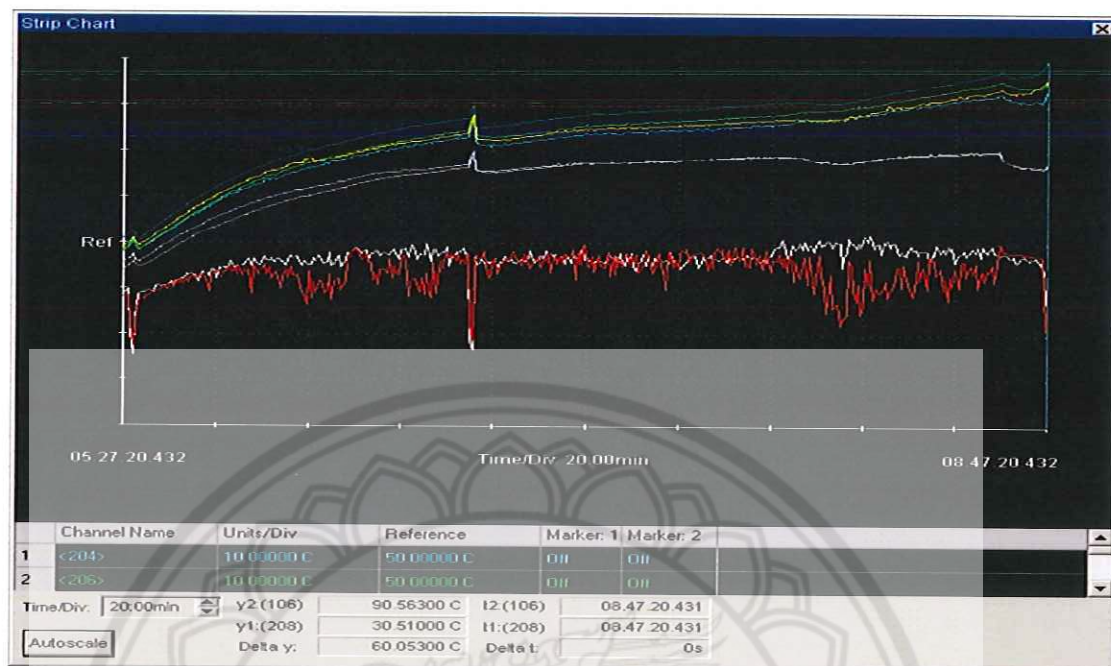


Figure 34 DC link capacitor voltage and chamber temperature trends during destructive test session

| Duty Cycle | Operating hours | MTBF [h] |
|------------|-----------------|----------|
| 40% | 9 | 320.370 |
| 50% | 12 | 256.520 |
| 60% | 15 | 213.891 |
| 75% | 18 | 171.212 |

Figure 35 Duty cycle vs MTBF

Photovoltaic Inverter: Thermal Characterization to Identify Critical Components

Catelani¹, M., Ciani¹, L. and Simoni, E. [22] study the critical components of a photovoltaic inverter from the thermal point of view. Generally, the trend of the MTBF (MeanTime Between Failure) vs temperature is linearly decreased when the temperature is increased while the MTBF versus the system electrical stress is decreased in parabolic curve when the system electrical stress is increased. Normally, the system electrical stress is increasing in the same way with temperature that confirming the important role in reliability. The MTBF vs temperature and system electrical stress is presented in Figure 26. From this reason, the thermal analysis of the inverter is presented and a series

of thermal tests were carried out in order to individuate the most critical components. It found that the most critical components are the DC capacitors and the insulated-gate bipolar

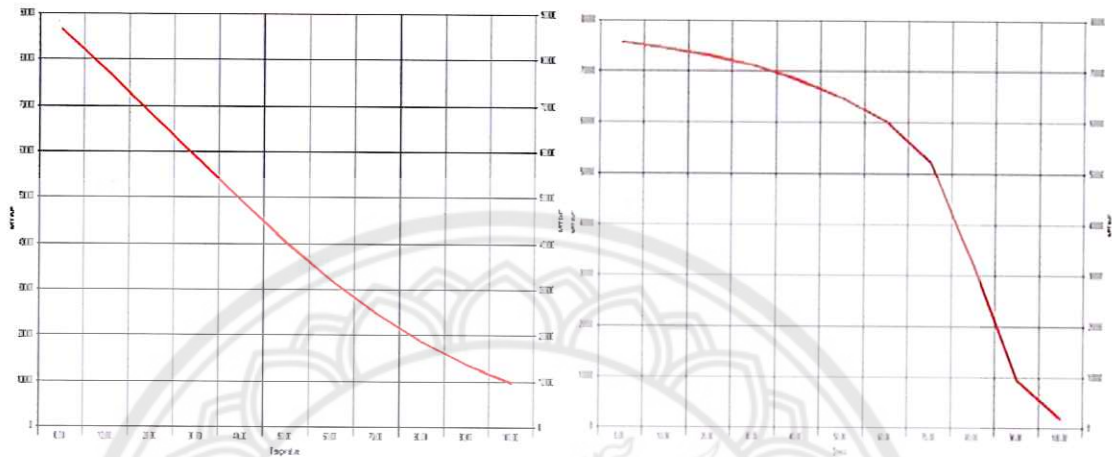


Figure 36 The MTBF vs temperature and system electrical stress

transistors (IGBT). From this point, the measurement set up that showed in Figure 27 is made and the PV inverter under test is powered and functioning during the test. A first thermal test phase was carried out with an internal temperature of the chamber of 50°C. The inverter under test is at the maximum operative temperature with maximum output power in order to put in evidence the behavior of the critical components. From the test, the temperature of IGBTs and DC capacitors are displayed in Figure 28. From the Figure, IGBT temperature is quite stable that no problems are present in the IGBT functioning while DC capacitors is constantly increasing without a stabilization due to an anomalous behaviors of such devices that represents the typical case of an uncorrected functioning of the inverter with the presence of a thermal escape. Moreover, it could leads to a rupture of the device. To solve this problem, the cooling system are designed

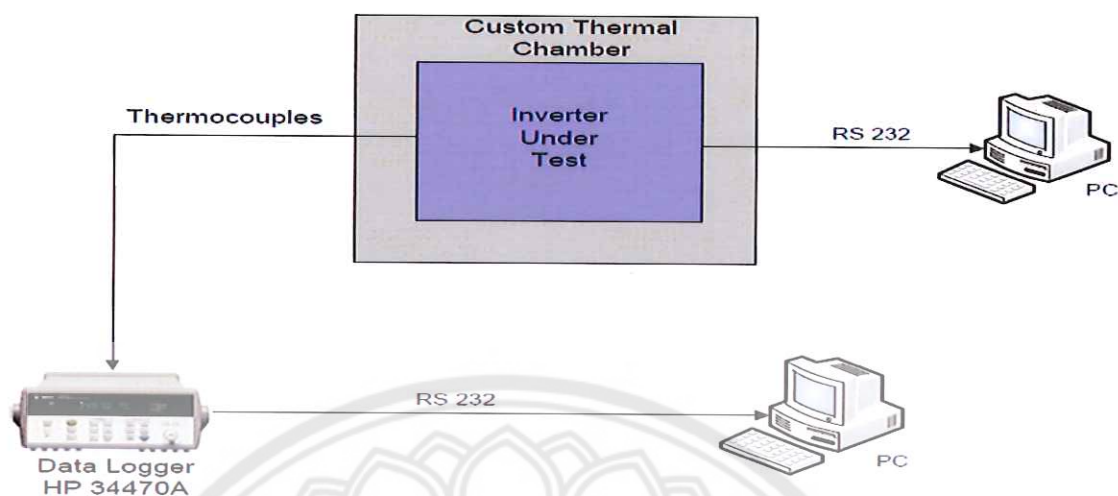


Figure 37 Measurement set-up

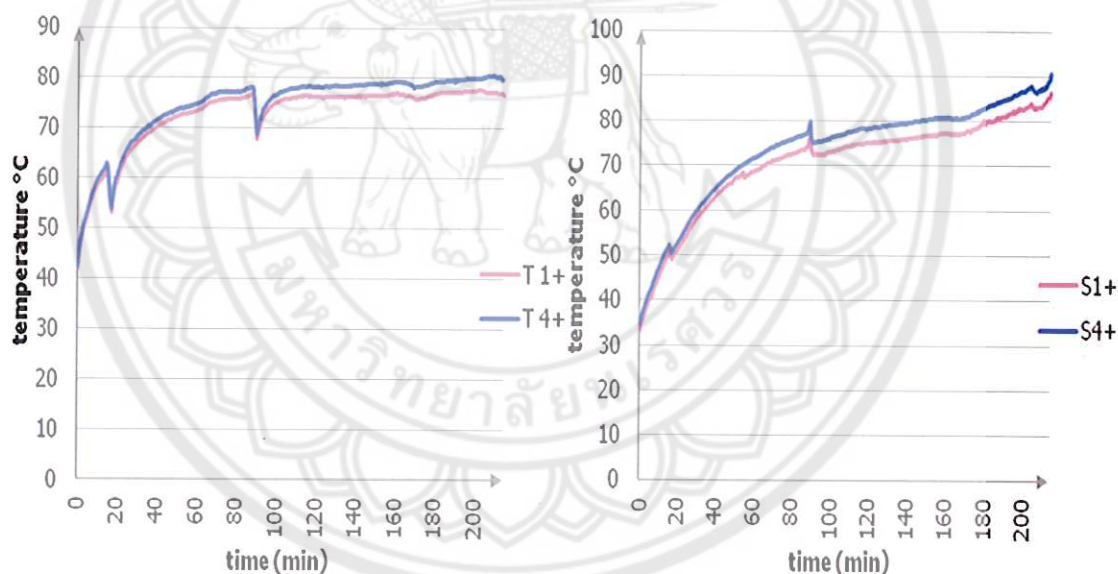


Figure 38 The temperature of IGBTs and DC capacitors

and installed. After that, the inverter is tested again and the temperature of DC capacitors is illustrated in Figure 29 that stabilized below 70 °C. The result of this study is possible to optimize the inverter design and therefore its energy yield taking into account the real operative condition presents when it is installed on the field. In this way, it will be also practicable to optimize the design of the diagnostic system of the PV inverter. Finally,

by means of the data obtained with this study it is also possible to improve the maintenance policy of the PV inverter hence its availability and that of the whole PV plant.

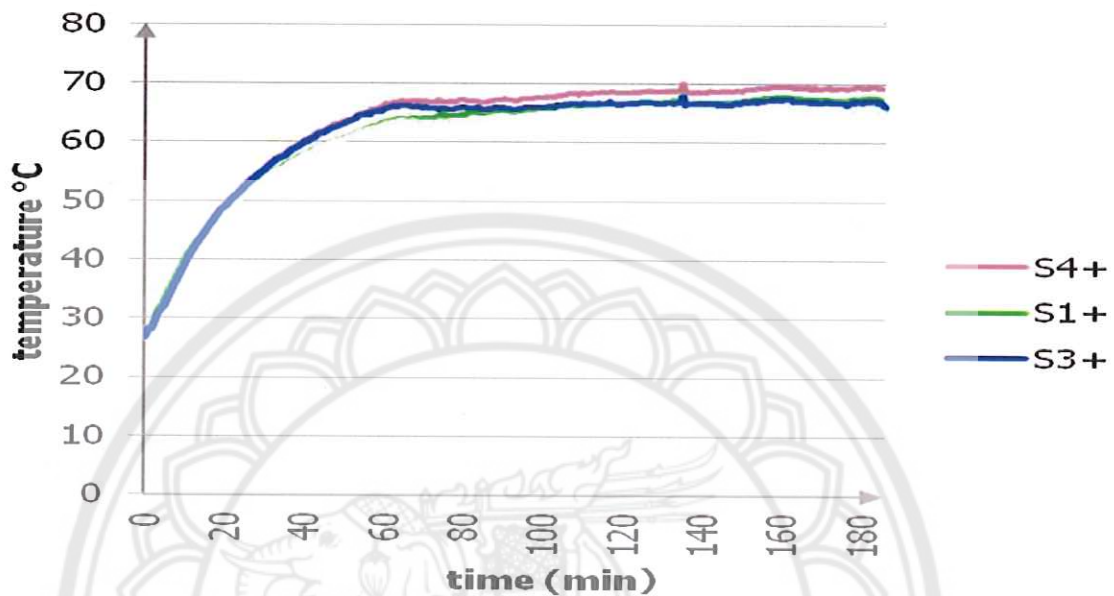


Figure 39 Capacitors temperature vs time after installed cooling system

Assessment of PV system Monitoring Requirement by Consideration of Failure Mode Probability

Pearsall1, N. M. and Atanasiu, B. [23] considers the failure modes that must be addressed by the monitoring, using results from a consultation process within the PV community based on a modified Failure Modes Effects Analysis (FMEA). The first task was to define the failure or loss modes that would be included. An initial list was considered, where delegates discussed the most important modes on the basis of their experience. For most operational problems, the main effect is a reduction in the energy output of the system. The cause of that reduction could be related to a single component or be at the system level. Thus the “failure” modes identified within the FMEA relate mainly to the causes of reduction. Table 15 provides a summary of the 31 modes that were included in the FMEA consultation. They are divided into three sections, A, B and C, relating respectively to module, system and environmental effects. The second task is estimating Risk Priority Number (RPN). The occurrence and severity indices for the different modes are represented in the FMEA and to indicate, where possible, the

information sources used to determine these. In most cases, the index was derived from a combination of actual field experience and expert opinion based on career experience. The two indices were then combined to give the RPN prior to detection. Finally, the RPN were averaged for each failure mode and normalized to provide a measure of the modes with the highest risk of substantial energy losses. The results are presented in Figure 30 and Table 16. Where a variation in either index with system type was indicated, this variation was preserved by calculating an average RPN for each suggested variation. The maximum and minimum values for each mode shown in Figure 30 show the extent of the variation in that mode. Where the two columns are the same height, no variations were suggested by the experts. In Table 16, the conditions under which higher RPN values are obtained for each mode are described. If we consider, the maximum RPN values for all modes, the analysis yields ten modes with RPNs above the average of 0.24. We will consider those ten modes in more detail. Table 17 summarizes the monitoring requirements to address these modes, remembering that the identification of losses is influenced by the frequency of measurement and the frequency with which the measurement data are analyzed. The updated European PV System Monitoring Guidelines will be issued at the end of 2009 for general use by all those with an interest in monitoring systems.

| Mode Ref. | Mode | Explanatory comments and consultation remarks |
|-----------|---|---|
| A01 | Module failure | Faults that lead to short circuit or open circuit failure of the module. Some of the other modes (particularly A04 and A05) can be the cause of this fault. The occurrence probability increases with the number of modules in the system, although the severity at system level decreases. |
| A02 | High level of module performance degradation | Degradation levels above those expected from manufacturer guarantees. The occurrence probability increases with the number of modules in the system. This would tend to occur for groups of modules rather than single modules where the cause is packaging, environment or manufacturing faults. |
| A03 | Broken or cracked cells; broken or cracked module glass | The occurrence probability increases with the number of modules in the system. Broken glass may not lead to electrical losses at least in the first instance, whereas broken cells are more problematic, so future analyses should separate these two modes. |
| A04 | Module junction box damage or fault | No comments. |
| A05 | Hot spot damage to module | No comments. |
| A06 | High module operating temperature | Where this is due to mounting/ventilation issues. |
| A07 | Bypass diode failure | No comments. |
| A08 | String failure | No comments. |
| B01 | Inverter failure | Faults that lead to complete shutdown of the inverter. Some of the other modes (particularly B09) can be the cause of this fault. The occurrence probability increases with the number of inverters in the system, although the severity at system level decreases. |
| B02 | Low inverter efficiency | Values that are substantially below the predicted value for the system design |
| B03 | Low MPP tracking efficiency | No comments. |
| B04 | Faulty circuit breakers or switches | Faulty or blown fuses should be explicitly included in this mode. |
| B05 | Damaged or faulty cabling | No comments. |
| B06 | Earthing or insulation faults | It was suggested that these are two separate faults, with earthing issues being considered at installation and insulation faults occurring during operation. |
| B07 | Array/inverter mismatch, incorrect sizing | Resulting in lower yield and efficiency than predicted |
| B08 | Accidental switch off of inverter | Prolonged disconnection but no technical faults |
| B09 | Overheating of inverter | May be the cause of an inverter failure (B01) |
| B10 | Fluctuation of grid specifications | Very dependent on local grid and load conditions. |
| B11 | Corrosion of contacts, connections | No comments. |
| B12 | Battery failure | No comments. |
| B13 | Poor charge controller performance | May lead to battery failure (B12) if not addressed. |
| B14 | Overheating of battery | May lead to battery failure (B12) if not addressed |
| B15 | Overconsumption (stand alone system) | System load levels substantially above design values. It was noted that this mode could be the cause of B12 (battery failure). |
| B16 | Damage from electrical arcing | The severity is very dependent on the location of the arcing damage, the system configuration and the potential for further damage from any fire risk. |
| C01 | Array shading | Additional to that accounted for in the system design. During operation, the most likely increase in shading will come from the growth of vegetation |
| C02 | Accumulation of dirt/snow/ice (requiring intervention) | No comments. |
| C03 | Lightning strikes, lightning induced damage | No comments. |
| C04 | Component damage due to extreme weather conditions | No comments. |
| C05 | Component damage due to animals, insects etc. | No comments. |
| C06 | Component damage due to vandalism | Deliberate damage to any part of the system |
| C07 | Theft of components | Leading to reduction in output. The severity is directly dependent on the nature of the theft and ranges from a few percentage points to loss of the whole system. Small systems in unmanned locations are more vulnerable to theft. |

Figure 40 Summary of failure/loss modes included in the FMEA

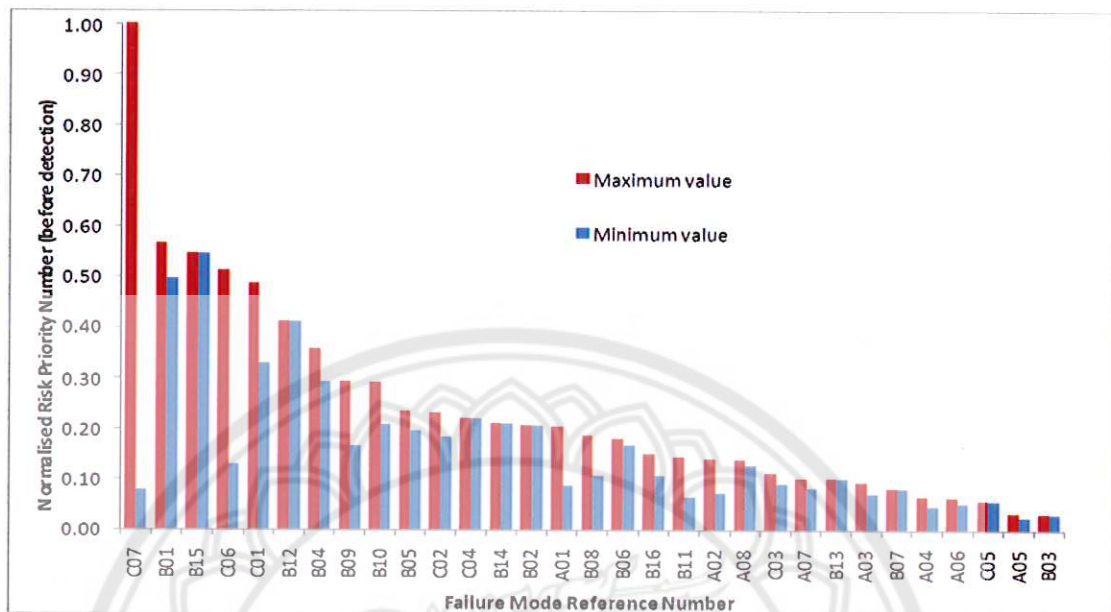


Figure 41 Normalised average RPN values for the 31 failure modes presented in descending order of maximum value. The two columns represent the maximum and minimum values obtained for that mode

| Mode Ref. No. | Mode | Higher RPN values assigned for: |
|---------------|---|---|
| A01 | Module failure | Large systems (>1MW) due to number of modules, concentrator systems due to thermal stress |
| A02 | High level of module performance degradation | Thin film compound technology (although noted that this is packaging dependent), hot and humid climates |
| A03 | Broken or cracked cells; broken or cracked module glass | Large systems (>1MW) due to number of modules, systems prone to vandalism |
| A04 | Module junction box damage or fault | Small and island systems due to the low number of strings |
| A05 | Hot spot damage to module | Slight increase for open circuit failure mode |
| A06 | High module operating temperature | BIPV systems, concentrator systems |
| A07 | Bypass diode failure | Small and island systems |
| A08 | String failure | Small systems due to the low number of strings |
| B01 | Inverter failure | Small increase in severity for small and island systems due to low number of inverters in system |
| B04 | Faulty circuit breakers or switches | Small and island systems |
| B05 | Damaged or faulty cabling | Small and island systems |
| B06 | Earthing or insulation faults | Locations with high humidity |
| B08 | Accidental switch off of inverter | Small and island systems |
| B09 | Overheating of inverter | Small, residential systems, island systems |
| B10 | Fluctuation of grid specifications | Locations with weak electrical grids |
| B11 | Corrosion of contacts, connections | Island systems |
| B16 | Damage from electrical arcing | Residential systems |
| C01 | Array shading | Residential systems, rural locations |
| C02 | Accumulation of dirt/snow/ice (requiring intervention) | Humid environment, concentrator systems |
| C03 | Lightning strikes, lightning induced damage | Locations with high frequency of strikes |
| C06 | Component damage due to vandalism | Urban systems, facade systems |
| C07 | Theft of components | Remote systems, unmanned systems |

Figure 42 Categorization of variations in RPN provided by the respondents to the consultation. The variations result in a change in one or both of the occurrence or severity index assigned and thus the resulting RPN value

| Mode Ref. | Mode Name | Measurements required to identify | Description of analysis | Frequency aspects | Other modes addressed by the same monitoring action |
|-----------|--------------------------------------|---|---|--|--|
| C07 | Theft of components | System output Visual inspection (manual or CCTV) | Problem indicated by reduced or zero output. Identification as theft needs further checks including visual inspection. | For high risk locations, regular visual checks may be advisable. Frequency of output data analysis likely to be dictated by other actions. | CCTV or other visual checks also address C06 and to a lesser extent C04 and C05. |
| B01 | Inverter failure | System output | Periodic check of system output – identification of cause of failure will require additional measurements and analyses. | Frequency of output analysis depends on system size but also likely to be defined by analysis requirements for other modes. | B08 (inverter switch off). |
| B15 | Overconsumption (stand alone system) | Battery index Availability to load Total system loads | Comparison of seasonal variation of battery index with expectation. Check with calculation of total system loads. | Frequency depends on the load variation and climate since the battery index will vary with season. This fault is also characterised by repeated non-availability of power. | Persistently low battery indices may be a precursor to B12 (battery failure) or indicate poor controller performance (B13). |
| C06 | Component damage due to vandalism | System output Visual inspection – manual or CCTV | Problem indicated by reduced or zero output. Identification as vandalism needs further checks including visual inspection. | For high risk locations, regular visual checks may be advisable. Frequency of output analysis likely to be dictated by other actions. | CCTV or other visual checks also address C07 and to a lesser extent C04 and C05. |
| C01 | Array shading | System output In-plane irradiance | Problem indicated by output variation not matching that of irradiance and by variation of effect with time and season. Can be confirmed by visual inspection. | Need to observe variation across the day – data intervals of not less than 10 minute averages recommended in most cases. Daily data need to be stored to allow sequential investigation. | A06 (partially), B03, B07, C02, B01, B08 and all other modes that rely on system output measurement at longer intervals. B09 and B10 if resolution allows inverter shutdowns to be observed. |
| B12 | Battery failure | System output Availability to load Battery capacity, battery voltage | Usually identified by a major reduction in system availability. May be characterised by capacity and voltage measurements. | Analysis of battery index may allow prevention of failure. Otherwise, analysis would be undertaken once fault is observed. | Related to B13 and B15 in terms of cause of the failure. |
| B04 | Faulty circuit breakers or switches | System output over time. | Fault identified by reduced or zero output. If available, string comparisons will help to identify problem. Further investigation needed to establish failure mode. | Frequency of analysis of system outputs dependent on the loss levels to be identified. Higher frequency for large systems. | All modes identified by sustained reduced output over a variety of operating conditions (A08, B05, B06, B11, B16, C03 – C07) |
| B09 | Overheating of inverter | Inverter operating period, inverter output, ambient or inverter temperature | Problem indicated by reduced output from inverter when temperature is high. Cause can be inferred from daily plots of variables and further analysis. | Similar data intervals to C01 and B10, with specific checks carried out during periods of hot weather. | See response to C01. |
| B10 | Fluctuation of grid specifications | Inverter output, irradiance, grid voltage and frequency (possible) | Problem indicated by output variation not matching that of irradiance and by periods of very low inverter output. Can be confirmed by inverter records of grid specifications if available. | Similar data intervals to C01 and B09, but required to show short term inverter drop-outs. Intervals of no more than 5 minutes recommended for average values, with sampling at no more than 1 minute intervals. | See response to C01. |
| B05 | Damaged or faulty cabling | System output over time. | Fault identified by reduced or zero output. If available, string comparisons will help to identify problem. Further investigation needed to establish failure mode. | Frequency of analysis of system outputs dependent on the loss levels to be identified. Higher frequency for large systems. | All modes identified by sustained reduced output over a variety of operating conditions (A08, B04, B06, B11, B16, C03 – C07) |

Figure 43 Summary of monitoring requirements for 10 modes with the highest derived RPN

Diagnostic architecture: A procedure based on the analysis of the failure causes applied to photovoltaic plants

Cristaldi, L., Faifer, M., Lazzaroni, M., Khalil, M.M.A.F., Catelani, M. and Ciani, L. [24] Analyze the failure modes and causes and diagnostic architectures for grid-connected photovoltaic system with one main inverter that presented in Figure 31. The PV power plant is possible separated into 3 main subsystems, photovoltaic modules connected in series and parallel, power conditioning subsystem that includes inverters and BOS (Balance Of System) subsystem that is composed by generator and module junction box, solar cable connectors, fuses, DC and AC wires, DC and AC switches. The failure modes of PV module can be classified in 6 modes that are encapsulation failures from discoloration and delamination, module corrosion failures from deterioration, broken interconnection and solder buses failures from thermal expansion and contraction or repeated mechanical stress, cells cracking failures from mechanical loads due to wind (pressure and vibrations) and snow (pressure), dust failures from different transmittance of light, and hot-spots failures from PV cell high temperature. The inverter failures can be classified into three major categories: manufacturing and inadequate design problems, control problems and electrical components failures. The failures of BOS components are considered the major reason behind the presence of non-producing modules in PV field. In fact, for these plants, high level of reliability is necessary in order to operate, without failures, in the time taking into consideration also the typical lifetime of these plants. To this aim the monitoring of both plant parameters and plant performances is a very important task that can be obtained, by means of a well-designed diagnostic and monitoring system. The smart monitoring of PV plants must be able to carry out the necessary performance measurements, evaluate the ageing of PV panels and early detect the possible failures previously described. Figure 32 shows a possible schematics diagram of the PV system smart performance monitoring that can be detected as reported the failure modes in the Table 18. The experimental activity

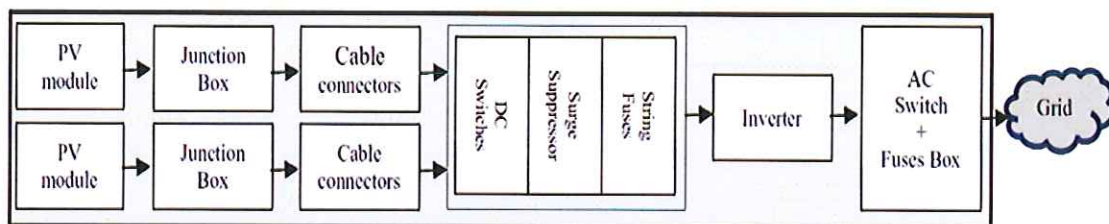


Figure 44 Simplified schematic diagram of photovoltaic plant

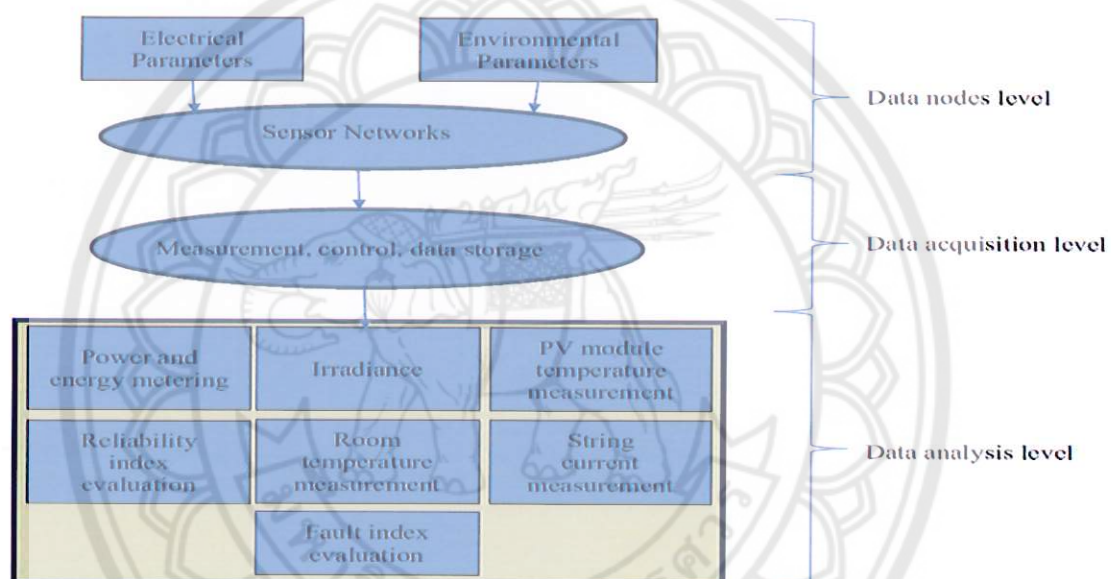


Figure 45 PV smart monitoring system

| Failure mode | Detectability | Requirement |
|--|--|--|
| Encapsulation | MPP value of the PV panel is below the value given by the model. Output of the other PV panels are good. We can compare the actual and model MPP | The PV panels have to be clean |
| Module corrosion | Model approach: a comparison between the value assigned to the series resistance during the characterization of the PV panel and the value estimated by means of the model | This failure mode can be detected only if the model algorithm allows to evaluate the parameter of the electrical model |
| Cells cracking | Model approach: open circuit voltage decrease so we have to compare the value obtained by the actual characteristic with the value given by the model | I-V curve has to be obtained by means an electronic load |
| Dust | It can be detected comparing the actual and model MPP. All PV panels of the string show the same problem | An algorithm that compares all the MPPs value |
| PV inverter: general failure | | If the plant has centralized or string inverter, the data base alarms has to be read by the monitoring system |
| BOS 1. Theft 2. Broken fuse 3. Broken cable | No string current | The three failure mode can be detected by means of devoted sensors |

Figure 46 Failure modes detection strategies

has been implemented by using a sun simulator and a test chamber. The acquired data have been obtained by a 5 W_p PV panel operating at about 25 °C. Table 19 reports the experimental data obtained by testing 10 PV panels. For each PV panel the MPP value has been obtained in two different conditions: first the PV panels have been tested when new or as good as new and carefully clean, second the same PV panels have been tested after a certain number of days during which they were exposed to the weather conditions according to a pattern reported in the last column of Table 19. This approach allows to improve complex system maintenance policies and, at the same time, to achieve a reduction of unexpected failure occurrences in the most critical components.

| # PV panel | MP considered for new PV (W) | MP considered for used PV (W) | Test conditions | Conditions classification (see Fig. 7) |
|------------|------------------------------|-------------------------------|------------------------------|--|
| 1 | 0.474 | 0.457 | Horizontal, no rain, 34 days | Increasing level ↑ |
| 2 | 0.471 | 0.443 | Horizontal, no rain, 34 days | |
| 3 | 0.448 | 0.418 | Horizontal, no rain, 34 days | |
| 4 | 0.467 | 0.455 | Horizontal, rain, 34 days | |
| 5 | 0.468 | 0.438 | Horizontal, rain, 34 days | |
| 6 | 0.506 | 0.489 | 30°, rain, 24 days | |
| 7 | 0.470 | 0.454 | 30°, rain, 24 days | |
| 8 | 0.474 | 0.456 | Horizontal, rain, 21 days | |
| 9 | 0.478 | 0.466 | Horizontal, no rain, 21 days | |
| 10 | 0.505 | 0.494 | Horizontal, no rain, 21 days | |

Figure 47 Results of the measurements performed during the test period

Reliability Performance Assessment in Modeling Photovoltaic Networks

Tonj, G. and Tonj, D.G. [25] present the reliability analysis of switched mode power converters estimating distribution parameters of different phases for PV useful-life period. The first step in analyzing the reliability is representing the system by an equivalent reliability block diagram (RBD) for the first level of detail to study the estimated reliability for typical PV system as represented in Figure33. In the reliability block diagram was taken into account the next parts of the PV system: The PV array (1), the PV array circuit combiner (2), the

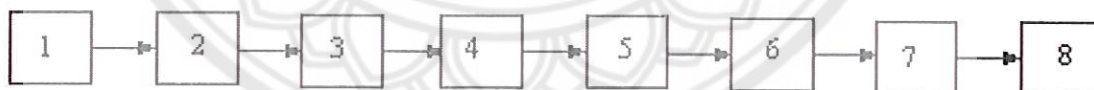


Figure 48 Reliability Block Diagram for a photovoltaic system

| PV system | Weibull parameters | | Correlation coefficient |
|---------------------------|--------------------|--------|-------------------------|
| | β | η | |
| PV array | 1.0783 | 1.0323 | 0.9632 |
| PV array circuit combiner | 1.0642 | 1.0215 | 0.9752 |
| Ground fault protector | 1.0564 | 1.0367 | 0.9748 |
| DC fuse switch | 1.0647 | 1.0204 | 0.9468 |
| AC/DC inverter | 1.0539 | 1.0194 | 0.9735 |
| AC fuse switch | 1.0745 | 1.0245 | 0.9784 |
| Utility switch | 1.0578 | 1.0576 | 0.9687 |
| Main service panel | 1.0739 | 1.0781 | 0.9877 |

Figure 49 The Weibull parameters values

ground fault protector (3), the DC fuse switch (4), AC/DC inverter (5), the AC fuse switch (6), the utility switch (7), the main service panel (8). It must be mentioned that the AC/DC inverter (5) and the main service panel (8) were considered separately because there were many cases when just one of them was damaged. If the resulting system level failures are used to extract Weibull distribution parameters, assuming that all failures are caused to only one failure mode, significant errors may be introduced. For the analyzed PV system it was calculated the empiric reliabilities which was compared with the reliabilities obtained using the analytical method. The parameter values and the correlation coefficients for each case are presented in Table 20. The values of Weibull parameters correspond the high values of the correlation coefficient. The analytical curve based on the parameters values were determined using the regression analysis and plotted in the Figure 34. From the Figure, the total reliability highly decrease after approximately 15.5 years of working of the PV system. From the analyzing, the initial failures are generally the result of manufacturing errors that are not caught in inspection prior to burn-in or placing in service. Failures resulting from time/stress dependent errors may occur in this period. Random failures and wear out failures are generally a factor of design. Wear out of mechanical parts also begins the moment the product is put into service. Photovoltaic (PV) energy system is assumed to work without interruptions over its entire life. In PV systems, the inverter is responsible

for the majority of failures, and most inverter failures are blamed on the aluminum electrolytic capacitors typically used in the dc bus.

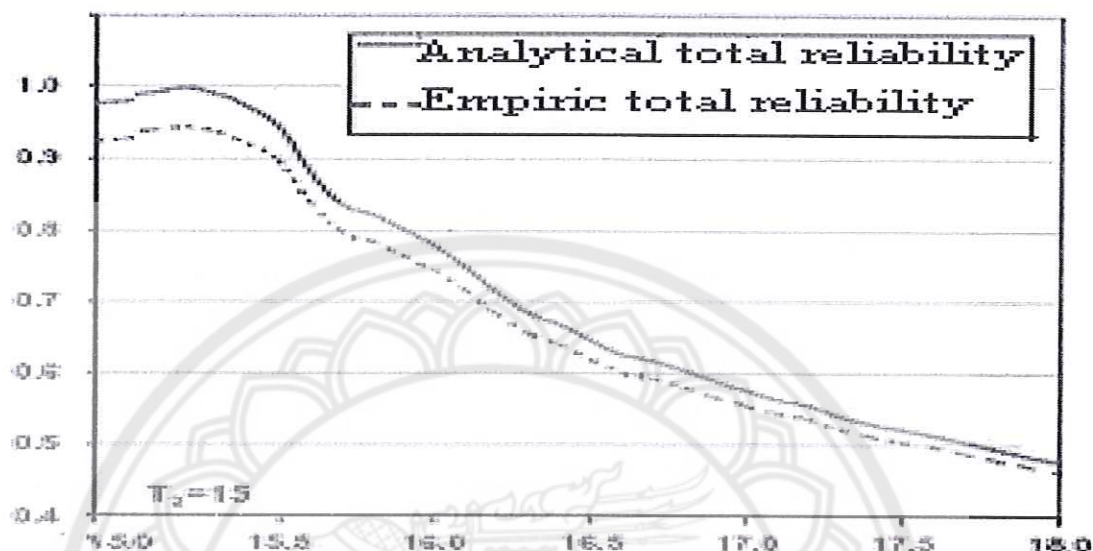


Figure 50 The total reliability of the PV system: 1- empiric total reliability; 2 – analytical total reliability

Information-based reliability weighting for failure mode prioritization in photovoltaic (PV) module design

Francis, R. and Colli, A. [26] present the prioritization of PV failure modes extending Colli using a Shannon information-weighted reliability approach is demonstrated. We call this information-weight the surprise index that developed for used within FMEA worksheets. The surprise index approach facilitates the prioritization of failure modes by weighting the consequence of their failures by the information in the failure generation model. In our case study, we modify FMEA data to compute the SI for a research solar PV array. The FMEA severity, occurrence and detection classifications are given in Table 21. The system under consideration is presented in Figure 35, consists of PV modules, racks, cables, string combiners, and power conditioning units. The DC and AC systems on both sides of the inverter unit are considered. Table 22 shows a portion of the FMEA worksheet for the PV modules, in particular considering crystalline silicon PV technologies. This table gives the severity, likelihood, and detection ratings for each failure mode considered, while Table 23 indicates the probabilities considered and the information scores for use

in computing the SI. Table 2 4 finally indicates the comparison between the SIs and RPNs. Notice that while some rankings are similar for both the SI and the RPN, some of the rankings are quite different. This evaluation highlights a couple of aspects. First, by using fairly broad likelihood categories, differences in failure mode probabilities over several orders of magnitude Table 21 FMEA severity and likelihood classifications used to calculate the RPN. Note that the RPN ranges from 1 to 125 in this application

| Severity ranking criteria | |
|-----------------------------|---|
| Rank | Description |
| 1 | Minor failure/degradation, hardly detected, no influence on the system performance. |
| 2 | Failure/degradation will be detected by plant owner/operator and/or will cause slight deterioration of parts or system performance. |
| 3 | Failure/degradation will be detected by plant owner/operator, will create dissatisfaction, and/or will cause deterioration of parts or system performance. |
| 4 | Failure/degradation will be easily detected by plant owner/operator, will create high dissatisfaction, and/or will cause extended deterioration of parts and system relevant non-functionality/loss of performance. |
| 5 | Failure/degradation will result in non-operation of the system or severe loss of performance. |
| Occurrence ranking criteria | |
| 1 | Unlikely - failure rate per unit-hour in the order of E-7 |
| 2 | Remote probability - failure rate per unit-hour in the order of E-6 |
| 3 | Occasional probability - failure rate per unit-hour in the order of E-5 |
| 4 | Moderate probability - failure rate per unit-hour in the order of E-4 |
| 5 | High probability - failure rate per unit-hour in the order of E-3 and E-2 |
| Detection ranking criteria | |
| 1 | Almost certain that the problem will be detected (chance 81-100 %) |
| 2 | High probability that the problem will be detected (chance 61-80 %) |
| 3 | Moderate probability that the problem will be detected (chance 41-60 %) |
| 4 | Low probability that the problem will be detected (chance 21-40 %) |
| 5 | None/minimal probability that the problem will be detected (chance 0-20 %) |

Figure 51 FMEA severity and likelihood classifications used to calculate the RPN. Note that the RPN ranges from 1 to 125 in this application

may be obscured. But the failure modes that may require special attention for contingency planning may have been overlooked if relying only on the RPN. The selected units may lead to reduced deliberation over contingency planning for highly unlikely, yet quite severe failures simply because of the qualitative scale selected. The objective of proper scoring is to improve the sensitivity and specificity of expert judgments by rewarding expert predictions that are both risky and correct. The surprise index may potentially aid in systematic evaluation of deep uncertainties in PV module design, as failure modes that might be overlooked using traditional PRA may be addressed using the information-based approach.

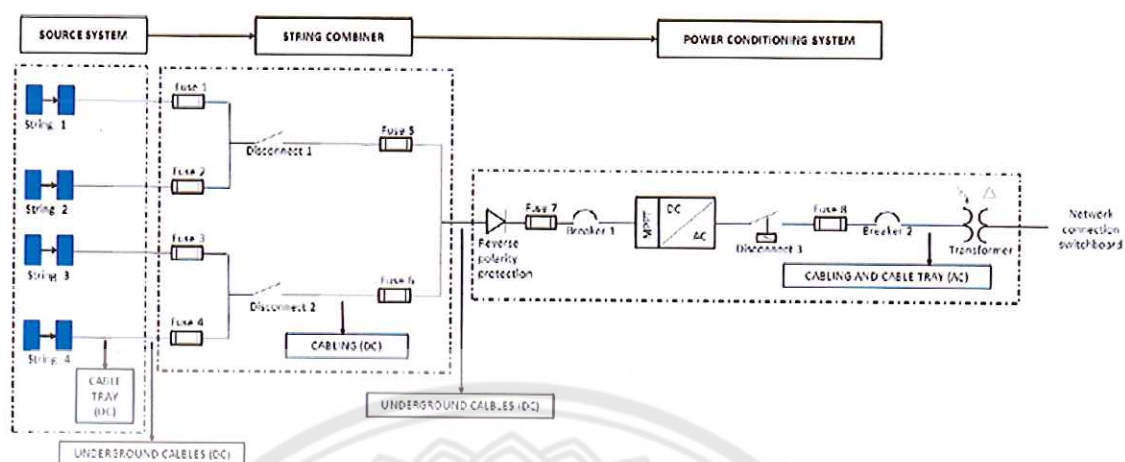


Figure 52 Simplified photovoltaic system model with the principal components of the BNL's NSERC PV array

| Sub-component | Function or Process | Potential Failure Mode | Potential Effects | Potential Causes | Severity Rating | Occurrence Rating | Detection Rating |
|---|----------------------|---------------------------------|---|--|-----------------|-------------------|------------------|
| Module (active components - cells and contacts) | Electric connections | Loss of electric function | No energy output, safety, fire | Shorts, arcs, open contacts. | 5 | 2 | 3 |
| | | Impairment of electric function | Reduced energy output, hot spot damage | High series resistance, low shunt resistance, aging, shading, soiling. | 4 | 2 | 4 |
| Junction box/bypass diode | Electric connections | Open contacts | No energy output | Disconnections, improper installation, corrosion | 5 | 1 | 3 |
| | | Short, arc in contacts | No energy output, safety, thermal damages, fire | Damaged insulation, aging, animals, lightning | 5 | 1 | 2 |
| | | Poor contact/intermittent | Reduced energy output, no energy output, thermal damage | Material defects, oxidation, aging | 4 | 1 | 4 |
| | | Shorted diode (end-to-end) | Reduced energy output, loss of module power | Material defects, aging, thermal stress, mechanical stress, electrical stress, contamination, processing anomaly | 4 | 1 | 4 |
| | | Open diode | Reduced energy output, thermal damages in module, fire, safety | Very high resistance, material defects | 3 | 1 | 5 |
| | | Parameter change in diode | Reduced energy output, improper intervention | Material defects, aging, continuous thermal stress | 3 | 1 | 5 |
| Connectors | Electric connections | Open | No energy output | Damage, disconnection, animals, vandalism, strong wind, pulled cables | 5 | 1 | 2 |
| | | Poor contact/intermittent | Reduced energy output, no energy output, thermal damage | Corrosion, improper installation, lightning damage | 5 | 1 | 4 |
| | | Short | No energy output, safety, thermal damages, fire | Damages, improper installation, disconnections, animals, vandalism | 4 | 1 | 5 |
| Encapsulation | Encapsulation | Loss of air tightness | Humidity/ water/ contaminant entrance, increased degradation, reduced energy output, no energy output | Bad lamination, high voltage stress, hot spots, high cell/module temperature, corrosive effects in the module structure, aging, damage from frame distortion, cleaning actions, extreme wind, snow load, vandalism, animals, lightning, earthquake, accidental impacts | 2 | 2 | 5 |

Figure 53 FMEA Worksheet excerpt for case study PV modules

| Sub-component | Function/Process | Potential Failure Mode | Considered probability | Information Score |
|---|----------------------|---------------------------------|------------------------|-------------------|
| Module (active components - cells and contacts) | Electric connections | Loss of electric function | 1.35E-06 | 14 |
| | | Impairment of electric function | 1.35E-06 | 14 |
| Junction box/bypass diode | Electric connections | Open contacts | 4.51E-07 | 15 |
| | | Short, arc in contacts | 4.51E-07 | 15 |
| | | Poor contact/intermittent | 4.51E-07 | 15 |
| | | Shorted diode (end-to-end) | 2.26E-07 | 15 |
| | | Open diode | 2.26E-07 | 15 |
| | | Parameter change in diode | 2.26E-07 | 15 |
| Connectors | Electric connections | Open | 4.51E-07 | 15 |
| | | Poor contact/intermittent | 4.51E-07 | 15 |
| | | Short | 4.51E-07 | 15 |
| Encapsulation | Encapsulation | Loss of air tightness | 4.06E-06 | 12 |

Figure 54 Information score for PV module failure modes

| Sub-component | Function/Process | Potential Failure Mode | Surprise Index | Risk Priority Number | SI Ranking | RPN Ranking |
|---|----------------------|---------------------------------|----------------|----------------------|------------|-------------|
| Module (active components - cells and contacts) | Electric connections | Loss of electric function | 203 | 30 | 9 | 2 |
| | | Impairment of electric function | 216 | 32 | 8 | 1 |
| Junction box/bypass diode | Electric connections | Open contacts | 219 | 15 | 7 | 8 |
| | | Short, arc in contacts | 146 | 10 | 10 | 11 |
| | | Poor contact/intermittent | 234 | 16 | 4 | 6 |
| | | Shorted diode (end-to-end) | 245 | 16 | 3 | 6 |
| | | Open diode | 230 | 15 | 5 | 8 |
| | | Parameter change in diode | 230 | 15 | 5 | 8 |
| Connectors | Electric connections | Open | 146 | 10 | 10 | 11 |
| | | Poor contact/intermittent | 292 | 20 | 1 | 3 |
| | | Short | 292 | 20 | 1 | 3 |
| Encapsulation | Encapsulation | Loss of air tightness | 124 | 20 | 12 | 3 |

Figure 55 Comparison of surprise index and risk priority number for PV module sub components

Performance and degradation analysis for long term reliability of solar photovoltaic systems

Sharma, V. and Chandel, S.S. [27] review the performance and degradation analysis studies of solar photovoltaic modules, accelerated aging testing under laboratory and outdoor field testing conditions. The factors affecting the performance of PV module are PV cell technologies, ambient temperature, solar irradiation, tilt

| Degradation mechanism | Stress factor | | | | | Accelerated stress test |
|---|------------------|----------|-----------------|----|--------------|-----------------------------------|
| | High temperature | Moisture | Thermal cycling | UV | High voltage | |
| Broken interconnect | ✓ | ✓ | | | ✓ | Thermal cycle |
| Broken cell | ✓ | | | | ✓ | |
| Solder bond failures | ✓ | ✓ | ✓ | | ✓ | |
| Junction box failure | ✓ | ✓ | | | | Damp heat exposure |
| Open circuits leading to Arcing | ✓ | | | | ✓ | |
| Corrosion | ✓ | ✓ | | | ✓ | |
| Delamination of encapsulant | ✓ | ✓ | ✓ | ✓ | ✓ | Humidity freeze |
| Encapsulant loss of adhesion and elasticity | ✓ | ✓ | ✓ | | ✓ | |
| Encapsulant discoloration | ✓ | | | ✓ | | |
| Hot spots | ✓ | | | | | Hot spot test |
| Shunts at the scribe lines | ✓ | ✓ | | | | |
| Electrochemical corrosion of TCO | ✓ | ✓ | | | ✓ | |
| Ground fault | | ✓ | | | ✓ | Dry and wet insulation resistance |
| Bypass diode failures | ✓ | | ✓ | | | |
| | | | | | | bypass diode thermal test |

Figure 56 Degradation mechanism, corresponding stress factors and accelerated aging tests

angle of PV module, and other factors such as dust accumulation, humidity, and air velocity. The common main parameters for evaluation of PV system performance are Final yield (Y_F), Reference yield (Y_R), Performance ratio (PR), PVUSA rating, Capacity factor (CF), and System efficiency. For PV module degradation modes, various degradation modes are finally responsible for performance loss and failure that are packaging material degradation, adhesion loss, interconnect degradation, moisture intrusion, and semiconductor device degradation. A summary of the degradation mechanism and corresponding stress factors causing the degradation and accelerated aging tests to study these defects is given in Table 25. The current PV module qualification standard tests are available in IEC 61215 for crystalline PV modules and IEC 61646 for thin film PV modules. According to qualification standard tests, eight modules are picked up randomly from the same batch and subjected to 18 rigorous tests in a fixed sequence. The modules of the whole batch out of which these modules

are picked up will be regarded as qualified if performance degradation during any of these tests or after any sequence of tests is within the acceptable limits ($< 5\%$). Out of the randomly selected eight modules, one module is kept as reference and is not subjected to any accelerated stress test. The second module is subjected to electrical characterization under sun simulator to determine performance at different radiation conditions, then bypass diode thermal test, and finally to hot spot endurance test to determine the ability of PV module to bear the localized heat due to partial shadowing of the cells/cracked/mismatched cells. The remaining six modules are divided into 3

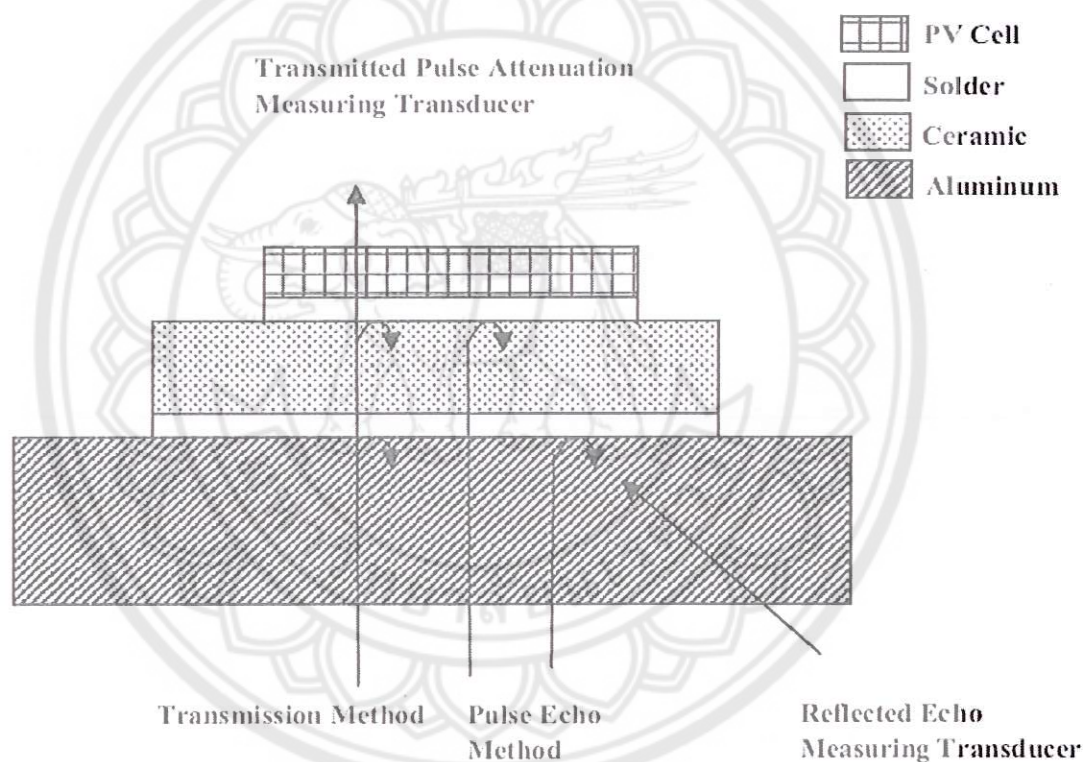


Figure 57 Ultrasonic inspection methodology

groups with two modules in each group and subjected to different mechanical and environmental tests. The important techniques for the failure mode analysis of PV modules that available in the past few year are Electrical characterization, Visual inspection, Ultrasonic inspection that displayed in Figure 36, Infrared imaging (IR imaging), Electroluminescence imaging (EL imaging), Attenuated total reflectance

infrared microscopy (ATIR), Scanning electron microscopy (SEM), and X-ray microtomography. Summary of failure mode analysis techniques is showed in Table 26.

| Name of the technique | Type of defect identified |
|--|---|
| (a) Non destructive ultrasonic imaging Infrared/thermal imaging Electroluminescence imaging (EL imaging) | Capable of locating air voids, debonding and delamination which are not visible Hotspot generation, increase in the series resistance Helpful in differentiating in the increased series resistance and reduced shunt resistance which is difficult because both of these defects lead to hotter areas in IR imaging Studying reliability and failure analysis issues such as μ -cracks in Si cells of PV module |
| Computed tomography (CT) using X-rays (b) Destructive scanning electron microscopy (SEM) X ray tomography | Study the morphology of the defect sample Studying the chemical changes which have occurred in the area of interest |

Figure 58 Summary of failure mode analysis techniques

Reliability assessment of photovoltaic power systems: Review of current status and future perspectives

Zhang, P., Li, W., Li, S., Wang, Y. and Xiao, W. [28] reviews the state-of-the-art technologies for evaluating the reliability of large-scale PV systems and the effect of PV interconnection on the reliability of local distribution system. The discussions are extended to emerging research topics including time varying and ambient-condition-dependent failure rates of critical PV system components, accurate operating models of PV generators in both interconnected and islanded modes, and the reliability evaluation of active distribution networks with PV penetration and transmission level Giga-PV system. A vision for the future research is presented, with a focus on the cyber-physical perspective of the PV reliability, modeling of PV voltage control scheme for reliability assessment, reliability assessment for PV systems under extreme events and PV reliability assessment considering cybersecurity. Large-scale grid-connected PV systems are usually connected in a centralized, a string/multi-string structure, and the micro-inverter system. When compare these topology, It found that the micro-inverter system has a potential to best optimize the PV power generation under partial shading conditions. At the same time, micro-inverter system may also improve reliability by reducing converter temperature and eliminating electrolytic capacitors. For reliability evaluation of critical components in PV system, it found that the PV modules can also

fail or degrade in their long-term lifecycle from many causes. Dust accumulation and PV connection topology are the important aspect associated with PV module reliability. Many studies present that total cross-tied (TCT) and bridge-linked (BL) configurations increase the operational lifetime of the PV arrays by 30%. The reliability of PV inverter depends on the performance of each component in PV inverter. A study indicate that failures often occur in switching stage and temperature is the most likely cause of failure. The electrolytic capacitor is the most dominant component for inverter failure while IGBT and MOSFET is the runner-up. Moreover, PV industry representatives at the DOE workshop agreed that the most urgent problem affecting inverter reliability is the quality of the dc-bus capacitors. The reliability of various structures of inverters such as single-stage, integrated topology, two-stage configuration, three-stage configuration AC-bus level, and DC-bus level are studied and the results show that higher system reliability can be achieved by using module-integrated inverters. Reliability evaluation methods of PV system that commonly used are Markov process method, Monte-Carlo simulation, State Enumeration, Reliability Block Diagram, and Fault Tree Analysis. For reliability indices for PV system, the traditional reliability indices such as mean time between failures (MTBFs), mean time to repairs (MTTRs), loss of load probability (LOLP), and loss of load hours (LOLHs) have been used in many studies. The loss of power probability (LPP) index which considered the extreme values of data as functions of certain recurrence intervals and The Yearly Expected Energy Production (YEEP) index that obtained based on a multi-state system model by considering both component failures and PV power outputs is introduced in a few papers. Future perspectives on PV reliability assessment is available in 4 topics that are Cyber-physical system perspective on reliability assessment of PV system, Modeling voltage control scheme in reliability assessment, PV reliability assessment under extreme weather conditions, and PV reliability assessment considering cyber vulnerability, attack and security. Reliability evaluation of power grids with PV systems are focused in 2 group that are active distribution network including PV microgrids and reliability for future Giga-PV system connected to power transmission grid.

From these literature review, they indicate that the availability and reliability of large scale PV power plant is dominated by inverter and electrolytic capacitor, IGBT, and MOSFET are the dominant components for inverter failure. The failure cause of these components is mainly from temperature and thermal stress. The inverter topologies is the factor that directly relate to inverter failure and reliability. From a few studies, they point out that the best system reliability can be possible achieved by using micro-inverter. From this point, the large scale PV power plant availability and reliability is also depended on the grid-connected PV system topologies.



CHAPTER III

METHODOLOGY

In this research, the availability and reliability of Decentralized Inverter PV Power Plant (DIPVP) and Centralized Inverter PV Power Plant (CIPVP) are evaluated for understanding energy harvest, levelized cost of energy (LCOE) and, financial internal rates of return (FIRR) for the energy producer or user. In addition, the result of the availability and reliability revaluation is possible used as the information to improve the preventative maintenance schedules, and budget for spares that result in reducing the maintenance cost projections over the system lifetime. The sample DIPVP and CIPVP are located in the same area in the central region of Thailand. The availability and reliability are analyzed and evaluated by using the measurement data and the efficiency and performance evaluation of DIPVP and CIPVP PV power plant as the referent data. The dissertation methodology is separated to 5 steps (Figure 37) as following;

1. Literature reviewing
2. PV power plant samples and data measuring
3. Efficiency and performance evaluation
4. Availability and reliability evaluation
5. Economic analysis

Literature reviewing

The literature reviewing in this research is displayed in the chapter II. The most of the literature that reviewed is concentrating in the availability and reliability of large scale PV power plant. Moreover, the availability, reliability, failure mode, and failure cause of the components in utility scale PV power station are also mentioned in the literature. The information from the literature reviewing is used as the idea to analyze and evaluate the availability and reliability of DIPVP and CIPVP in this research. The

result of this research is possible used to predict the energy harvest, LCOE and IRR and improve the preventative maintenance schedules, and budget for spares.

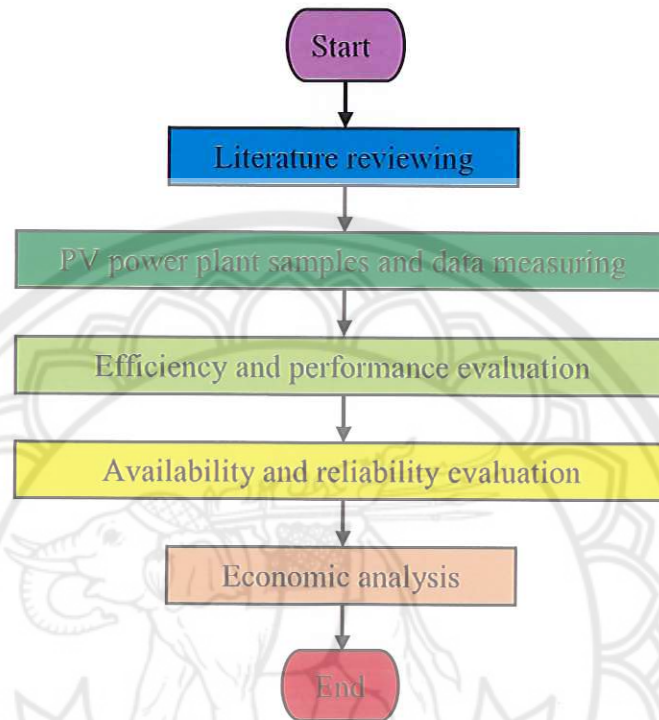


Figure 58 The dissertation methodology

From the information in the literature reviewing, higher availability and reliability are representing the better economical yields. Consequently, availability and reliability evaluation criteria are designed and presented in Table 27 by using the parameters that effect to availability and reliability. Downtime is the main factor that effect to availability. It is dominated by the combination of inverter, other component, and grid failure with failure detecting and repair period. Reliability depends on failure probability that is calculated from inverter failure.

PV power plant samples and data measuring

1. PV power plant samples

An objective of this dissertation is to analyze and compare reliability and availability of PV power system applying decentralized and centralized inverter concepts. Therefore the selecting of PV power plant samples have to focus on decentralized and centralized inverter topology of PV power plant and limit the effect of other factor such as whether condition, geography, utility grid condition, and other factors. From this point, two 5 MW PV power plant that are DIPVP that constructed with the decentralized inverter concept with string inverter and CIPVP that constructed with the centralized

Table 5 Availability and reliability evaluation criteria

| Availability evaluation criteria | Characteristic | |
|----------------------------------|---|---|
| | DIPVP | CIPVP |
| Inverter failure | Always occur but effect only a very small part of the PV power plant. | Rarely occur but effect the big part of the PV power plant. |
| Other component failure | Randomly occur depend on the component condition. Effect only a very small part for LV component and big part for MV component. | Randomly occur depend on the component condition. Effect only a very small part for LV component and big part for MV component. |
| Grid failure | Randomly occur depend on grid stability and effect all PV power plant | Randomly occur depend on grid stability and effect all PV power plant |
| Failure detecting period | Long period from the high inverter number | Short period from the low inverter number |
| Repair period | Short period for replacing inverter | Long period for service from manufacturer |

Table 5 (cont.)

| Availability evaluation criteria | Characteristic | |
|-------------------------------------|--|---|
| | DIPVP | CIPVP |
| Inverter failure | Always occur but effect only a very small part from the high number of inverter. | Rarely occur but effect the big part from the low number of inverter. |

inverter concept are selected as the PV power plant samples. Because of these PV power plants are located in the same district and province in the central region of Thailand and the distant between these PV power stations is only 8.37 km., the whether condition, geography, utility grid condition is not different and the effect from these factors are limited. In addition, the reliability and availability evaluation result of DIPVP and CIPVP is mainly dominated by the decentralized and centralized inverter concepts of the PV power plant samples that respond to the first objective of this dissertation. The specification of DIPVP and CIPVP is presented in Table 28. From the Table, the DC and AC output of both PV power plant is equal that means the effect of the different total power output from the PV array and inverter is eliminated. From the PV power plant information, the main components in both PV power plants are installed with the good quality and meeting the relating standard. Especially, inverter that is the most critical component and dominating the availability and reliability of the PV power plants are installed in different area for DIPVP and CIPVP. The string inverters in the DIPVP are installed outdoor under PV arrays while the central inverter in the CIPVP are installed indoor in the substation. From this reason, it is possible to predict the failure rate of these inverters. The failure rate of string inverter is possible higher than the failure rate of central inverter because it have to operate under extreme conditions such as high ambient temperature, high humidity, strike of lightning or surge, and other extreme conditions. There conditions increase the thermal stress, accelerate ageing and degradation, or event destroy the inverter. The specification of significant components in DIPVP and CIPVP are displayed in Appendix.

Table 6 The specification of DIPVP and CIPVP

| PV power plant features | DIPVP | CIPVP |
|--|---------------------------|-------------------------|
| PV power plant topology | Decentralized inverter | Centralized inverter |
| DC/AC Output power (MW_p/MW) | 5.75/5.00 | 5.75/5.00 |
| PV module technology | mc-Si | micromorph |
| PV module power/Total number (W/module) | 230/25,000 | 142-145/40,440 |
| PV array voltage/PV array number (V/array) | 294.4/1250 | 595-605/20 |
| Inverter type | String inverter | Central inverter |
| Inverter power/Total number (kW/inverter) | 4/1250 | 250/20 |
| Inverter output system and voltage | 1 Ø 230 VAC | 3 Ø 400 VAC |
| Junction box number/MDB number | 139/5 | 780/4 |
| Transformer size/Transformer number (kVA/transformer) | 1,000-1,500/5 | 1,250/4 |

2. Data measuring

The important operating parameters of DIPVP and CIPVP such as solar irradiance, ambient temperature, PV module temperature, PV array voltage, PV array current, inverter output voltage, inverter output current, inverter output power, inverter status, common coupling point (CCP) voltage, CCP current, and CCP power is measured with 1 minute interval time or faster. The list of sensors and instruments that used for measuring the significant parameters in both PV power plant are available in Table 29. For solar irradiance, ambient temperature, and PV module temperature, their measured data are converted to RS 485 and transfer to the server of the monitoring system. PV array voltage, PV array current, inverter output voltage, inverter output current, inverter output power, and inverter status are measured by the sensors in the inverters while CCP voltage, CCP current, and CCP power are measured by power meter. These measured data are transferred to the server of the monitoring system by

RS 485 of inverters and power meter. All measure data are recorded in the server of the monitoring system in DIPVP and CIPVP. The single line diagram of data measuring

Table 7 The list of sensors and instruments that used for measuring the significant parameters in both PV power plant

| Parameters | Sensors and instruments | |
|-------------------------|-------------------------|--------------------|
| | DIPVP | CIPVP |
| Solar irradiance | SMP 11 pyranometer | CMP 11 pyranometer |
| Ambient temperature | RTD pt-100 | RTD pt-100 |
| PV module temperature | RTD pt-100 | RTD pt-100 |
| PV array voltage | Inverter | Inverter |
| PV array current | Inverter | Inverter |
| Inverter output voltage | Inverter | Inverter |
| Inverter output current | Inverter | Inverter |
| Inverter output power | Inverter | Inverter |
| Inverter status | Inverter | Inverter |
| CCP voltage | Power meter | Power meter |
| CCP current | Power meter | Power meter |
| CCP power | Power meter | Power meter |

and recording of DIPVP and CIPVP are presented in Figure 38 and 39 respectively. The specification of the important sensors and instruments that used for measuring the significant parameters is displayed in Appendix.

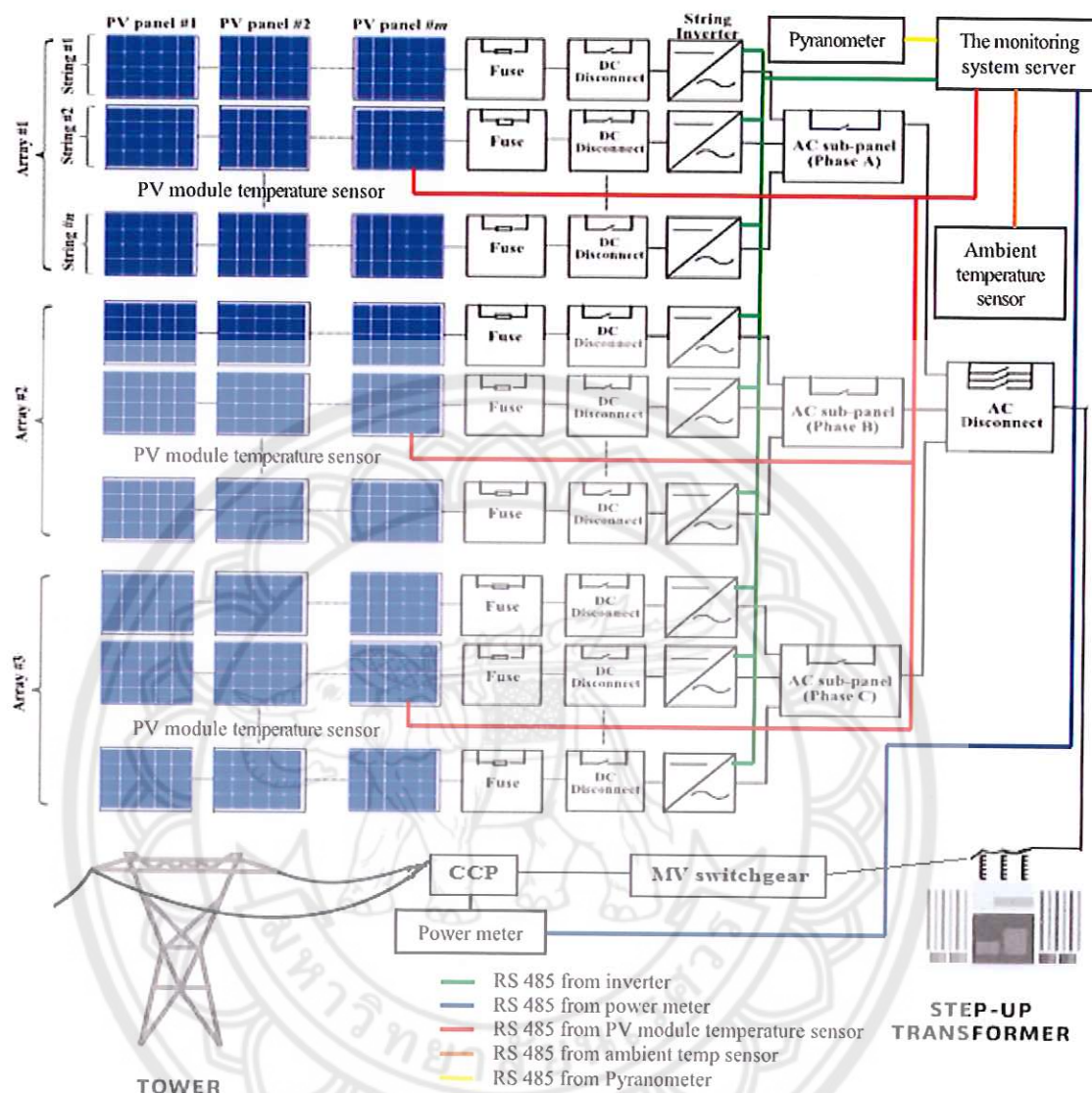


Figure 60 The single line diagram of data measuring and recording of DIPVP

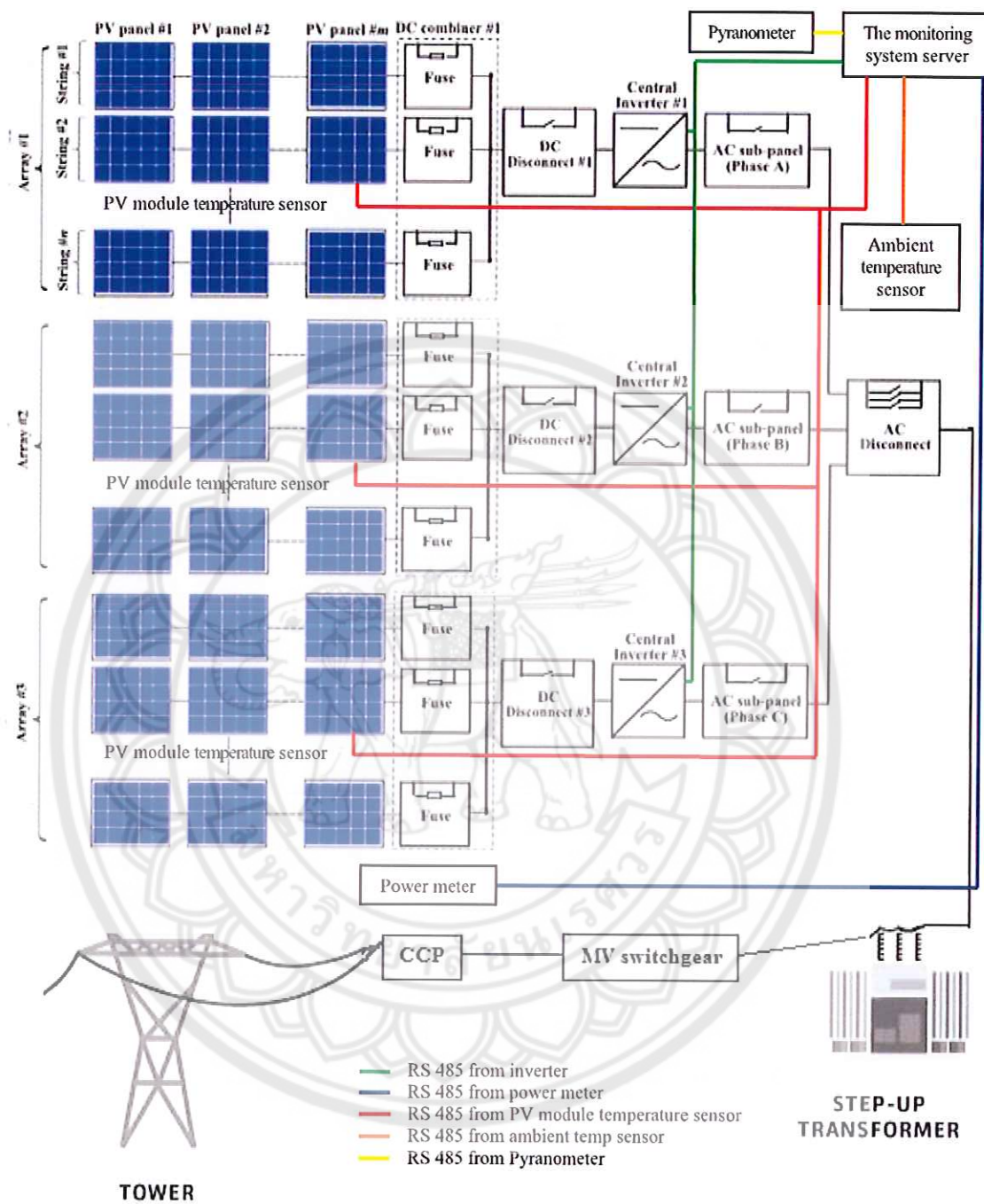


Figure 61 The single line diagram of data measuring and recording of CIPVP

Efficiency and performance evaluation

The technical analysis processes of IEC 61724 standard and EU Guidelines, 4.3 [29] are used to evaluate the efficiency and performance of PVMG in this research. The important parameters for analysis is presented follow this:

The array yield Y_A represents the number of hours per day that the array would need to operate at its nominal power P_0 to contribute the same daily array energy to the system as was monitored.

$$Y_A = E_A / P_0 \quad (1)$$

Y_A = Array yield (kWh/ W_p)

E_A = Annual mean yields (kWh)

P_0 = Nominal power (W_p)

The final PV system yield Y_f is the portion of the daily energy of the entire PV plant which is delivered to the load per kilowatt peak of installed PV array.

$$Y_f = Y_A \eta_{LOAD} \quad (2)$$

Y_f = Final PV system yield (kWh/ W_p)

η_{LOAD} = Load efficiency

$$\eta_{LOAD} = E_{use} / E_{in} \quad (3)$$

E_{use} = Total system output energy (kWh)

$$E_{use} = E_L + E_{TUN} + E_{TSN} \quad (4)$$

E_L = Net energy to load (kWh)

E_{TUN} = Net energy to utility grid (kWh)

E_{TSN} = Net energy to storage (kWh)

E_{in} = Total input energy (kWh)

$$E_{in} = E_A + E_{BU} + E_{FUN} + E_{FSN} \quad (5)$$

E_{BU} = Energy from back-up system (kWh)

E_{FUN} = Net energy from utility grid (kWh)

E_{FSN} = Net energy from storage (kWh)

The reference yield Y_r represents the solar energy theoretically available per kilowatt peak of installed PV per day.

$$Y_r = H_I / G_{ref} \quad (6)$$

Y_r = Reference yield (kWh/W_p)

H_I = Global irradiation in the plane of the array (kWh/m²)

G_{ref} = STC reference in plane irradiance (W/m²)

The array capture losses L_C are caused by operating cell temperatures higher than 25 °C (thermal capture losses) and by miscellaneous causes such as:

1. Low irradiance
2. Wiring, string diodes
3. Partial shading, contamination, snow covering, non-homogenous irradiance
4. Maximum power point tracking errors
5. Reduction of array power caused by inverter failures or by fully charged accumulator (standalone systems)
6. Spectral losses, losses caused by glass reflections (use of pyranometers)

$$L_C = Y_r - Y_A \quad (7)$$

L_C = Array capture losses (kWh/W_p)

System losses L_S are gained from inverter conversion losses in grid-connected systems and from accumulator storage losses in stand-alone systems.

$$L_S = Y_A - Y_f \quad (8)$$

L_S = System losses (kWh/ W_p)

The performance ratio PR indicates the overall effect of losses on the array's nominal power due to array temperature, incomplete utilization of irradiation, and system component inefficiencies or failures.

$$PR = Y_f / Y_r \quad (9)$$

PR = Performance ratio

The mean array efficiency $\eta_{A,mean}$ represents the mean energy conversion efficiency of the PV array, which is useful for comparison with the array efficiency η_{A0} at its nominal power P_0 . The difference in efficiency values represents diode, wiring and mismatch losses as well as energy wasted during plant operation.

$$\eta_{A,mean} = E_A / E_{S,A} \quad (10)$$

$\eta_{A,mean}$ = Mean array efficiency

$E_{S,A}$ = Total solar energy on array plane (kWh)

$$E_{S,A} = H I A_A \quad (11)$$

A_A = Array area

The fraction of the energy from all sources which was contributed by the PV array is F_A . For stand-alone systems without back-up energy ($E_{BU} = 0$) and grid connection ($E_{FUN} = 0$), this fraction is equal to one, because the useful energy to the loads is totally supplied by the solar irradiation and the energy flows from and to the battery are not considered ($E_{FSN} = 0$). For all PV power stations, which take no energy from the grid ($E_{FUN} = 0$), F_A is also equal to one.

$$F_A = E_A / E_{in} \quad (12)$$

F_A = PV array fraction

The matching factor MF is the product of the performance ratio (PR) and the array fraction F_A . This MF indicator was introduced with respect to stand-alone hybrid systems for a better illustration of the performance. The matching factor is valuable for all hybrid systems (F_A less than one) and for grid-connected systems with a considerable contribution from the grid (F_A less than one). The matching factor indicates how the PV generated energy matches the electrical load while using a back-up contribution (SAS) or energy from the grid (GCS).

$$MF = PR F_A \quad (13)$$

MF = Matching factor

The usage factor UF, being the ratio of the energy supplied by the PV array (E_A) and the potential PV production (E_{pot}), has been introduced to demonstrate how the system is using the potential energy. E_{pot} is a measured energy quantity, which is equal to E_A ($UF = 1$) for all grid-connected systems and differs from E_A for all SAS presenting PV array disconnection due to a fully charged battery. UF values are used to highlight the different operation of SAS having the same PR and allow the detection of system problems.

$$UF = E_A / E_{pot} \quad (14)$$

UF = Usage factor

E_{pot} = Potential energy (kWh)

The BOS efficiency η_{BOS} represents the mean energy conversion efficiency of the BOS in system. The difference in efficiency values represents BOS and mismatch losses as well as energy wasted during plant operation.

$$\eta_{BOS} = (E_L + E_{TSN} - E_{FSN} + E_{TUN} - E_{FUN}) / (E_A + E_{BU}) \quad (15)$$

η_{BOS} = BOS efficiency

The overall PV plant efficiency η_{tot} represents the mean energy conversion efficiency of the overall PV plant. The difference in efficiency values represents array capture losses and system losses as well as energy wasted during overall PV plant operation.

$$\eta_{tot} = \eta_{A,mean} \eta_{LOAD} \quad (16)$$

η_{tot} = Overall PV plant efficiency

Availability and reliability evaluation

1. Availability and reliability theory

Several standard reliability metrics are commonly used to express and evaluate the number of failures or downtime of a system. Industry-specific definitions and standard metrics have also been developed. For grid connected inverters, no industry-specific standard reliability metrics have been adopted. In addition, some metrics are commonly used without specifying the details of their definitions. What follows is the reliability metrics that can be useful by themselves or adapted for application to PV inverters.

Reliability, typically denoted R or $R(T)$, is commonly defined as the probability of success, the idea that an item is fit for a purpose with respect to time, the capacity of a designed, produced or maintained item to perform as required over time, the capacity of a population of designed, produced or maintained items to perform as required over specified time, the resistance to failure of an system over time, the durability of an system, or the probability that a system will operate properly for a specified time period under the design operating conditions without failure. Statistically, reliability can be expressed as:

$$R(T) = 1 - F(T) = 1 - \int_0^T f(t) dt \quad (17)$$

$R(T)$ = Reliability

$F(T)$ = The probability of failure over a specified time period T

$f(t)$ = The failure probability distribution

Clearly, for this definition of reliability to be meaningful, the time interval, T , must be stated. In addition, failure must be clearly defined. For example, in the case of an inverter, failure may be defined simply as the inability to produce power, or it may include loss of auxiliary functions such as data transmission. With the increasing complexity of remote monitoring and control systems at the inverter level, this distinction is becoming increasingly important. For PV inverters, $R(T)$ can be estimated for a population of N inverters that are fielded as:

$$R(T) = 1 - (N_f(T)/N) \quad (18)$$

N = Population of inverters that are fielded

N_f = The total number of inverters that failed in the sample population during the time period $(0, T)$

Mean time to failure (MTTF) and mean time between failures (MTBF) are commonly used metrics in the PV inverter industry, but are also some of the most difficult

to interpret. Strictly defined, MTTF is the expected time to failure (and replacement) of non-reparable systems such as residential PV inverters:

$$MTTF = \int_0^{\infty} t f(t) dt \quad (19)$$

MTTF = the expected time to failure and replacement of non-reparable systems

In the case of reparable systems such as commercial PV inverters, MTBF is used, and is defined similarly as the expected time between two successive failures (and repairs). For brevity, MTTF is used here to also represent MTBF. Several considerations should be taken into account when specifying or interpreting MTTF. Most of these arise from the fact that MTTF is typically estimated with the following equation:

$$MTTF = T_{\text{Total}} / Y \quad (20)$$

T_{Total} = The total number of inverter hours for a given population

Y = the total number of failures in that population during that time period

One important consideration specific to estimating MTTF with equation 20 is that it produces an average value for the interval from which the data is taken. Referring to the bathtub curve, failure rates are typically changing during the infant mortality and wear-out periods. Therefore, using field data from these periods to calculate MTTF will result in an average failure rate for that time period, and does not provide information about the changing failure rate, which can be very important in understanding the expected total number of failures during the lifetime of an inverter population.

The renewal function, $M_i(T)$ gives the expected number of failures of a component during the time interval $(0, T)$. This function takes into account both the failure probability distribution, and immediate renewal of the component after repair. The renewal function is the solution to the fundamental renewal equation:

$$M_i(T) = F_i(T) + \int_0^T M_i(T-t) f_i(t) dt \quad (21)$$

$M_i(T)$ = the expected number of failures of a component during the time interval (0,T)

This equation is recursive in $M_i(T)$, and, for most failure probability distribution functions, must be solved numerically. The expected number of repairs per unit time (per year for example) is the differential of $M_i(T)$:

$$m_i(t) = dM_i(t) / dt \quad (22)$$

$m_i(t)$ = The expected number of repairs per unit time

Note, that equations 21 and 22 are specific to a single component in an inverter. To estimate the number of repairs of all components in an inverter, the component renewal functions can be summed.

A simple nonparametric failure rate can show this either cumulatively or as a rate. For a sample population of N inverters with at least T years of operation, the cumulative failure rate can be calculated from the number of failures observed. The average number of cumulative failures per inverter in the first T years of operation for a given inverter population can be estimated as:

$$CFR(T) = \frac{1}{N} \sum_{j=1}^N Y_j(T) \quad (23)$$

$CFR(T)$ = The average number of cumulative failures per inverter in the first T years of operation for a given inverter population

$Y_j(T)$ = The number of failures or repairs for the j -th inverter on the interval (0,T)

N = The total number of inverters in the sample population

To calculate the failure and/or repair rate from the cumulative failure rate, differentiate:

$$FR(T) = dCFR(t) / dt \quad (24)$$

Note that $CFR(T)$ and $FR(t)$ are similar to $M_i(T)$ and $m_i(t)$, respectively. The difference is that $M_i(T)$ and $m_i(t)$ are based on $f_i(t)$ and can be used to predict failure rates for any time period, while $CFR(T)$ and $FR(t)$ are based on field data and are limited to the time period of the data provided. However, $FR(t)$ may still be useful for failure prediction by serving as a data set for fitting a parameterized failure rate model that can be extrapolated into the future. Another important note is that $CFR(T)$ and $M_i(T)$ are not cumulative failure probability distributions like $F(T)$, which, by definition, must approach unity as T goes to infinity. $CFR(T)$ and $M_i(t)$ can be greater than unity because they reflect the number of expected failures of reparable equipment, which can be repaired more than once over a time interval.

One of the most basic ways of quantifying lost energy production is simply inverter downtime multiplied by average inverter power. Given existing field data from a population of N inverters that operated for time T , it is possible to estimate average cumulative downtime per inverter on an interval $(0, T)$ by summing the downtimes due to individual inverter failures:

$$D(T) = \frac{1}{N} \sum_{j=1}^N D_j(T) \quad (25)$$

$D(T)$ = Average cumulative downtime per inverter on an interval $(0, T)$

$D_j(T)$ = The downtime due to failure and repair of the j -th inverter on the interval $(0, T)$

To calculate the downtime per inverter per unit time from the average cumulative downtime, simply differentiate:

$$d(t) = dD(t) / dt \quad (26)$$

$d(t)$ = Downtime per inverter per unit time from the average cumulative downtime

When calculating downtime, an important distinction is whether it excludes hours when energy cannot be produced such as nighttime.

Availability is considered one of the most important reliability metrics for repairable systems. It is generally defined as the ratio of (a) the total time a functional unit is capable of being used during a given interval to (b) the length of the interval, the probability that a system will be operable when called upon. Likewise, unavailability is the probability that a system will not be available when called upon. There are many forms and definitions of availability, mostly differing by what is included in the downtime and total time, and whether steady state is assumed or not. One of the forms most applicable to PV inverters is operational availability (A_O)

$$A_O = \text{Uptime} / \text{Total time} = 1 - (\text{Downtime} / \text{Total time}) \quad (27)$$

A_O = Operational availability

Uptime = The time that the equipment performs its intended purpose when called upon

Downtime = The time that the equipment does not perform its intended purpose when called upon

Total time = The total time that the equipment could be called upon to perform its intended purpose

In the definition of A_O , downtime includes both indirect and direct maintenance and repair time as well as logistics time and waiting or administrative downtime. In calculating A_O for PV inverters, two main approaches can be taken:

considering only times when power production is possible (daylight hours), or considering all field time (both daytime and nighttime). IEEE Std. 762, which defines metrics for electric power generating equipment, seems to suggest availability should consider both daytime and nighttime hours by defining Availability Factor (AF) as:

$$AF = (AH / PH) 100 \quad (29)$$

AF = Availability Factor

AH = Available hours, which includes both service hours (producing power) and reserve shutdown hours (available to but not producing power)

PH = Period hours, which is the entire time the equipment is in the active state (but not necessarily producing power)

AH therefore may consist of both daytime and nighttime hours when a PV inverter is able to produce power. For PV inverters, AF is very simple to calculate: the downtime hours are simply added together, whether they occur during daytime or nighttime, and are divided by the total field time of the inverter, and the result is subtracted from unity. An alternate operational availability metric for PV inverters, which we will term A_{DC} , could be defined whereby Total Time is the time when conditions are sufficient to produce power, as opposed to the “period time” or “active time” described by IEEE Std. 762. Note that this approach would not include in total time any of the following:

1. Periods of darkness from approximately sundown minus 30 minutes to sunrise plus 30 minutes.
2. Cloudy or bad weather hours when there is insufficient irradiance or when weather conditions prohibit the field from generating power such as when the arrays are pointed off sun during very high winds.
3. Times when there is natural or induced damage to the PV field or to the AC grid, such as being hit by lightning.

To yield a correct formulation of availability for A_{DC} , Downtime must also only be accrued during periods when Total Time is accrued.

2. Availability and reliability evaluation constraint

Because of the monitoring system of DIPVP is not accurately report inverter failure and the inverter number is enormous, it has to manually find these failure inverter by field surveying and estimate the inverter failure detecting time. Moreover, the time that used to replace the failure inverter is not recorded. Therefore the inverter replacing time should be estimated too. From this reason, the inverter failure detecting time is estimated at 4 hour while the inverter replacing time is estimated at 1 hour. For the monitoring system of DIPVP, the inverter failure is real time reported and the inverter repaired period is also recorded. For other components and grid failure, they are detected, reported, and recorded by the DIPVP and CIPVP monitoring system and PV power plant operators. For the evaluation period, the data from the monitoring system of DIPVP and CIPVP and other data during MAY 2013 to October 2014 that about 18 months are used in the availability and reliability evaluation. This period data can present the availability and reliability DIPVP and CIPVP in infant mortality and random failure period while wear-out have to use long term data for evaluation.

3. Economic analysis

The economic analysis of DIPVP and CIPVP are based on Net Present Value (NPV), Internal Rate of Return (IRR), and Cost per Unit and Levelized cost of Energy (LCOE) in evaluation. There are 3 significant factors that used in the economic analysis of PVMG. These factors are present follow this:

3.1 Net Present Value (NPV)

The net present value (NPV) method for evaluating the desirability of investments can be defined as follows:

$$NPV = \frac{B_1}{(1+i)} + \frac{B_2}{(1+i)^2} + \dots + \frac{B_n}{(1+i)^n} - TIC = \sum_{n=1}^N \frac{B_n}{(1+i)^n} - TIC \quad (30)$$

Or

$$NPV = \sum_{n=0}^N \frac{B_n}{(1+i)^n} - \sum_{n=0}^N \frac{C_n}{(1+i)^n} = PVB - PVC \quad (31)$$

- B_n = Expected benefit at the end of year n
 TIC = Total initial cost (investment)
 C_n = Expected cost at the end of year n
 i = Discount rate, i.e., the required minimum annual rate on new investment
 n = Project's duration in years
 N = Project's period
 PVB = Present Value Benefit
 PVC = Present Value Cost

3.2 Internal Rate of Return (IRR)

The internal rate of return (IRR) is another time – discounted measure of investment worth. The IRR is defined as that rate of discount which equates the present value of the stream of net receipt with the initial investment outlay:

$$NPV = \sum_{n=0}^N \frac{B_n}{(1+i)^n} - \sum_{n=0}^N \frac{C_n}{(1+i)^n} = PVB - PVC \quad (32)$$

Where, “ i ” denotes the internal rate of return (IRR). An alternative and equivalent definition of the IRR is the rate of discount which equates the NPV of the cash flow to zero:

$$NPV = \sum_{n=0}^N \frac{B_n}{(1+i)^n} - \sum_{n=0}^N \frac{C_n}{(1+i)^n} = 0 \quad (33)$$

There are two methods to compute IRR:

1. Trial and error

- 1.1 Given the cash flow and investment outlay
- 1.2 Choose a discount rate
- 1.3 Calculate the project's NPV
- 1.4 If $NPV > 0$, choose a higher discount rate and go to no. 3
 If $NPV < 0$, choose a lower discount rate and go to no. 3
 If $NPV = 0$, then choose discount rate = IRR

2. Interpolation

2.1 Arithmetically

3. Giving a lower discount rate: i_L ; $NPV > 0$

4. Giving an upper discount rate: i_U ; $NPV < 0$

$$IRR = i_L + (i_U - i_L) \frac{NPV_L}{(NPV_L - NPV_U)} \quad (34)$$

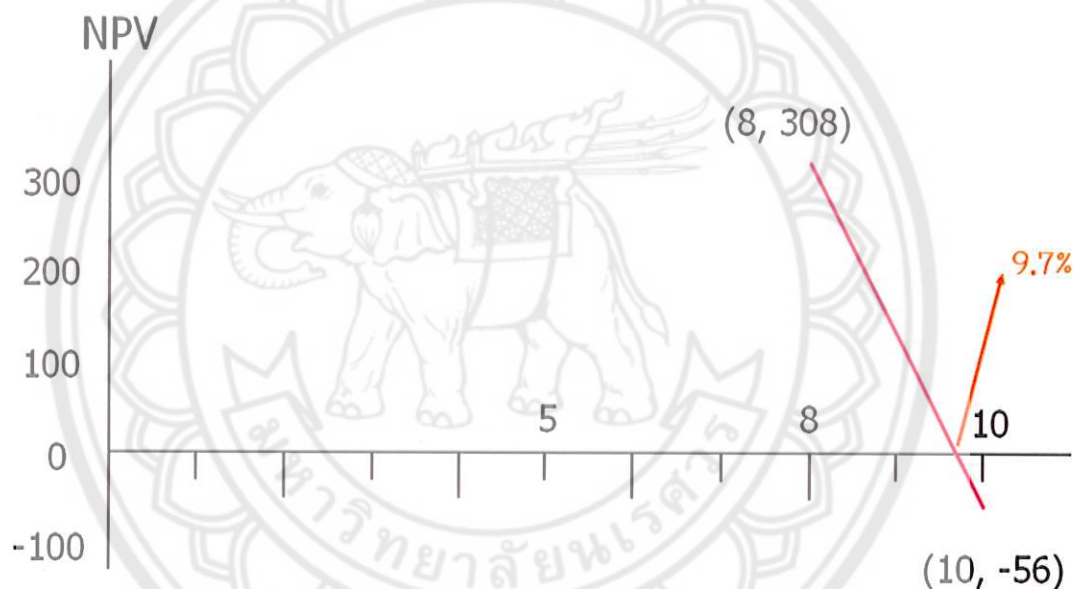


Figure 62 Graphical method of IRR computation

In graphical method, calculate NPV assuming one value of IRR. Then, calculate NPV for another IRR. Then draw a graph of NPV against IRR. Hence, desired IRR is the value where NPV line crosses IRR line, i.e., when the NPV value is equal to zero. Figure 40 is present graphical method of IRR computation.

3.3 Cost per Unit and Levelized cost of Energy (LCOE)

The cost per unit method is an economic evaluation technique that used in economic analysis. Total cost consists of fixed and variable costs. Fixed costs do not change based on production. Examples of fixed costs include rent, utilities and salary of employees. Variable costs vary based on the number of units produced such as raw materials, packaging, and wages of hourly workers. The cost per unit is based

on the total fixed cost, variable cost and the number of units produced during an accounting period. Cost per unit can be defined as follows:

$$\text{Cost per unit} = \text{Total cost} / \text{total unit} \quad (35)$$

The levelized cost of electricity (LCOE) is the net present value of the unit-cost of electricity over the lifetime of a generating asset. It is often taken as a proxy for the average price that the generating asset must receive in a market to break even over its lifetime. It is a first-order economic assessment of the cost competitiveness of an electricity-generating system that incorporates all costs over its lifetime: initial investment, operations and maintenance, cost of fuel, cost of capital. The levelized cost is that value for which an equal-valued fixed revenue delivered over the life of the asset's generating profile would cause the project to break even. This can be roughly calculated as the net present value of all costs over the lifetime of the asset divided by the total electricity output of the asset

$$\text{LCOE} = \frac{\sum_{t=1}^n \frac{I_t + M_t + F_t}{(1+r)^t}}{\sum_{t=1}^n \frac{E_t}{(1+r)^t}} \quad (36)$$

I_t = Investment expenditures in the year t

M_t = Operations and maintenance expenditures in the year

F_t = Fuel expenditures in the year t

E_t = Electricity generation in the year t

r = Discount rate

n = Life of the system

CHAPTER IV

RESULT AND DISCUSSION

Efficiency and performance evaluation result

DIPVP and CIPVP has been COD sine 24 April 2013. The collected data that used in the efficiency and performance evaluation of DIPVP and CIPVP are in May 2013 to October 2014 period that is about 18 months. However, the monitoring data of these PV power plant are very complicated and impossible to evaluate every parameters. Especially, L_c and L_s cannot calculate from the collected data. Only total losses (L_T) that is the sum of L_c and L_s is possible calculated from these data. Consequently, only Y_r , Y_f , L_T , PR, and η_{tot} are evaluated in this dissertation. After analyzing the collected data follow the technical analysis processes of IEC 61724 standard and EU Guidelines, the efficiency and performance evaluation result of DIPVP and CIPVP during May 2013 to October 2014 is presented in Table 30. Y_r , Y_f , L_T , PR, and η_{tot} of DIPVP and CIPVP during May 2013 to October 2014 is displayed in Figure 41, 42, 43, 44, and 45 respectively. From the table, average Y_r of DIPVP and CIPVP are 4.88 and 5.04 h/day that not significantly different. When compares with the annual daily average solar radiation of Thailand at 5.05 kWh/m² day that given by DEDE, the daily average solar radiation of DIPVP at 4.88 kWh/m² day is a little bit lower while the daily average solar radiation of DIPVP at 5.05 kWh/m² day is equal. Y_f of these PV power plant in each month is nearly the same and the average Y_f of DIPVP and CIPVP are 3.83 and 3.87 h/day respectively that is approximately the same. Most of L_T in each month of DIPVP and CIPVP are not different except in January to April 2014 that is significantly different. The cause of the different L_T is possible from the lack of PV module cleaning in CIPVP that result in higher L_T in this period. PR of DIPVP and are almost the same in each month except in January to April 2014 that is the result from the higher L_T of CIPVP in this period. Almost of PR in each month of DIPVP and CIPVP are nearly the same except in January to April 2014 that DIPVP has a little bit better PR from the lower L_T in this period. DIPVP clearly has higher η_{tot} than CIPVP nearly 2 times in every month. The cause of different in η_{tot} of these PV power plant is mainly from the

Table 8 The efficiency and performance evaluation result of DIPVP and CIPVP during May 2013 to October 2014

| Month | DIPVP | | | | | CIPVP | | | | |
|---------|----------------------|-------|-------|-------|--------------|----------------------|-------|-------|-------|--------------|
| | Evaluated parameters | | | | | Evaluated parameters | | | | |
| | Y_r | Y_f | L_T | PR | η_{tot} | Y_r | Y_f | L_T | PR | η_{tot} |
| | h/day | h/day | h/day | % | % | h/day | h/day | h/day | % | % |
| May 13 | 5.20 | 4.14 | 1.06 | 79.62 | 11.28 | 5.53 | 4.29 | 1.24 | 77.55 | 7.04 |
| Jun 13 | 4.59 | 3.67 | 0.92 | 79.96 | 11.32 | 4.69 | 3.75 | 0.94 | 79.94 | 7.26 |
| Jul 13 | 4.17 | 3.33 | 0.84 | 79.86 | 11.31 | 4.40 | 3.53 | 0.87 | 80.19 | 7.28 |
| Aug 13 | 4.62 | 3.69 | 0.93 | 79.87 | 11.31 | 4.66 | 3.74 | 0.92 | 80.29 | 7.29 |
| Sep 13 | 3.98 | 3.17 | 0.81 | 79.65 | 11.28 | 4.09 | 3.28 | 0.82 | 80.07 | 7.27 |
| Oct 13 | 4.80 | 3.83 | 0.97 | 79.79 | 11.30 | 4.88 | 3.82 | 1.06 | 78.24 | 7.10 |
| Nov 13 | 4.76 | 3.77 | 0.99 | 79.20 | 11.22 | 5.06 | 3.91 | 1.15 | 77.32 | 7.02 |
| Dec 13 | 5.65 | 4.47 | 1.18 | 79.12 | 11.21 | 5.88 | 4.55 | 1.33 | 77.35 | 7.02 |
| Jan 14 | 5.89 | 4.57 | 1.32 | 77.59 | 10.99 | 6.05 | 4.38 | 1.67 | 72.43 | 6.58 |
| Feb 14 | 5.29 | 4.15 | 1.14 | 78.45 | 11.11 | 5.42 | 3.91 | 1.51 | 72.18 | 6.55 |
| Mar 14 | 5.43 | 4.18 | 1.25 | 76.98 | 10.90 | 5.74 | 4.14 | 1.60 | 72.14 | 6.55 |
| Apr 14 | 5.44 | 4.22 | 1.22 | 77.57 | 10.99 | 5.61 | 4.20 | 1.41 | 74.88 | 6.80 |
| May 14 | 5.36 | 4.09 | 1.27 | 76.31 | 10.81 | 5.37 | 4.09 | 1.28 | 76.12 | 6.91 |
| Jun 14 | 4.50 | 3.50 | 1.00 | 77.78 | 11.02 | 4.39 | 3.42 | 0.97 | 77.80 | 7.06 |
| Jul 14 | 4.25 | 3.39 | 0.86 | 79.76 | 11.30 | 4.44 | 3.45 | 0.98 | 77.82 | 7.06 |
| Aug 14 | 4.43 | 3.50 | 0.93 | 79.01 | 11.19 | 4.50 | 3.51 | 0.99 | 78.06 | 7.09 |
| Sep 14 | 4.73 | 3.68 | 1.05 | 77.80 | 11.02 | 4.92 | 3.78 | 1.14 | 76.83 | 6.98 |
| Oct 14 | 4.71 | 3.66 | 1.05 | 77.66 | 11.00 | 5.06 | 3.88 | 1.19 | 76.53 | 6.95 |
| Average | 4.88 | 3.83 | 1.04 | 78.66 | 11.14 | 5.04 | 3.87 | 1.17 | 76.99 | 6.99 |

PV module technologies. Multicrystalline silicon PV module that used in DIPVP has efficiency about 14.60% while micromorph PV module that used in CIPVP has efficiency about 9.35%. The efficiency different of these PV module are nearly 2 times that result in the different η_{tot} of these PV power plant is nearly 2 times too.

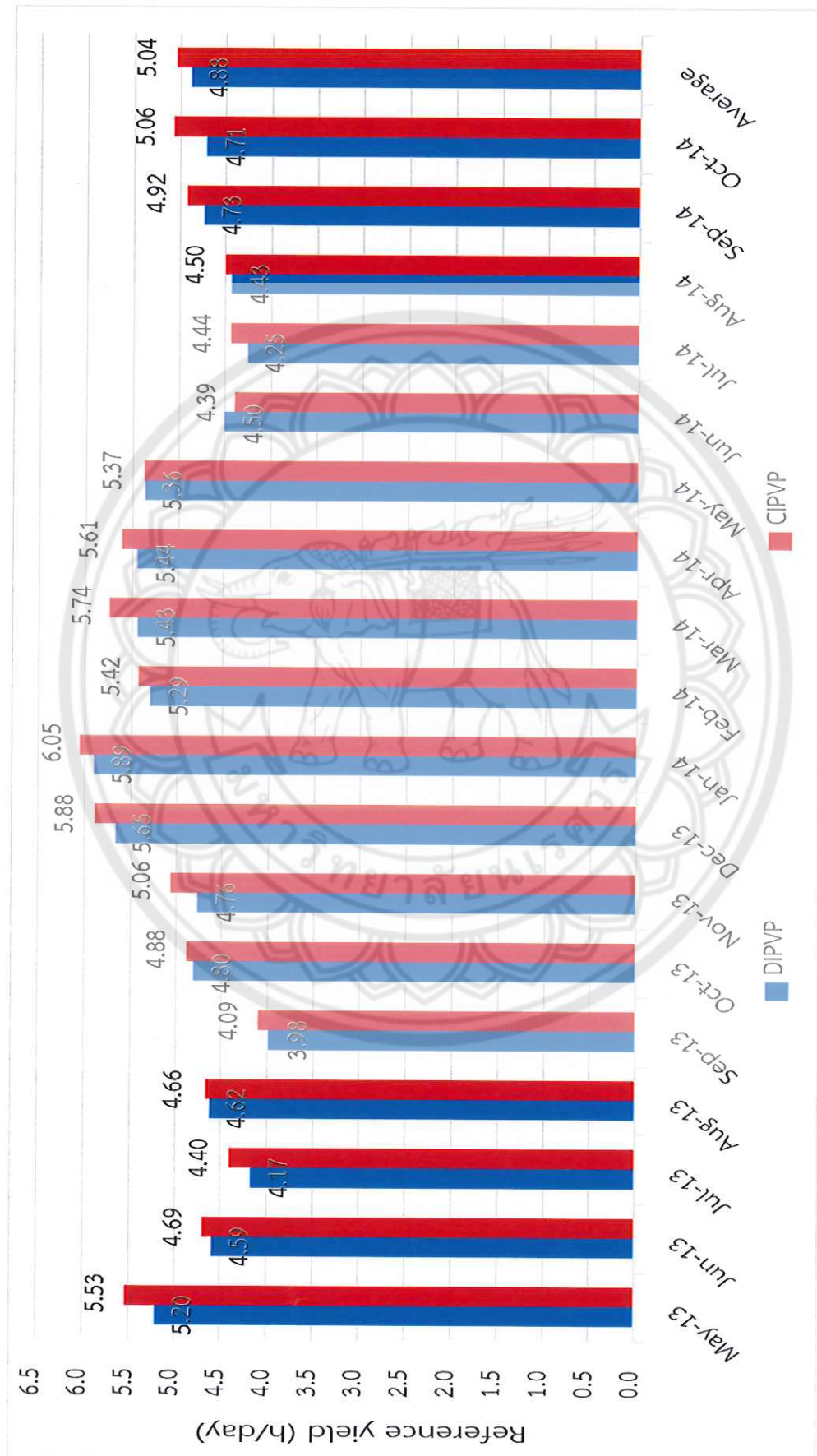


Figure 63 Yr. of DIPVP and CIPVP during May 2013 to October 2014

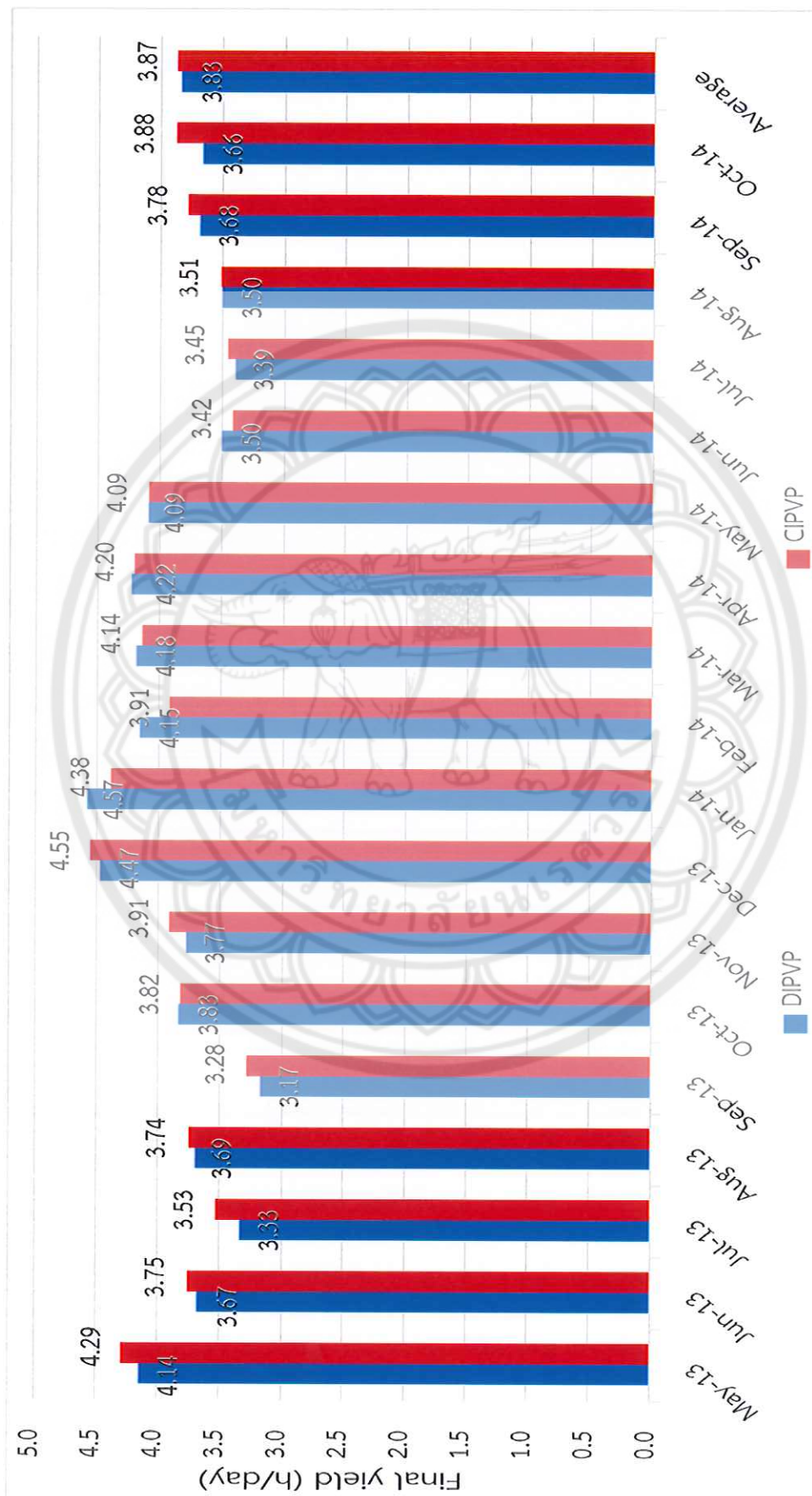


Figure 64 Y_r of DIPVP and CIPVP during May 2013 to October 2014

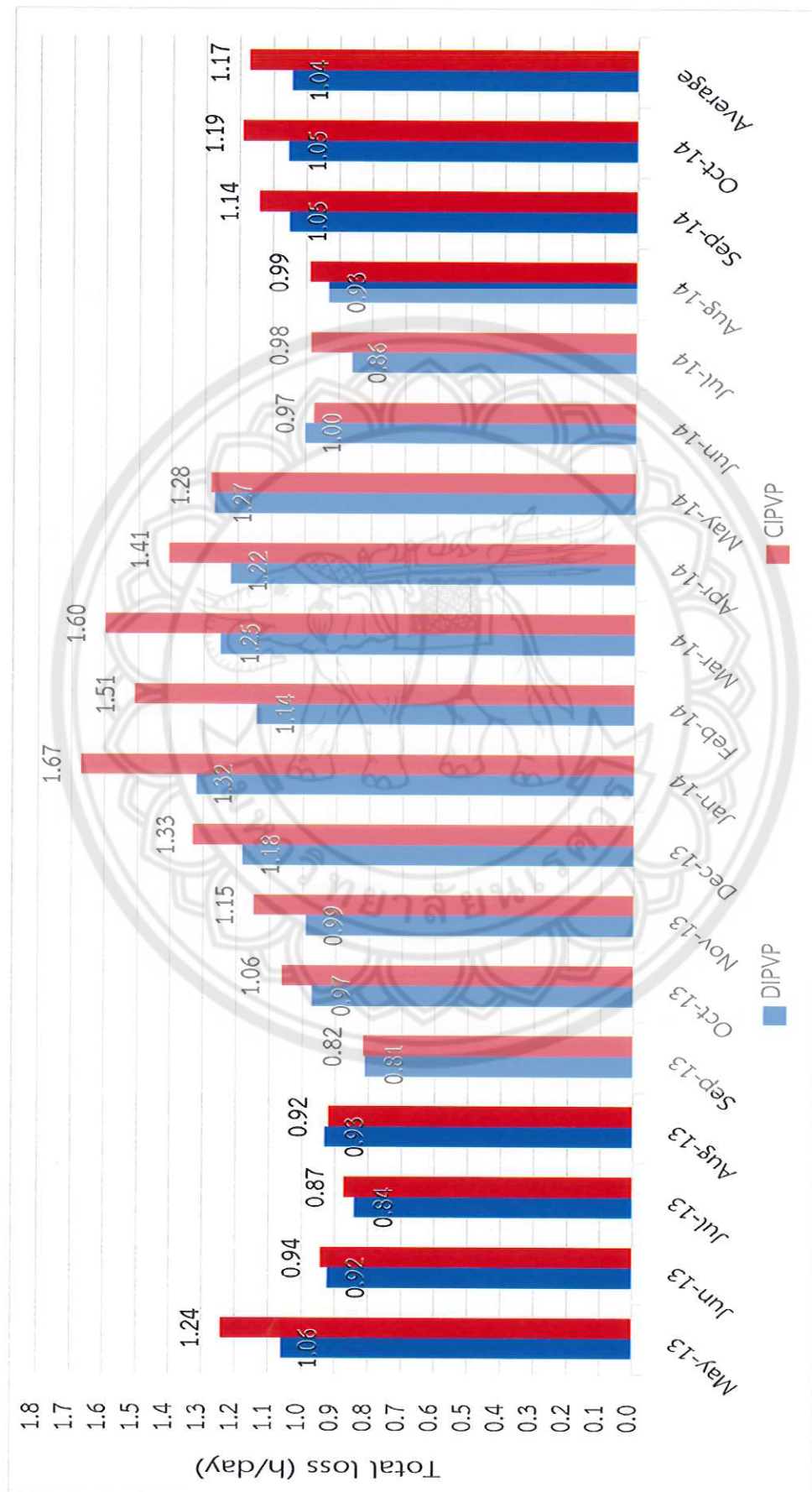


Figure 65 L_t of DIPVP and CIPVP during May 2013 to October 2014

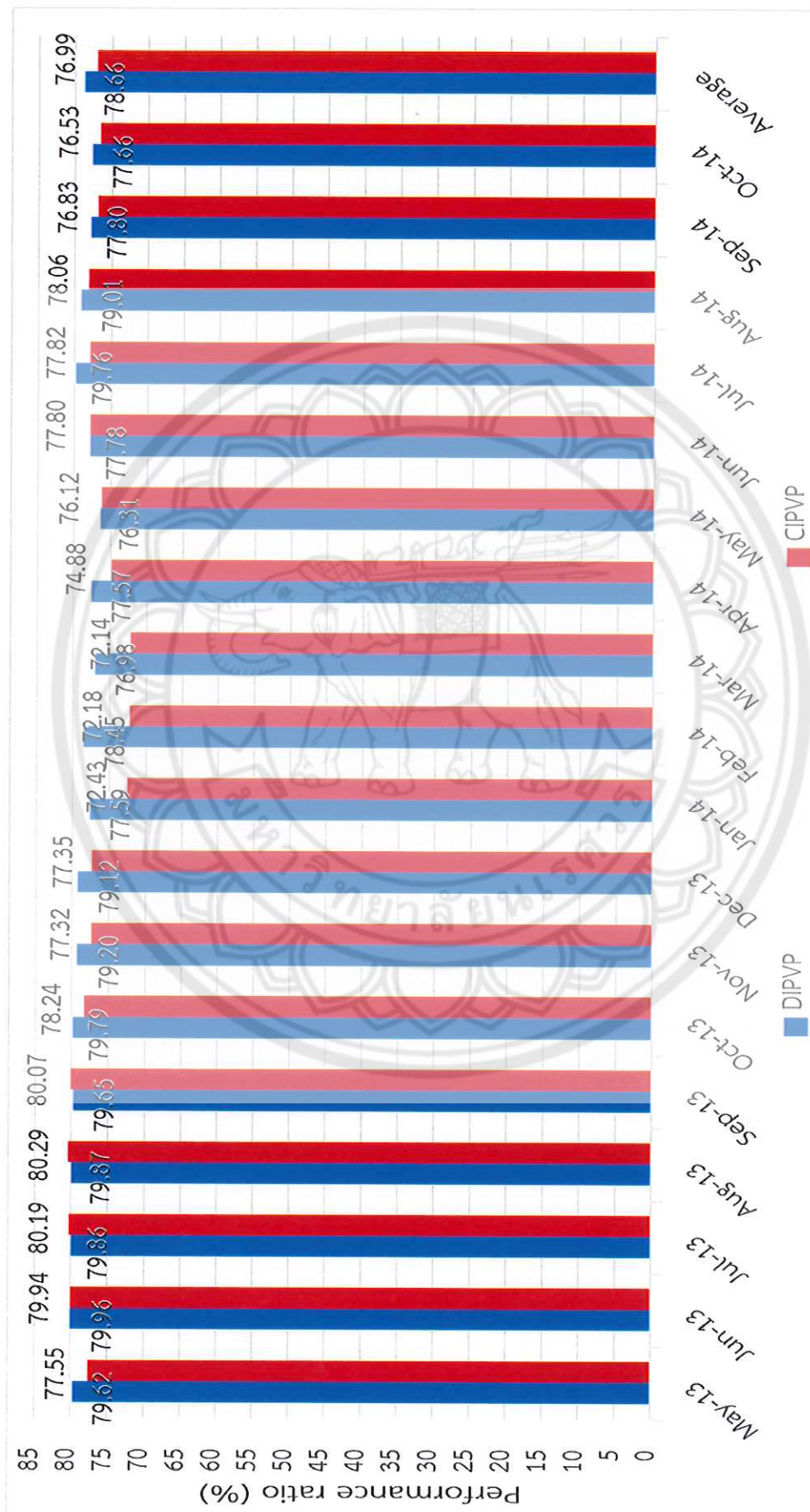


Figure 66 PR of DIPVP and CIPVP during May 2013 to October 2014

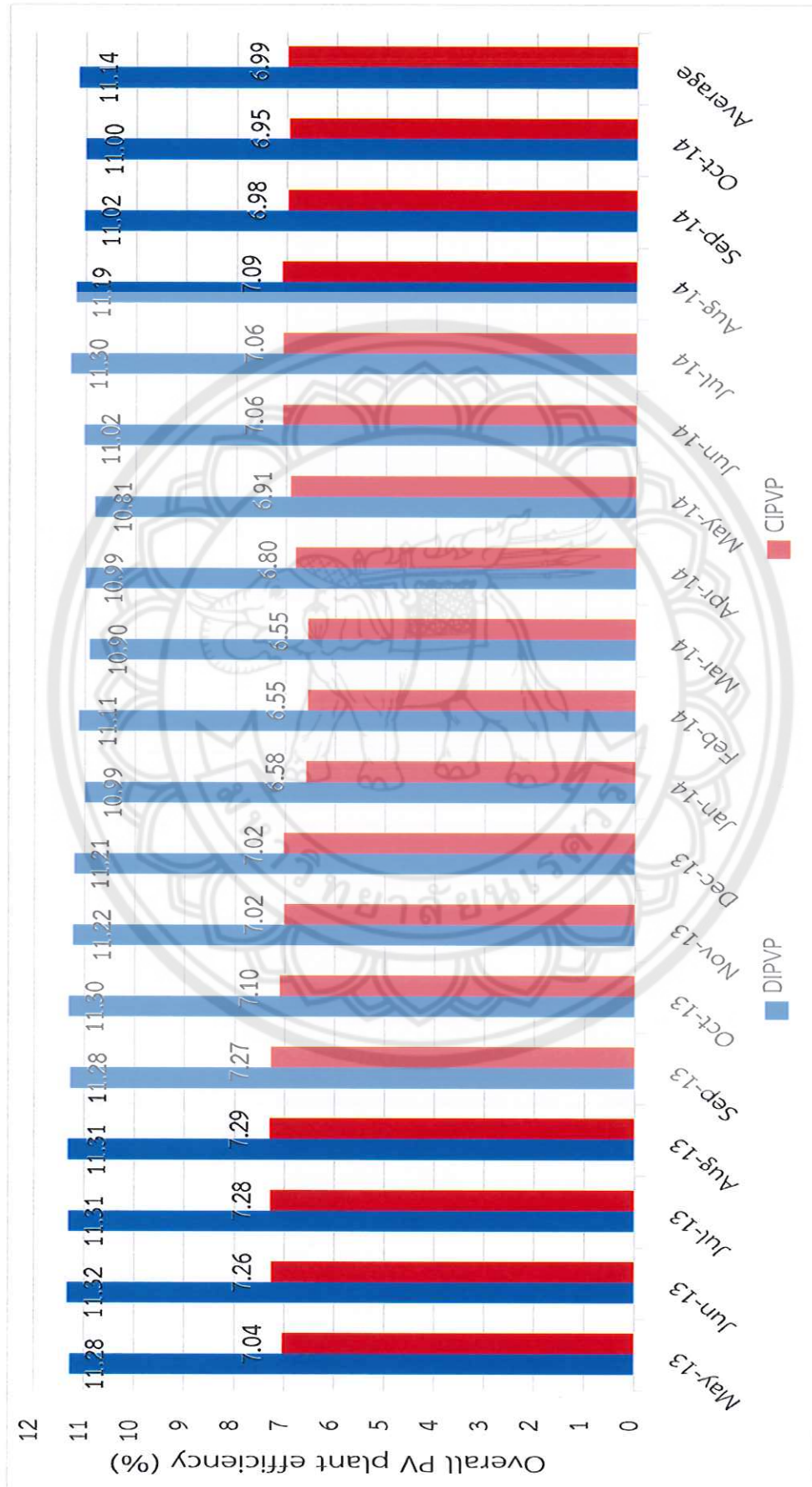


Figure 67 η_{tot} of DIPVP and CIPVP during May 2013 to October 2014

From the efficiency and performance evaluation result, it found that almost of evaluated parameters of DIPVP and CIPVP have no significant different except η_{tot} . The different PV module technologies is the main cause of the different η_{tot} . However, the different η_{tot} of these PV power plant is not directly effect to the availability and reliability evaluation. From these reasons, the reliability and availability evaluation result of DIPVP and CIPVP is mainly dominated by the decentralized and centralized inverter concepts of the PV power plan because the other factors that effect to the reliability and availability of these PV power plant is almost the same.

Availability and reliability evaluation result

After evaluating the availability and reliability of DIPVP and CIPVP, the evaluated result is presented as follows:

1. Inverter, other PV power plant component, and grid failures analysis result

Because of failure time of inverter, other PV power plant component, and grid effect to the generated power output of DIPVP and CIPVP in different degree, the failure time of each PV power plant component and grid have to estimate in equivalent PV power plant downtime form. In this form, the failure time of each PV power plant component and grid are calculated to the equivalent time that the PV power plants completely shutdown or stop operation. From the inverter, other PV power plant component, and grid failures analysis during May 2013 to October 2014, the equivalent PV power plant downtime of the inverter, other PV power plant component, grid, and total in DIPVP and CIPVP during May 2013 to October 2014 are displayed in Table 31 and Figure 46, 47, 48, and 49 respectively. From the table, the equivalent PV power plant downtime of the inverter in DIPVP is distributing in every month while CIPVP is concentrating in October 2014. The total equivalent PV power plant downtime of the inverter in DIPVP is lower than CIPVP. However, the equivalent PV power plant downtime of the inverter in CIPVP is possible lower than DIPVP when the failures analysis is longer because the inverter equivalent PV power plant downtime of CIPVP is very hardly occur while CIPVP is always occur in every month. For other PV power plant component, the equivalent PV power plant downtime of both PV power plants are scattering occur in many months. The total equivalent PV power plant downtime of

Table 9 The equivalent PV power plant downtime of the inverter, other PV power plant component, grid, and total in DIPVP and CIPVP during May 2013 to October 2014

| Month | Equivalent PV power plant downtime | | | | | | | |
|---------|------------------------------------|----------------|---------------|----------------|-------------------|----------------|---------------|----------------|
| | DIPVP | | | | CIPVP | | | |
| | Inverter (Min) | Other (Min) | Grid (Min) | Total (Min) | Inverter (Min) | Other (Min) | Grid (Min) | Total (Min) |
| May 13 | 7.92 | 0.00 | 217.00 | 224.92 | 0.00 | 0.00 | 0.00 | 0.00 |
| Jun 13 | 11.03 | 0.00 | 213.00 | 224.03 | 0.00 | 0.00 | 27.00 | 27.00 |
| Jul 13 | 8.63 | 0.00 | 674.00 | 682.63 | 0.00 | 0.00 | 334.00 | 334.00 |
| Aug 13 | 6.23 | 0.00 | 264.00 | 270.23 | 0.00 | 0.00 | 18.25 | 18.25 |
| Sep 13 | 9.83 | 0.00 | 254.00 | 263.83 | 0.00 | 387.75 | 50.00 | 437.75 |
| Oct 13 | 10.08 | 0.00 | 47.00 | 57.08 | 0.00 | 25.25 | 0.00 | 25.25 |
| Nov 13 | 5.52 | 0.00 | 0.00 | 5.52 | 0.00 | 13.00 | 20.00 | 33.00 |
| Dec 13 | 12.72 | 0.00 | 10.00 | 22.72 | 0.00 | 0.00 | 0.00 | 0.00 |
| Jan 14 | 18.50 | 0.12 | 4.00 | 22.62 | 0.00 | 0.00 | 75.00 | 75.00 |
| Feb 14 | 10.57 | 15.12 | 10.00 | 35.69 | 0.00 | 0.00 | 0.00 | 0.00 |
| Mar 14 | 12.23 | 345.34 | 46.00 | 403.57 | 0.00 | 0.00 | 0.00 | 0.00 |
| Apr 14 | 12.72 | 0.33 | 2.00 | 15.05 | 0.00 | 0.00 | 11.00 | 11.00 |
| May 14 | 18.17 | 0.29 | 5.00 | 23.45 | 0.00 | 0.00 | 10.00 | 10.00 |
| Jun 14 | 10.80 | 88.00 | 51.00 | 149.80 | 0.00 | 0.00 | 0.00 | 0.00 |
| Jul 14 | 12.48 | 0.00 | 21.00 | 33.48 | 0.00 | 0.00 | 0.00 | 0.00 |
| Aug 14 | 12.00 | 77.14 | 20.00 | 109.14 | 0.00 | 10.25 | 20.00 | 30.25 |
| Sep 14 | 11.77 | 0.00 | 49.00 | 60.77 | 0.00 | 26.00 | 0.00 | 26.00 |
| Oct 14 | 11.52 | 13.54 | 99.00 | 124.06 | 262.50 | 45.00 | 0.00 | 307.50 |
| Total | 202.72 | 539.88 | 1986.00 | 2728.59 | 262.50 | 507.25 | 565.25 | 1335.00 |
| Average | 11.26 | 29.99 | 110.33 | 151.59 | 14.58 | 28.18 | 31.40 | 74.17 |

the other PV power plant component in CIPVP is slightly lower than DIPVP. The equivalent PV power plant downtime of the grid in DIPVP and CIPVP are distributing in every month. Nevertheless, the equivalent PV power plant downtime of the grid in DIPVP in each month usually far higher than CIPVP. Moreover, the total equivalent PV power

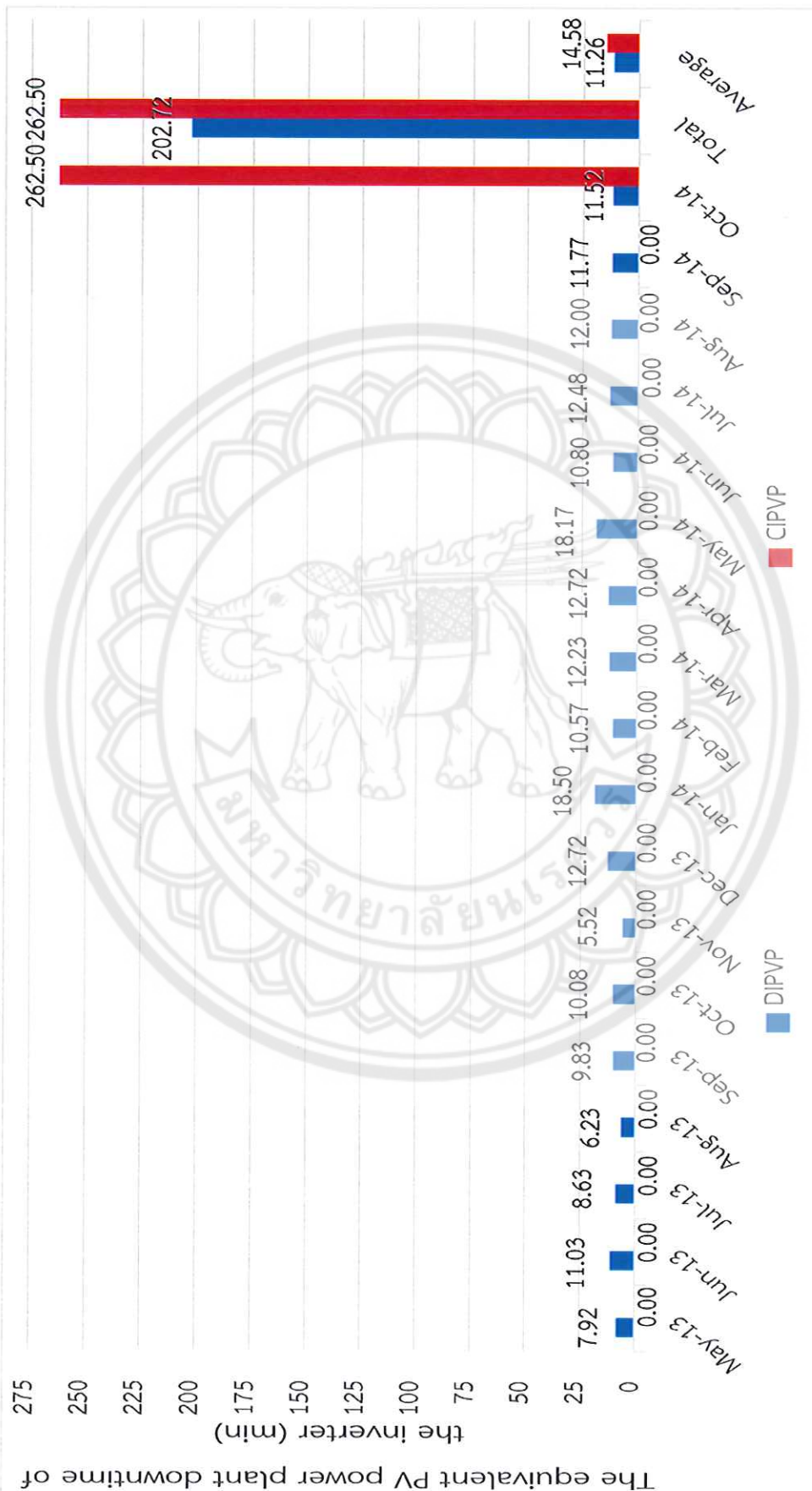


Figure 68 The equivalent PV power plant downtime of the inverter in DIPVP and CIPVP during May 2013 to October 2014

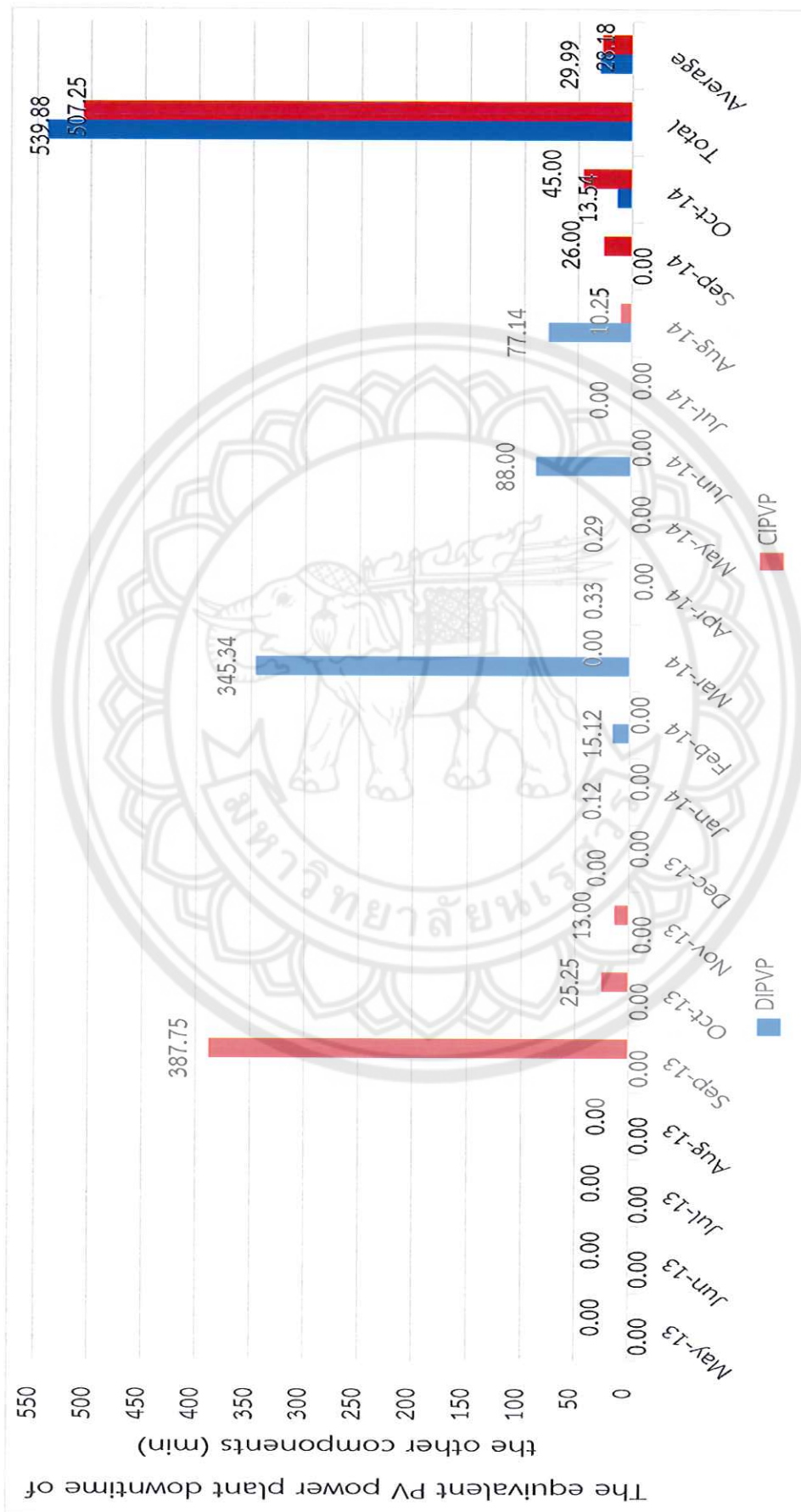


Figure 69 The equivalent PV power plant downtime of the other PV power plant component in

DIPVP and CIPVP during May 2013 to October 2014

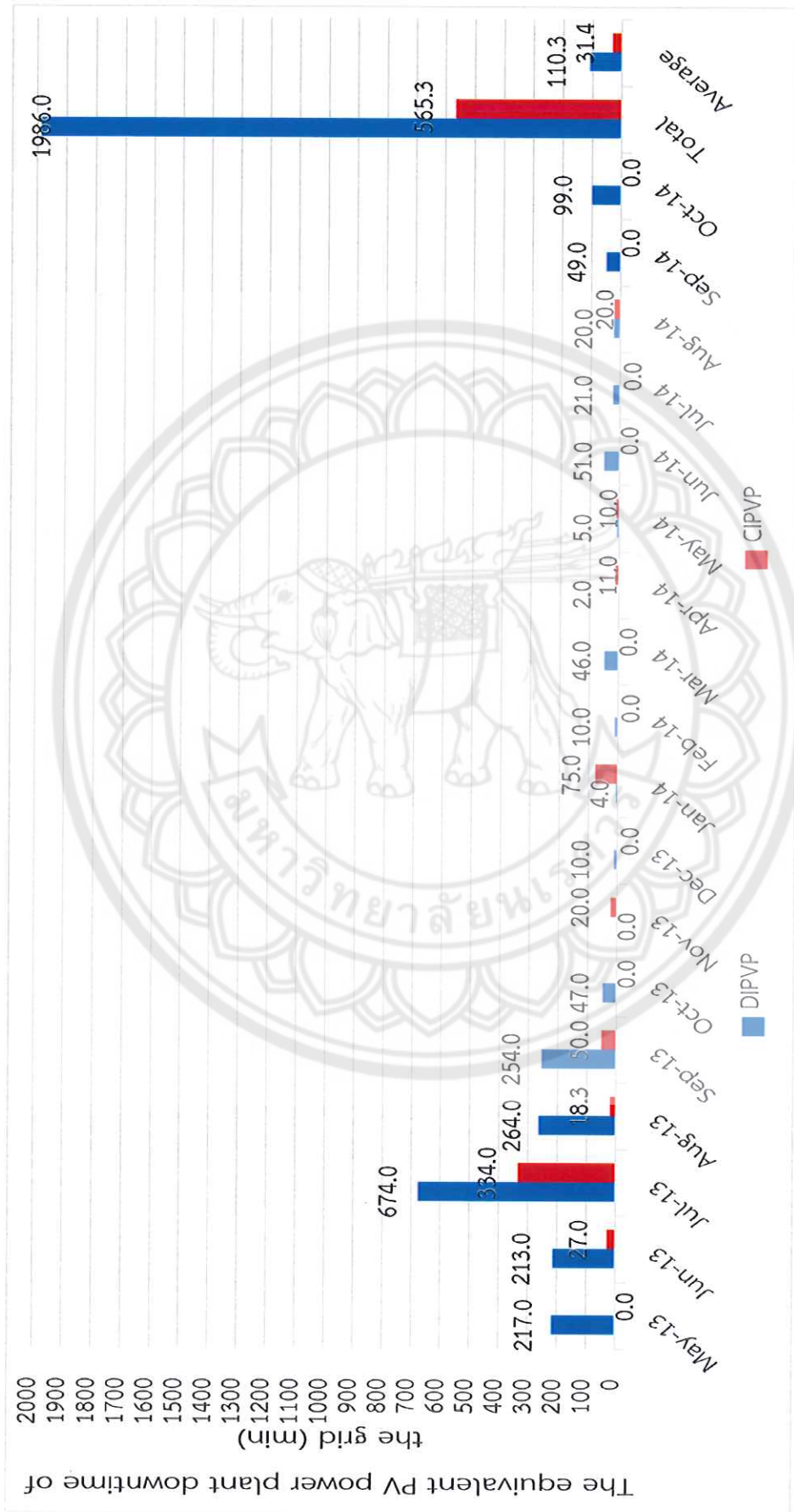


Figure 70 The equivalent PV power plant downtime of the grid in DIPVP and CIPVP during May 2013 to October 2014

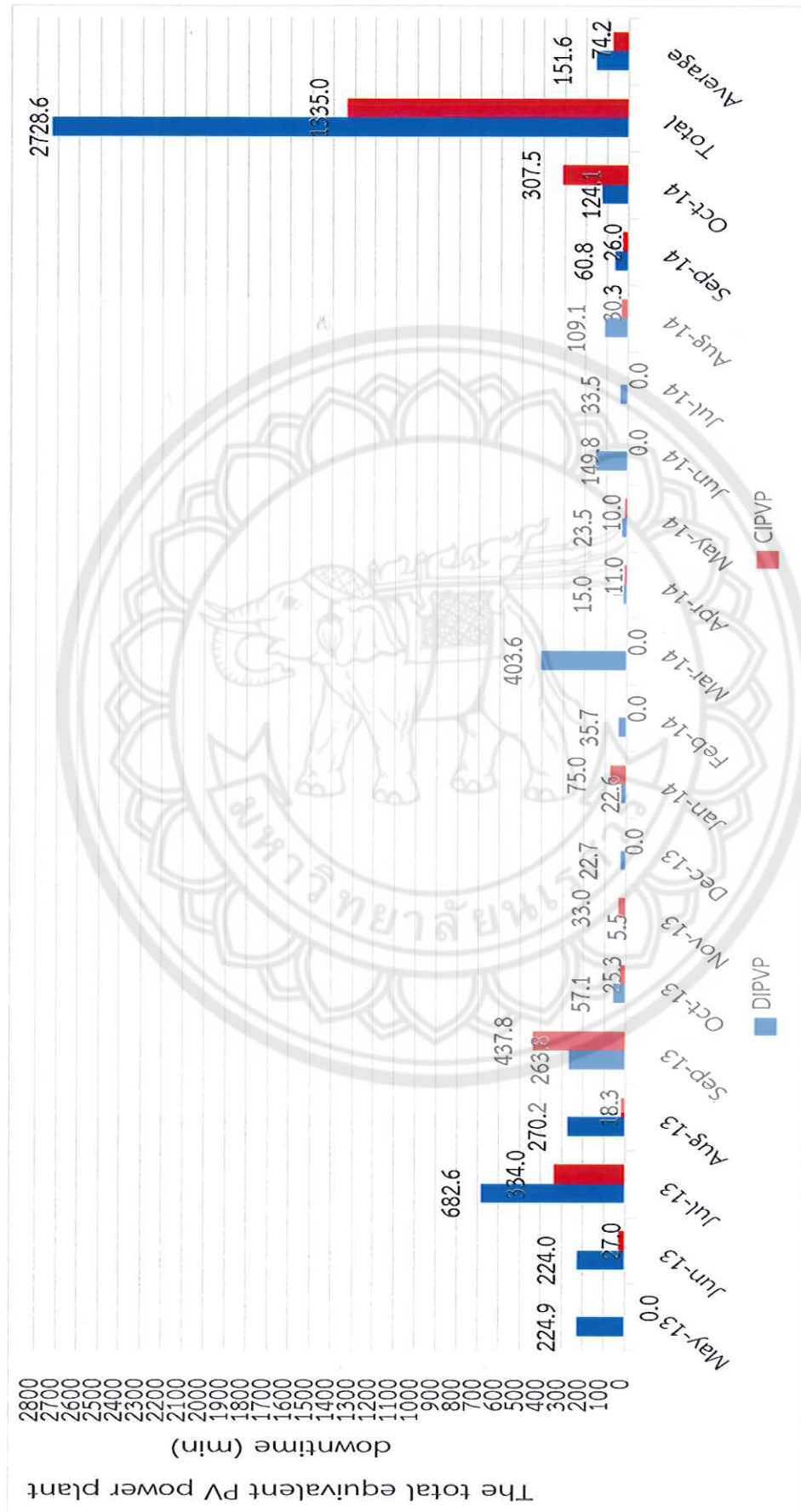


Figure 71 The total equivalent PV power plant downtime in DIPVP and CIPVP during May 2013 to October 2014

plant downtime of the grid in DIPVP is also far higher than DIPVP too. The total equivalent PV power plant downtime of DIPVP is available in every month while CIPVP is not available in many months. In addition, the total equivalent PV power plant downtime of DIPVP is far higher than CIPVP. The cause of the far higher total equivalent PV power plant downtime is mainly from the grid equivalent PV power plant downtime of DIPVP during May to September 2013 that grid network in of the PV power plant is still not modified. From these result, it found that grid failure plays the most important role in the total equivalent PV power plant downtime and the other PV power plant components is the second important factor. The MV equipment failure is the most significant factor that dominate the equivalent PV power plant downtime of the other PV power plant component failure because this failure effects the entire PV power plant while other component failure effects only a part of PV power plant. For inverter failure, string inverter failure always occur in every month but effects to only a very small part of the PV power plant while central inverter failure hardly occur only a time per year but effect to the large part of the PV power plant. From this point, the equivalent PV power plant downtime of the string inverter is really constant in each month while the central inverter is always zero but peak only a time per year. It is result that the equivalent PV power plant downtime of the central inverter depend on the analysis period.

2. Availability evaluated result

The availability evaluation of DIPVP and CIPVP is based on the total time and the equivalent PV power plant downtime data. The total time is the total period that the equipment could be called upon to perform its intended purpose or the enough irradiance exists and all other external conditions are met that the system will function as intended and produce rated power. From this definition, it is possible to estimate the total time of DIPVP and CIPVP from the monitoring data of these PV power plant. From the monitoring data, the estimated total time of each day are classified in 3 group that based on the DIPVP and CIPVP operation period. First, long operation period during May to August is the period that these PV power plant operate for 12 hours during 6.30 to 18.30. Second, medium operation period during September to October and March and April is the period that these PV power plant operate for 11.5 hours during 6.45 to 18.15. Third, short operation period during November to February is the period that these PV power plant operate for 11 hours during 7.00 to 18.00. Because of an objective of this

dissertation is analyzing and comparing reliability and availability of PV power system applying decentralized and centralized inverter concepts, the total time without grid failure is a necessary parameter that has to estimate for higher accurate availability evaluation. The estimated total time and total time without grid failure of DIPVP and CIPVP in each month during May 2013 to October 2014 is available in Table 32 and Figure 50. From the table, the total time in each month is various follow the number of day in each month and the operation period group. The total time without grid failure of CIPVP is higher than DIPVP about 1,421 minute that indicate the higher stability of CIPVP grid network specially during May to September 2013. However, the total time without grid failure of these PV power plant are not different after September 2013 that point out the grid network improvement of DIPVP. From the total time and the equivalent PV power plant downtime data, the availability of DIPVP and CIPVP during May 2013 to October 2014 are evaluated and the availability evaluation is separated in 2 cases that are the availability with and without grid failure. The evaluation result of the availability with and without grid failure in DIPVP and CIPVP during May 2013 to October 2014 is illustrated in Table 33 and Figure 51 and 52. From the table, the availability with grid failure of CIPVP is higher than DIPVP in nearly every month except in September 2013, November 2013, January 2014, and October 2014. The average availability with grid failure of CIPVP at 99.65 % is also higher than DIPVP at 99.29 %. The cause that dominate the availability with grid failure of DIPVP is mainly from the grid failure that higher than CIPVP about 4 times. For inverter, and other PV power plant component failure, they are not significant different in DIPVP and CIPVP and far lower than grid failure that almost not effecting to the availability with grid failure of both PV power plants. From this result, it is not obviously specifying the availability of the PV power system that applying decentralized or centralized inverter concept is higher to comply the first objective of this thesis. To complete the first objective, the availability without grid failure in DIPVP and CIPVP have to evaluate. From the evaluation result in Table 31, the availability without grid failure of CIPVP is higher than DIPVP in nearly every month except in September 2013, October 2013, November 2013, January 2014, and October 2014. However, the average availability without grid failure of CIPVP at 99.80 % is

Table 10 The estimated total time and total time without grid failure of DIPVP and CIPVP in each month during May 2013 to October 2014

| Month | The estimated total time (Minute) | | |
|---------|-----------------------------------|----------------------------------|----------------------------------|
| | With grid failure | Without grid failure of DIPVP | Without grid failure of CIPVP |
| May 13 | 22,320 | 22,103 | 22,320 |
| Jun 13 | 21,600 | 21,387 | 21,573 |
| Jul 13 | 22,320 | 21,646 | 21,986 |
| Aug 13 | 22,320 | 22,056 | 22,302 |
| Sep 13 | 20,700 | 20,446 | 20,650 |
| Oct 13 | 21,390 | 21,343 | 21,390 |
| Nov 13 | 19,800 | 19,800 | 19,780 |
| Dec 13 | 20,460 | 20,450 | 20,460 |
| Jan 14 | 20,460 | 20,456 | 20,385 |
| Feb 14 | 18,480 | 18,470 | 18,480 |
| Mar 14 | 21,390 | 21,344 | 21,390 |
| Apr 14 | 20,700 | 20,698 | 20,689 |
| May 14 | 22,320 | 22,315 | 22,310 |
| Jun 14 | 21,600 | 21,549 | 21,600 |
| Jul 14 | 22,320 | 22,299 | 22,320 |
| Aug 14 | 22,320 | 22,300 | 22,300 |
| Sep 14 | 20,700 | 20,651 | 20,700 |
| Oct 14 | 21,390 | 21,291 | 21,390 |
| Total | 382,590 | 380,604 | 382,025 |
| Average | 21,255 | 21,145 | 21,224 |

the same with DIPVP. The result evidently stipulates the availability of the PV power system that applying decentralized and centralized inverter concept in the evaluation period and complies the first objective of this dissertation. The cause that dominate the availability without grid failure of DIPVP and CIPVP are inverter, and other PV power plant component failure. The other PV power plant component failure is randomly occur

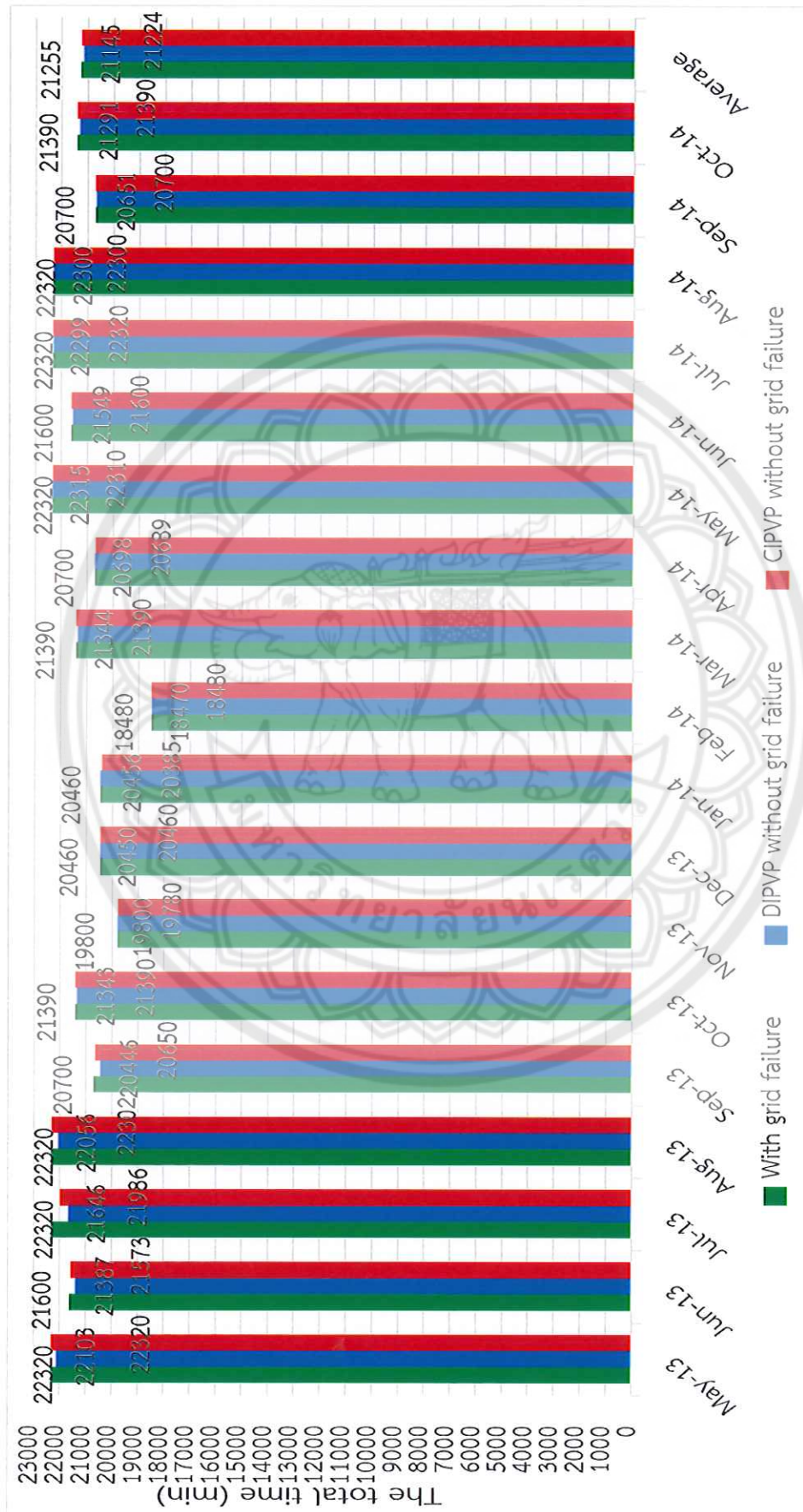


Figure 72 The estimated total time and total time without grid failure of DIPVP and CIPVP in each month during May 2013 to October 2014

Table 11 The evaluation result of the availability with and without grid failure in DIPVP and CIPVP during May 2013 to October 2014

| Month | The availability of DIPVP (%) | | The availability of CIPVP (%) | |
|---------|-------------------------------|----------------------|-------------------------------|----------------------|
| | With grid failure | Without grid failure | With grid failure | without grid failure |
| May 13 | 98.99 | 99.96 | 100.00 | 100.00 |
| Jun 13 | 98.96 | 99.95 | 99.88 | 100.00 |
| Jul 13 | 96.94 | 99.96 | 98.50 | 100.00 |
| Aug 13 | 98.79 | 99.97 | 99.92 | 100.00 |
| Sep 13 | 98.73 | 99.95 | 97.89 | 98.12 |
| Oct 13 | 99.73 | 99.95 | 99.88 | 99.88 |
| Nov 13 | 99.97 | 99.97 | 99.83 | 99.93 |
| Dec 13 | 99.89 | 99.94 | 100.00 | 100.00 |
| Jan 14 | 99.89 | 99.91 | 99.63 | 100.00 |
| Feb 14 | 99.81 | 99.86 | 100.00 | 100.00 |
| Mar 14 | 98.11 | 98.32 | 100.00 | 100.00 |
| Apr 14 | 99.93 | 99.94 | 99.95 | 100.00 |
| May 14 | 99.89 | 99.92 | 99.96 | 100.00 |
| Jun 14 | 99.31 | 99.54 | 100.00 | 100.00 |
| Jul 14 | 99.85 | 99.94 | 100.00 | 100.00 |
| Aug 14 | 99.51 | 99.60 | 99.86 | 99.95 |
| Sep 14 | 99.71 | 99.94 | 99.87 | 99.87 |
| Oct 14 | 99.42 | 99.88 | 98.56 | 98.56 |
| Average | 99.29 | 99.80 | 99.65 | 99.80 |

with the no different rate in the both PV power plants. The inverter failure is continuously occur in DIPVP while hardly occur in CIPVP. From this point, the trend of the average availability without grid failure when extend the evaluation period in DIPVP is really constant while CIPVP is continuously increasing until the next inverter failure that the average availability without grid failure is sharply decreasing again.

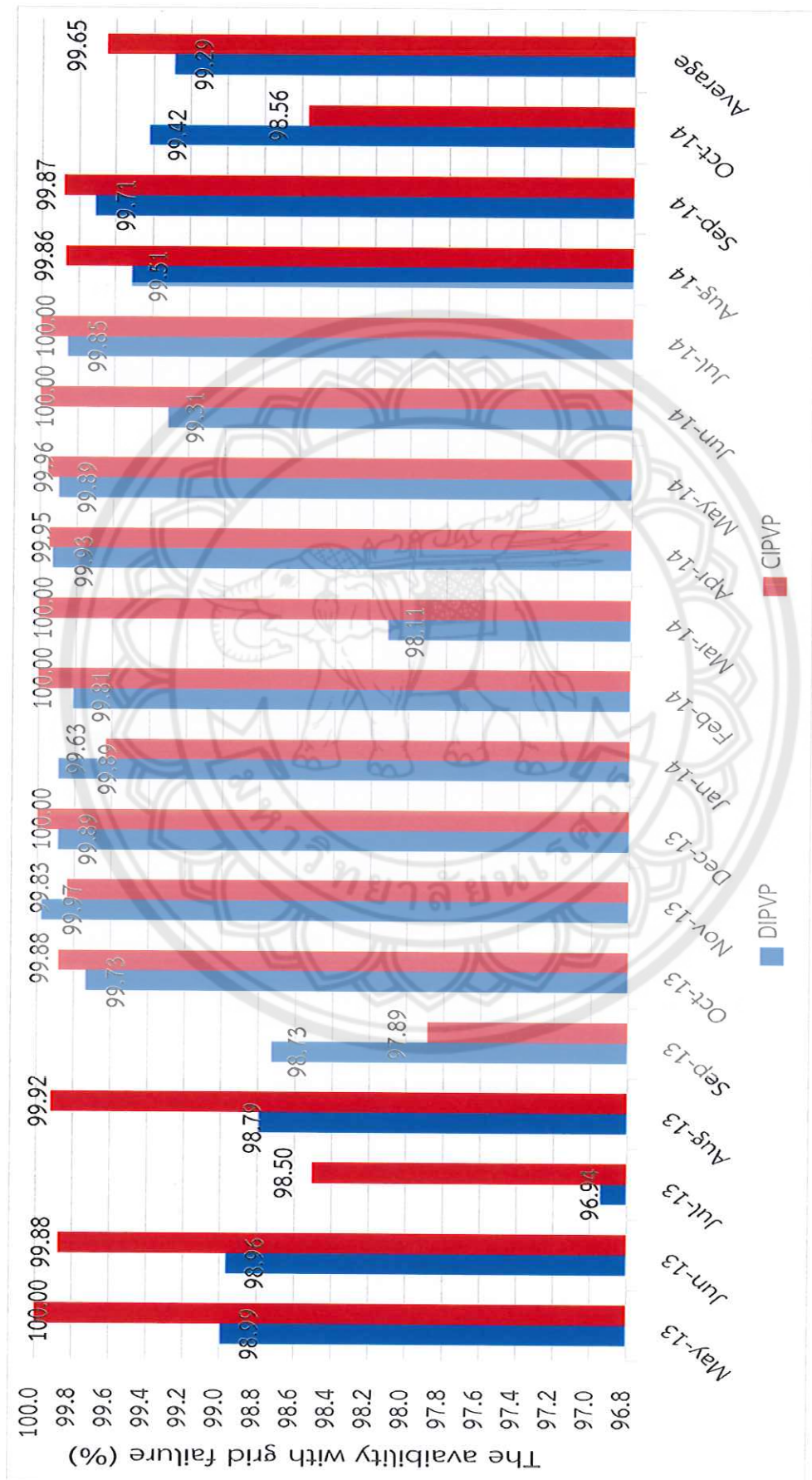


Figure 73 The evaluation result of the availability with grid failure in DIPVP and CIPVP during May 2013 to October 2014

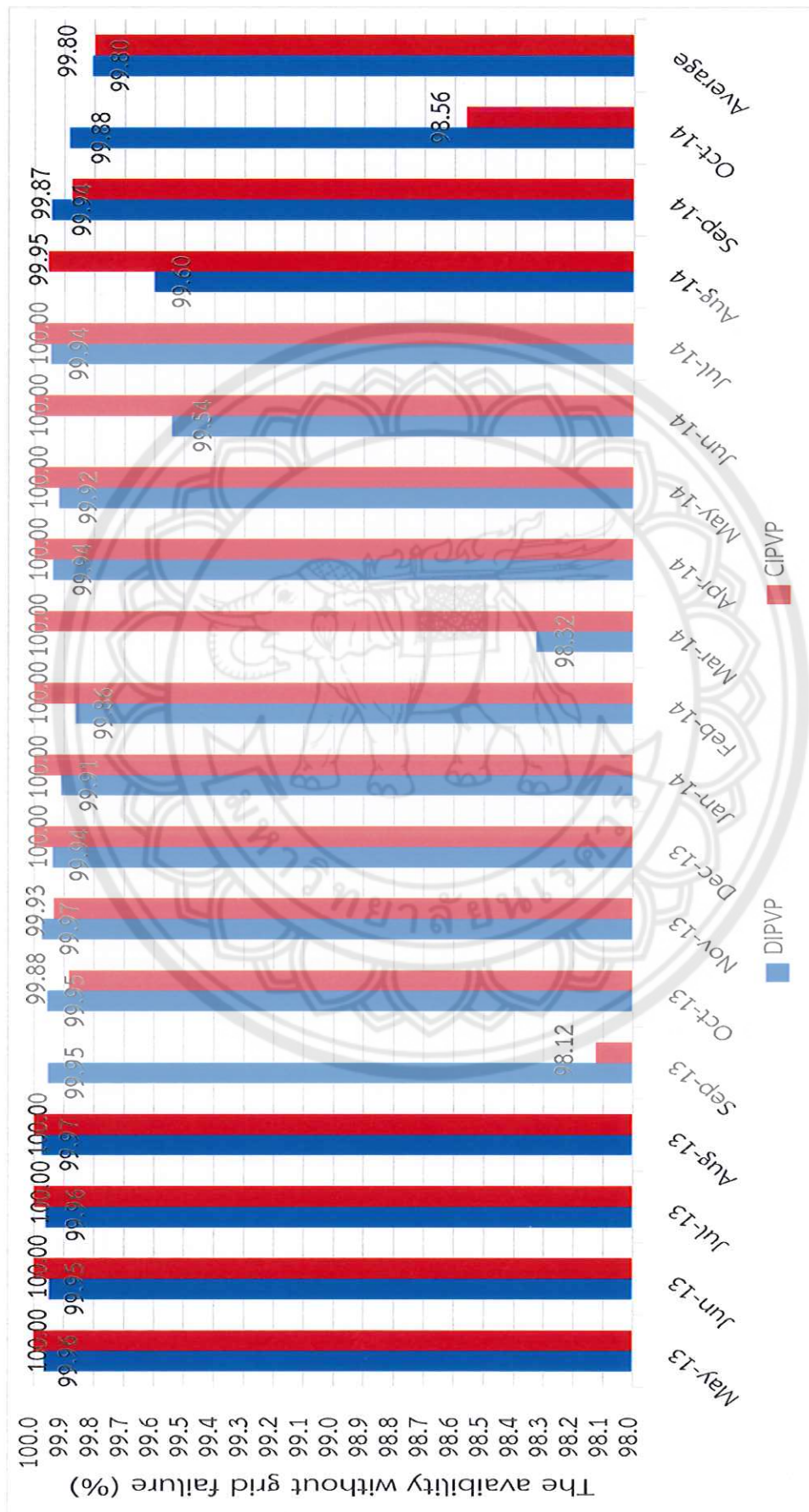


Figure 74 The evaluation result of the availability without grid failure in DIPVP and CIPVP during May 2013 to October 2014

The availability evaluated result clearly indicates that the PV power system applying decentralized and centralized inverter concepts have not significant different in availability during evaluation period. However, the availability trend of the PV power system applying decentralized concept is really steady while centralized inverter concepts is sharply decreasing when inverter failure occur and continuously increasing until the next inverter failure. To evaluate the higher precise availability of the PV power system applying decentralized and centralized inverter concepts, the life time evaluation period at 25 years is necessary for availability evaluation of the PV power system applying both concepts. This evaluated result complete a part of the first objective of this dissertation.

3. Reliability evaluated result

The definition of reliability is the probability that a system will operate properly for a specified time period under the design operating conditions without failure. From the definition, the number of each PV power plant component and the failure data of each component in the PV power plant are necessary in the reliability evaluation. However, these necessary data are not complete for DIPVP and CIPVP. Therefore the reliability evaluation is scope in only inverter because the necessary data for inverter reliability evaluation in DIPVP and CIPVP are available for evaluation. In addition, the first objective of this thesis is focusing on the reliability of PV power system applying decentralized and centralized inverter concepts that inverter play the most important role in these PV system concepts. The inverter reliability evaluation result of DIPVP and CIPVP is possible pointing out the entire PV power plant reliability trend of these PV power plant. The inverter reliability evaluation of DIPVP and CIPVP is based on the total number of inverters that failed in the sample population during the time period and total number of inverters in these PV power plant. Because of the inverter number of DIPVP and CIPVP are not equal, it has to estimate the inverter failure of these PV power plant in the inverter failure probability form. The evaluation period is between May 2013 and October 2014. The inverter failure probability and the inverter reliability evaluated result of DIPVP and CIPVP during May 2013 to October 2014 is presented in Table 34 and Figure 53 and 54. From the table, the inverter failure probability in each month of DIPVP is fluctuation between 1.84 and 6.16 % while CIPVP is constant at 100 % except in October 2014. The total inverter failure probability of DIPVP at 67.60 % is

far higher than CIPVP at 10 % that is the result from the massive inverter failure number at 854 inverters in DIPVP during evaluation period. From the evaluated result, the inverter reliability in each month of DIPVP is scattering in 93.84 to 98.16 % range while CIPVP is stable at 100% except in October 2014. The total inverter reliability of DIPVP at 32.40 % is far lower than CIPVP at 90 % that is the result from the great inverter failure probability at 67.60 % in DIPVP during evaluation period. The result obviously specifies

Table 12 The inverter failure probability and the inverter reliability evaluated result of DIPVP and CIPVP during May 2013 to October 2014

| Month | DIPVP | | CIPVP | |
|--------|---------------------|-------------|---------------------|-------------|
| | Failure probability | Reliability | Failure probability | Reliability |
| | (%) | (%) | (%) | (%) |
| May 13 | 2.64 | 97.36 | 0.00 | 100.00 |
| Jun 13 | 3.68 | 96.32 | 0.00 | 100.00 |
| Jul 13 | 2.88 | 97.12 | 0.00 | 100.00 |
| Aug 13 | 2.08 | 97.92 | 0.00 | 100.00 |
| Sep 13 | 3.28 | 96.72 | 0.00 | 100.00 |
| Oct 13 | 3.36 | 96.64 | 0.00 | 100.00 |
| Nov 13 | 1.84 | 98.16 | 0.00 | 100.00 |
| Dec 13 | 4.24 | 95.76 | 0.00 | 100.00 |
| Jan 14 | 6.16 | 93.84 | 0.00 | 100.00 |
| Feb 14 | 3.52 | 96.48 | 0.00 | 100.00 |
| Mar 14 | 4.08 | 95.92 | 0.00 | 100.00 |
| Apr 14 | 4.24 | 95.76 | 0.00 | 100.00 |
| May 14 | 6.08 | 93.92 | 0.00 | 100.00 |
| Jun 14 | 3.60 | 96.40 | 0.00 | 100.00 |
| Jul 14 | 4.16 | 95.84 | 0.00 | 100.00 |
| Aug 14 | 4.00 | 96.00 | 0.00 | 100.00 |
| Sep 14 | 3.92 | 96.08 | 0.00 | 100.00 |
| Oct 14 | 3.84 | 96.16 | 10.00 | 90.00 |
| Total | 67.60 | 32.40 | 10.00 | 90.00 |

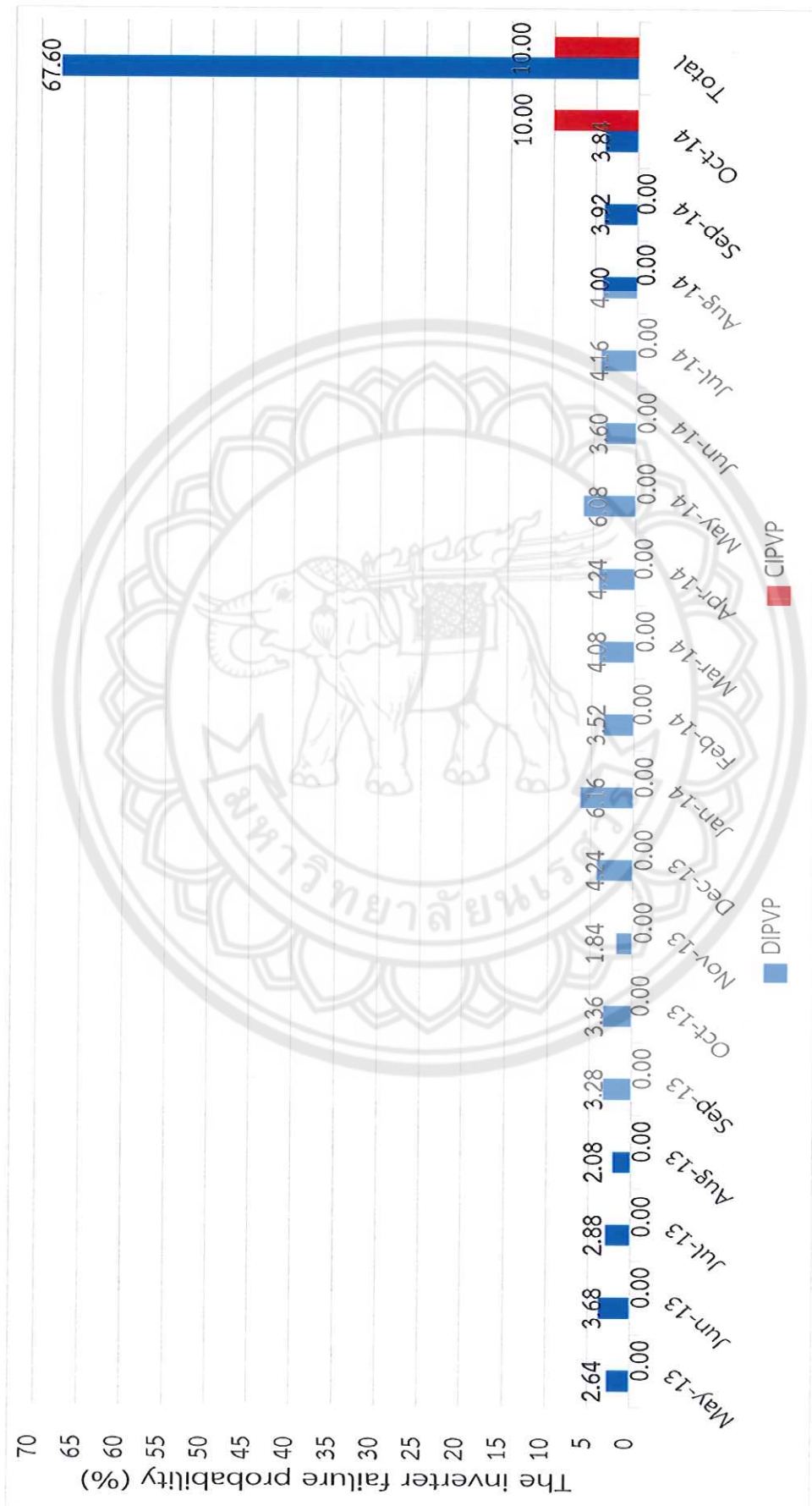


Figure 75 The inverter failure probability evaluated result of DIPVP and CIPVP during May 2013 to October 2014

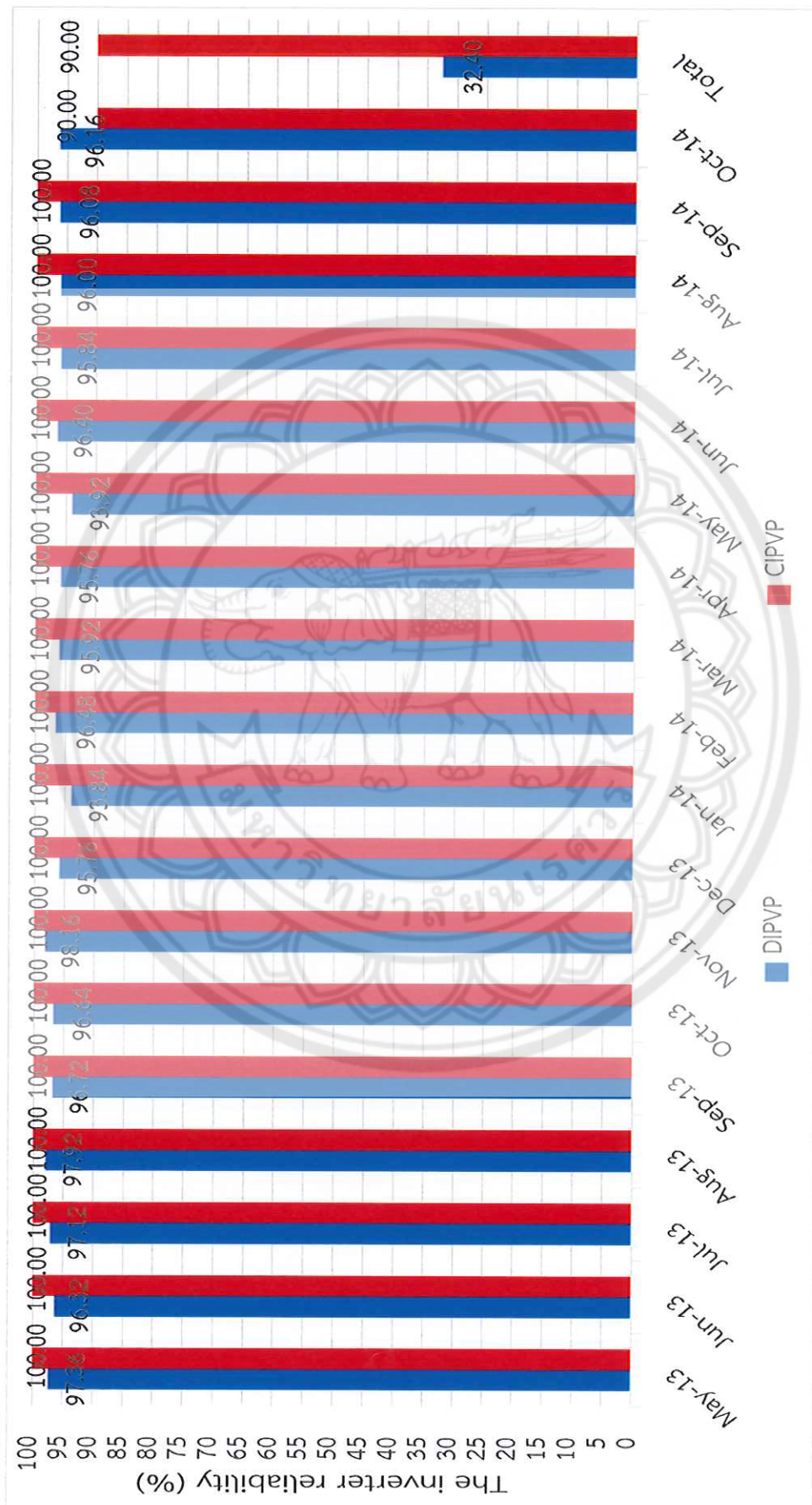


Figure 76 The inverter reliability evaluated result of DIPVP and CIPVP during May 2013 to October 2014

that the reliability of central inverter is far higher than string inverter. Moreover, it is possible to imply that the reliability of the PV power system applying centralized inverter concepts is far higher than decentralized inverter concepts and complies the first objective of this dissertation. The cause that dominate the inverter reliability of DIPVP and CIPVP are inverter failure. This failure is continuously occur in DIPVP while hardly occur in CIPVP. The continuous inverter failure in DIPVP is possible from the outdoor installation that the inverter has to endure extreme weather condition and thermal stress. In addition, the manufacturing quality is another cause of high inverter failure in DIPVP. From this reason, the trend of the total reliability when extend the evaluation period in DIPVP is continuously decreasing while CIPVP is standing at the same value until the next inverter failure that the total reliability is decreasing again.

The reliability evaluated result explicitly mentions that the reliability of central inverter is far better than string inverter and it can signify that the PV power system applying decentralized inverter concepts has far worse reliability than centralized inverter concepts during evaluation period. Furthermore, the reliability trend of the PV power system applying decentralized concept is endlessly reducing while centralized inverter concepts is decreasing when inverter failure occur and steadying until the next inverter failure. To evaluate the higher accurate reliability of the PV power system applying decentralized and centralized inverter concepts, the total PV power plant component failure and the life time evaluation period at 25 years is essential for reliability evaluation of the PV power system applying both concepts. This evaluated result complete another part of the first objective of this dissertation.

Economic analysis result

In the economic analysis, there are 3 indicators such as Cost per Unit or Levelized cost of Energy (LCOE), Net Present Value (NPV), and Internal Rate of Return (IRR) that calculated by using the performance, availability, and reliability evaluation result in DIPVP and CIPVP. In addition, these indicators are estimated based on 25 year system life time, PV system energy output degradation at 0.8 %/year, electricity cost increasing at 2 %/year with the initial electricity cost at 3,679.6 Baht/MWh for peak period with 244 days/year and 2,176.0 Baht/MWh for off peak period with 121 days/year, CO₂ price at 640 Baht/ton, and O&M cost at 2% of

investment cost/year and increasing at 3 %/year. For NPV, IRR, and COE calculation, the discount factor is 4 %. The investment and replacement cost are 250 and 25 million Baht for 5 MW PV power plant. 8.0 Baht/kWh adder for 10 year (Feed in tariff) is the considered subsidy case in this economic analysis. There are 2 availability options that are the availability with and without grid failure are diagnose in the economic analysis. For the economic analysis result in each indicator, it is presented follow this:

1. Cost per Unit and Levelized Cost of Energy (LCOE)

Cost per Unit and Levelized Cost of Energy (LCOE) are the indicators that specify the total production cost per unit of product. So, the subsidy scheme is not effect to these indicators. The different of these indicators are the discount factor that not included in Cost per Unit but included in LCOE. The actual availability of DIPVP and CIPVP are 99.29 and 99.65 % respectively. Cost per Unit with the actual availability of DIPVP and CIPVP are 2,895.87 and 2,880.70 Baht/MWh respectively or 2.90 and 2.88 Baht/kWh respectively while LCOE with the actual availability of these PV power plants are 3,721.93 and 3,702.46 Baht/MWh respectively or 3.72 and 3.70 Baht/kWh respectively. For the availability without grid failure case, DIPVP and CIPVP have the availability at 99.80 %. Cost per Unit with these availability of DIPVP and CIPVP are 2,880.84 and 2,876.45 Baht/MWh respectively or 2.88 Baht/kWh while LCOE with the availability without grid failure of these PV power plants are 3,702.61 and 3,696.96 Baht/MWh respectively or 3.70 Baht/kWh. Cost per Unit and LCOE with the both availability case of DIPVP and CIPVP are showed in Figure 55. From the Figure, Cost per Unit and LCOE with the actual availability of DIPVP are higher than CIPVP about 15.171 and 19.498 Baht/MWh respectively or 0.015 and 0.020 Baht/kWh respectively while Cost per Unit and LCOE with the availability without grid failure of DIPVP are higher than CIPVP about 4.393 and 5.646 Baht/MWh respectively or 0.004 and 0.006 Baht/kWh respectively. On the one hand, this result reflexes the influence of grid failure to Cost per Unit and LCOE. On the other hand, the PV power system applying centralized or decentralized inverter concepts is not significant domination to Cost per Unit and LCOE. However, Cost per Unit of these PV power plants are still higher than the present electricity

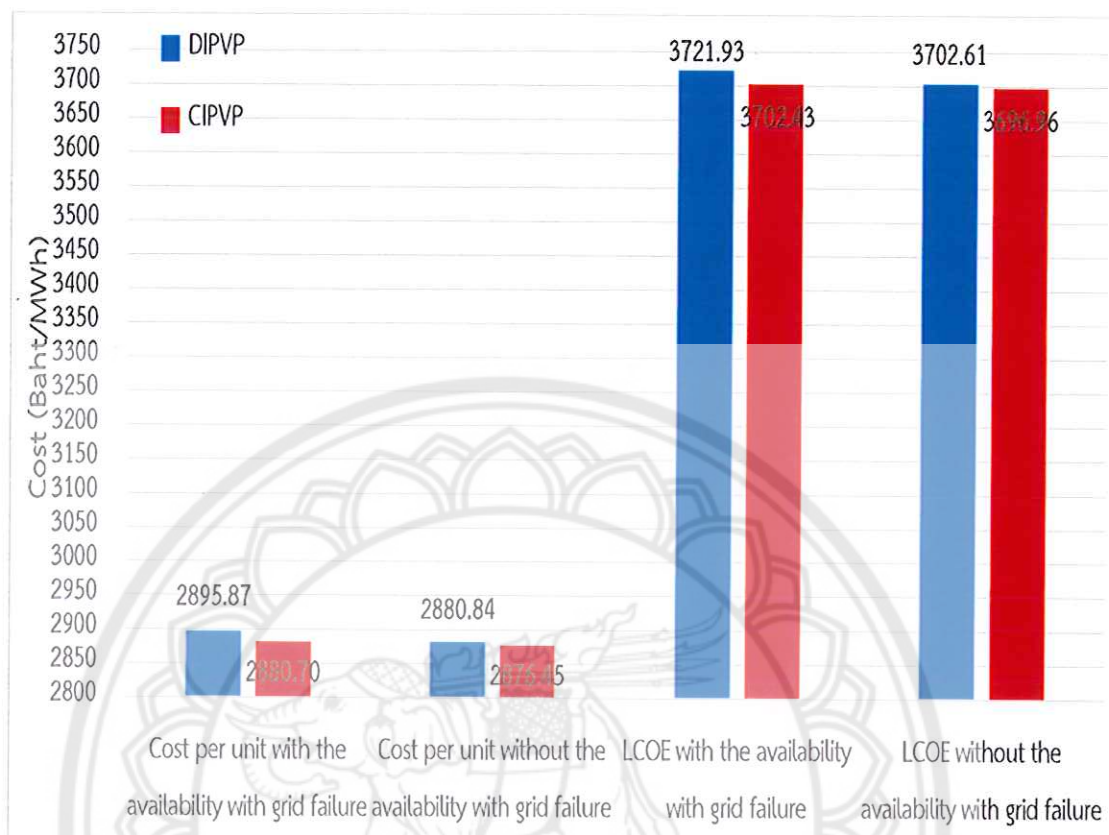


Figure 77 Cost per Unit and LCOE with the both availability case of DIPVP and CIPVP

cost in Thailand during off peak period and LCOE of these PV power plants are a little bit higher than present electricity cost in Thailand during off peak period that indicate the infeasibility in commercial of these PV power plant in no subsidy case but feasibility in commercial for 8.0 Baht/kWh adder for 10 year subsidy case. The result of Cost per Unit and LCOE comply a part of the second objective in this thesis.

2. Net Present Value (NPV)

The availability with grid failure of DIPVP and CIPVP are 99.29 and 99.65 % respectively while the availability without grid failure of these PV power plants are 99.80 and 99.80 % respectively. For 8.0 Baht/kWh adder for 10 year subsidy case, Net Present Value (NPV) with the availability with grid failure of DIPVP and CIPVP are 452.58 and 457.30 million Baht respectively while NPV with the availability without grid failure of these PV power plants are 457.25 and 458.63 million Baht respectively. NPV

with the both availability case of DIPVP and CIPVP are displayed in Figure 56. From the Figure, NPV with the availability with and without grid failure of DIPVP is lower

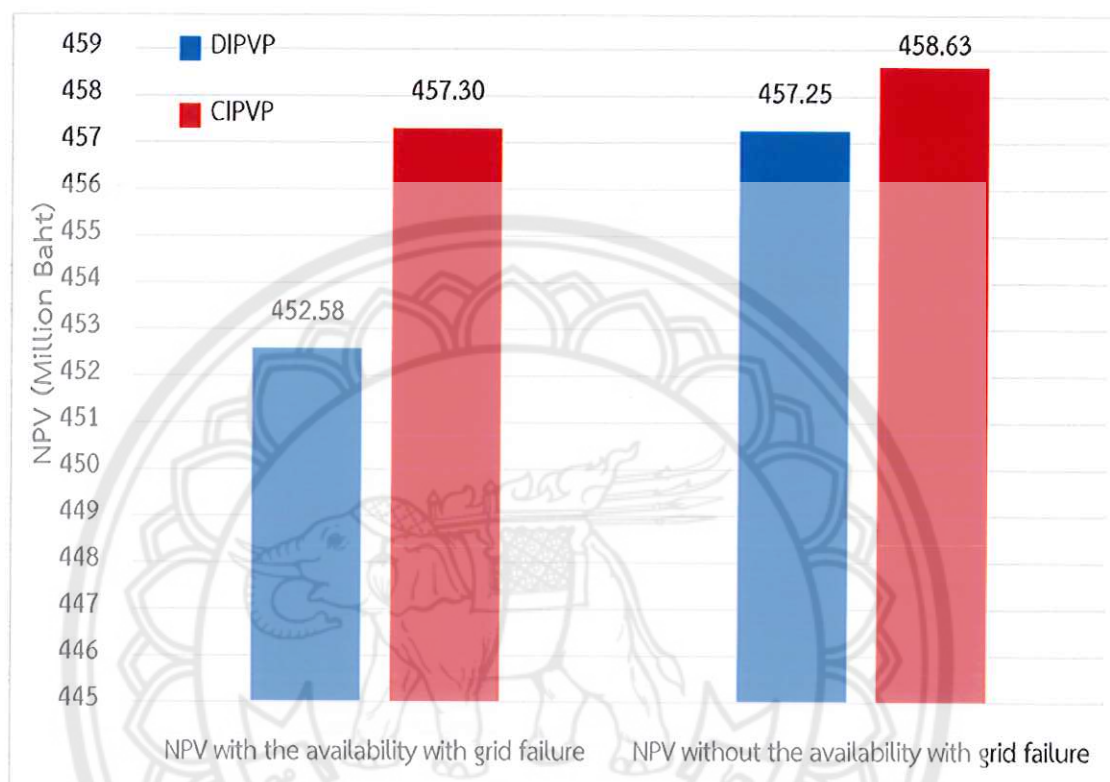


Figure 78 NPV with the both availability case of DIPVP and CIPVP PV power plant

CIPVP about 4.72 and 1.38 million Baht respectively. From this point, it presents that the grid failure effect is far higher than the effect from the PV power system applying centralized or decentralized inverter concepts in NPV analysis. NPV in such high value of DIPVP and CIPVP in 8.0 Baht/kWh adder for 10 year subsidy case is supporting the feasibility in commercial of these PV power plant. The result of NPV complies a part of the second objective in this dissertation.

3. Internal Rate of Return (IRR)

For 8.0 Baht/kWh adder for 10 year subsidy case, Internal Rate of Return (IRR) with the availability with and without grid failure at 99.29 and 99.80 % respectively of DIPVP and CIPVP are 24.67 and 24.86 % respectively while IRR with the availability with and without grid failure at 99.65 and 99.80 % respectively of CIPVP are 24.86 and

24.92 % respectively. IRR with the both availability case of DIPVP and CIPVP are displayed in Figure 57. From the Figure, IRR with the availability with and without grid failure of DIPVP is lower than CIPVP about 0.19 and 0.06 % respectively. This result stipulates that the grid failure influence is far higher than the domination from the PV

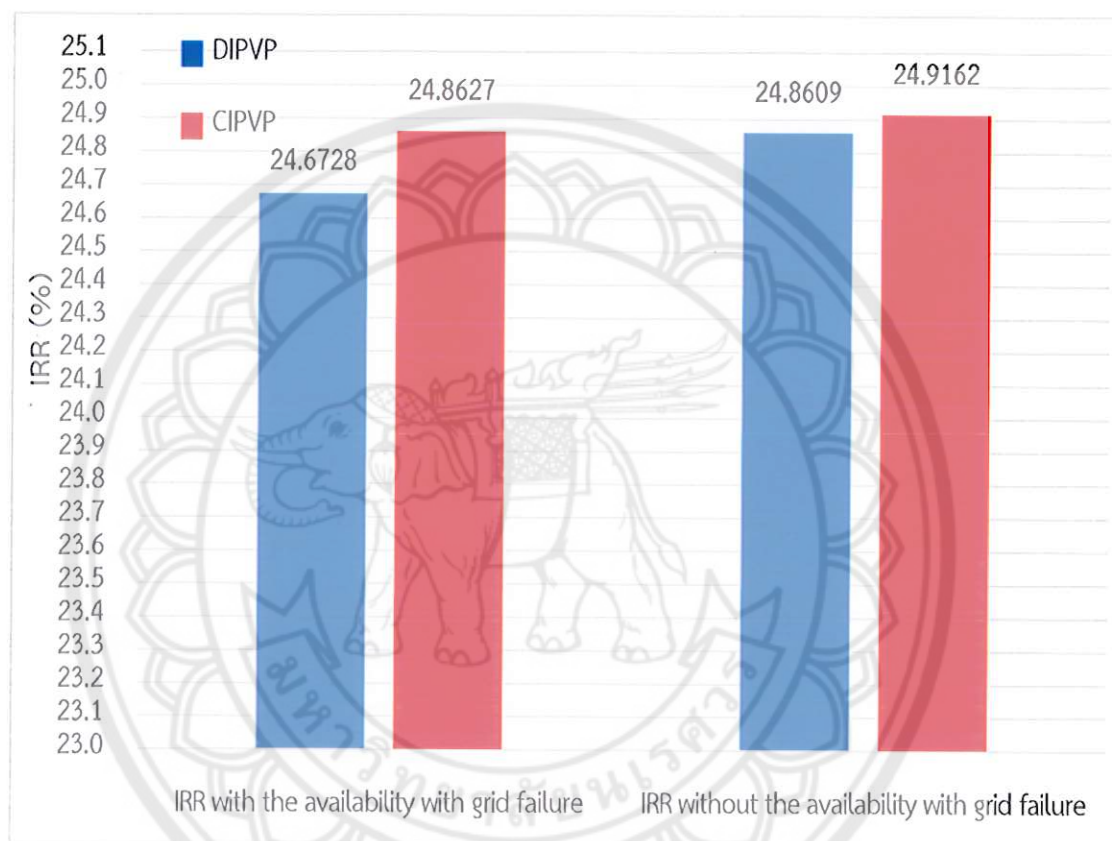


Figure 79 IRR with the both availability case of DIPVP and CIPVP PV power plants

power system applying centralized or decentralized inverter concepts in IRR analysis. In addition, the no significant different of IRR with the availability without grid failure in DIPVP and CIPVP are an evident to prove that the centralized or decentralized inverter concepts are not potentially effect to IRR of these PV power plant. The IRR that higher than 24% of DIPVP and CIPVP in 8.0 Baht/kWh adder for 10 year subsidy case is proving the feasibility in commercial of these PV power plant. The IRR result complies the final part of the second objective in this dissertation.

From the economic analysis result, all of the indicators point out that the grid failure influence is far higher than the effect from the PV power system applying centralized or decentralized inverter concepts in the economic analysis. Moreover, the centralized or decentralized inverter concepts are not potentially domination the economic analysis result. For 8.0 Baht/kWh adder for 10 year subsidy case, all of the indicators point out that DIPVP and CIPVP is feasibility in commercial. These economic analysis results complete the second objective of this dissertation.



CHAPTER V

CONCLUSION AND RECOMMENDATION

Analyzing the availability and reliability of PV power plant is important for planning and long-term operation, because the analysis helps predict system behavior over time and devise appropriately timed maintenance plans. It is a significant factor for the operator to be able to assess system availability and reliability under long-term operations in order to optimize decisions in design, engineering, procurement, construction, and service that result in PV power plant economic improvement. There are many studies already on the availability and reliability of PV power system applying centralized and decentralized inverter concept but almost of these study based on climate and environment in other country. Therefor the outcome of these study cannot completely use in Thailand. Availability and reliability of PV power system applying decentralized inverter concept concentrate on central and string inverter, climate, and environment in Thailand. Two 5 MW PV power plant that are DIPVP for the decentralized inverter concept with string inverter and CIPVP for the centralized inverter concept are selected as the PV power plant samples. These PV power plant are located in the same area in the central region of Thailand that is a good representative for the centralized and decentralized inverter concept, climate, and environment in Thailand. The summary study result during May 2013 to October 2014 of this dissertation is presenting in 3 groups. First, efficiency and performance evaluation result is presented in Table 35. Second, availability and reliability evaluation result is displayed in Table 36. Third, economic analysis result is showed in Table 37.

Table 35 Efficiency and performance evaluation result

| Parameters | DIPVP (Decentralized) | CIPVP (Centralized) |
|--|-----------------------|---------------------|
| Reference yield (Y_r) | 4.88 h/day | 5.04 h/day |
| Final PV system yield (Y_f) | 3.83 h/day | 3.87 h/day |
| Total losses (L_T) | 1.04 h/day | 1.17 h/day |
| Performance ratio (PR) | 78.66 % | 76.99 % |
| Overall PV plant efficiency (η_{tot}) | 11.14 % | 6.99 % |

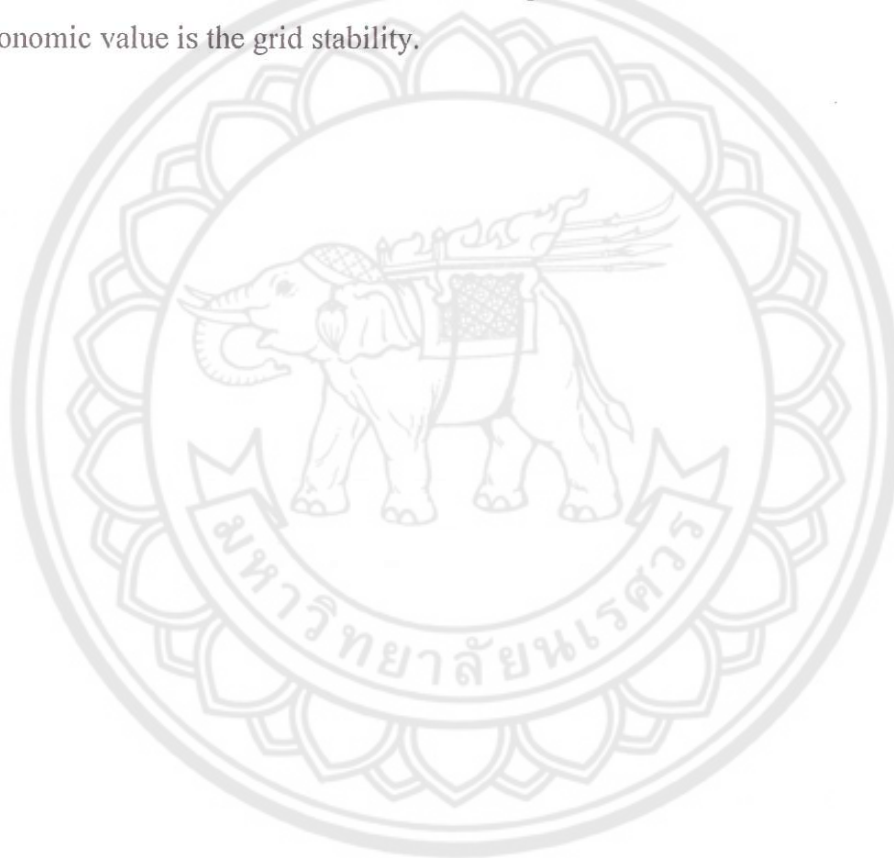
Table 36 Availability and reliability evaluation result

| Parameters | DIPVP (Decentralized) | CIPVP (Centralized) |
|------------------------------------|-----------------------|---------------------|
| Inverter downtime | 202.72 minutes | 262.50 minutes |
| Other component downtime | 539.88 minutes | 507.25 minutes |
| Grid downtime | 1,986.00 minutes | 565.25 minutes |
| Total downtime | 2,728.59 minutes | 1,335.00 minutes |
| Availability with grid failure | 99.28 % | 99.65 % |
| Availability without grid failure | 99.80 % | 99.80 % |
| Total inverter failure probability | 67.60 % | 10.00 % |
| Inverter reliability | 32.40 % | 90.00 % |

Table 37 Economic analysis result

| Parameters | DIPVP (Decentralized) | CIPVP (Centralized) |
|------------------------------------|-----------------------|---------------------|
| Cost per unit with grid failure | 2.90 Baht/kWh | 2.88 Baht/kWh |
| Cost per unit without grid failure | 2.88 Baht/kWh | 2.88 Baht/kWh |
| LCOE with grid failure | 3.72 Baht/kWh | 3.70 Baht/kWh |
| LCOE without grid failure | 3.70 Baht/kWh | 3.70 Baht/kWh |
| NVP with grid failure | 452.58 million Baht | 457.30 million Baht |
| NVP without grid failure | 457.25 million Baht | 458.63 million Baht |
| IRR with grid failure | 24.67 % | 24.86 % |
| IRR without grid failure | 24.86 % | 24.92 % |

From Table 34, the result presents no significant different except η_{tot} that is the result from PV module technologies. From Table 35, the result display no important different in inverter and other component downtime and availability except grid downtime. For reliability, centralized inverter concept is far higher than decentralized concept. To evaluate the higher precise availability and reliability of the PV power system applying decentralized and centralized inverter concepts, the life time evaluation period at 25 years is necessary. From Table 36, the result shows no remarkable different on the economic aspect. The most influential factor of the economic value is the grid stability.





REFERENCES

REFERENCES

- [1] Department of Alternative Energy Development and Efficiency Ministry of Energy. (2008). **Renewable Energy Development Plan (REDP 2008-2022)**. Bangkok: n.p.
- [2] Department of Alternative Energy Development and Efficiency Ministry of Energy. (2008). **Alternative Energy Development Plan (AEDP 2012-2021)**. Bangkok: n.p.
- [3] Jäger-Waldau A. (2013). **Report EC-JRC Institute for Energy and Transport: 2013**. Brussels: Publications Office of the European Union.
- [4] Jäger-Waldau A. (2014). **Report EC-JRC Institute for Energy and Transport: 2014**. Brussels: Publications Office of the European Union.
- [5] Energy Regulatory Commission of Thailand. (March 18, 2014). **Solar Energy Regulation**. Retrieved March 18, 2014, from <http://www.erc.or.th/ERCWeb2/Front/News/NewsDetail.aspx?rid=2323&CatId=1&muid=36&prid=21&IsPrint=1>
- [6] Thansettakij News paper. (March 18, 2014). **Solar Energy Business**. Retrieved March 18, 2014, from http://www.thanonline.com/index.php?option=com_content&view=article&id=261456:2015-01-13-17-35-45&catid=88:2009-02-08-11-23-46&Itemid=418#.VQlWdY6UeSp
- [7] Fife, J.M and Morris, R.W. (2009). System Availability Analysis for a Multi-megawatt Photovoltaic Power Plant. Proceeding Photovoltaic Specialists Conference (PVSC), **IEEE**, 34, 1221-1226.
- [8] Fife, J.M., Scharf, M., Hummel, S.G. and Morris, R.W. (2010). Field Reliability Analysis Methods for Photovoltaic Inverters. Proceeding Photovoltaic Specialists Conference (PVSC), **IEEE**, 35, 2767-2772.

- [9] Arnett, J.C. and others; Schaffer, L. A.; Rumberg, J. P.; Tolbert, R. E. L. (1984). Design, installation and performance of the ARCO Solar one-megawatt power plant. Proceedings of the Fifth International Conference (EC Photovoltaic Solar Energy Conference), **Athens**, 2(14), 314-323.
- [10] Wenger, H.J. and others. (1991). Decline of the Carrisa Plains PV power plant. Proceedings of Photovoltaic Specialists Conference, **IEEE**, 34(5), 41-49.
- [11] Stadt Hemau. (2003). **In Hemau liefert der weltweit größte Solarpark umweltfreundlichen Strom aus der Sonne**. Retrieved April 13, 2013, from <http://www.hemau.de/index.asp?NAVIID=%7B21B64141-C02C-4194-8A02-7D54CA2AB16F%7D>
- [12] Bundesumweltministerium (BMU). (2004). **The Renewable Energy Sources Act. Bundesgesetzblatt 2004 I No. 40**. Retrieved April 13, 2013, from http://www.bmu.de/files/english/pdf/application/pdf/eeg_en.pdf
- [13] Geosol. (2004). **Leipziger Land project**. Retrieved April 13, 2013, from <http://www.geosol.de/sites/default/files/references/GERMANY%20REFERENCE%20Leipziger%20Land%20-%20EN.pdf>
- [14] Collins, E., Dvorack, M., Mahn, J., Mundt, M. and Quintana, M., (2009). Reliability Availability Analysis of a Field Photovoltaic System, Proceeding Photovoltaic Specialists Conference (PVSC). **IEEE**, 34, 2316-2321.
- [15] Gabriele Zini, Christophe Mangeant and Jens Merten (2011). Reliability of large-scale grid connected photovoltaic systems. **Renewable Energy**, 36, 2334-2340.
- [16] H. S. Huang, J.C. Jao, K. L. Yen and C. T. Tsai. (2011). Performance and Availability Analysis of PV Generation Systems in Taiwan. **World Academic of Science, Engineering and Technology**, 5(6), 309-313.
- [17] John H. Wohlgemuth. (2008). Reliability of PV systems. **Proceeding of International Society for Optical Engineering Conference**. 10(7048), 98-107.

- [18] Moradi-Shahrabak, Z., Tabesh, A. and Yousefi, G. R. (2014). Economical Design of Utility-Scale Photovoltaic Power Plants With Optimum Availability. **IEEE Transaction on Industrial Electronics**, 61(7), 3399-3406.
- [19] Ahadi, A., Ghadimi, N. and Mirabbasi, D. (2014). Reliability assessment for components of large scale photovoltaic systems. **Journal of Power Sources**, 264, 211-219.
- [20] Sintamarean, N.C., Wang, H., Blaabjerg, F. and Rikken, P.de P. (2014). A design tool to study the impact of mission-profile on the reliability of SiC-based PV-inverter devices. **Microelectronics Reliability**, 54, 1655-1660.
- [21] Catelani, M., Ciani, L. and Reatti, A. (2014). Critical components test and reliability issues for Photovoltaic Inverter. **Proceeding IMEKO TC4 International Symposium**, 20, 592-596.
- [22] Catelani, M., Ciani, L. and Simoni, E. (2012). Photovoltaic Inverter: Thermal Characterization to Identify Critical Components. **Proceeding IMEKO World Congress Metrology for Green Growth, TC01**, 1-5. 12(2), 100-105.
- [23] Pearsall, N. M. and Atanasiu, B. (2009). Assessment of PV system Monitoring Requirement by Consideration of Failure Mode Probability. **Proceeding European Photovoltaic Solar Energy Conference**, 24, 3896-3903.
- [24] Cristaldi, L., Faifer, Marco., Lazzaroni, M., Khalil, M.M.A.F., Catelani, M. and Ciani, L. (2015). Diagnostic architecture: A procedure based on the analysis of the failure causes applied to photovoltaic plants. **Measurement**, 67, 99-107.
- [25] Tonf, G. and Tonf, D.G. (2014). Reliability Performance Assessment in Modeling Photovoltaic Networks. **Proceedings International Conference on Environment, Ecosystems and Development (EED' 14)**, 12, 63-68.
- [26] Francis, R. and Colli, A. (2014). Information-based reliability weighting for failure mode prioritization in photovoltaic (PV) module design. **Proceedings Probabilistic Safety Assessment & Management conference (PSAM 12)**, 12, 215.

- [27] Sharma, V. and Chandel, S.S. (2013). Performance and degradation analysis for long term reliability of solar photovoltaic systems. **Renewable and Sustainable Energy Reviews**, 27, 753-767.
- [28] Zhang, P., Li, W., Li, S., Wang, Y. and Xiao, W. (2013). Reliability assessment of photovoltaic power systems: Review of current status and future perspectives. **Applied Energy**, 104, 822-833.
- [29] Ulrike Jahn. (2008). **Analysis of Photovoltaic Systems, Report IEA-PVPS Task 2-01: 2000**. Fribourg: NET Nowak Energie & Technologie AG.





APPENDIX A SOLAR MODULE

Solar Module**PPV-220M6 / 230M6 / 235M6****220/230/235Wp Multicrystalline silicon photovoltaic module**

1. Assembled by 60 pcs of 6" multicrystalline solar cell with average efficiency rate 13.54% - 14.47%
2. Bypass diode on the module minimized the efficiency dropping ratio caused by shades
3. Modules are constructed of high quality clear anodized aluminum frames and high transparency, low-iron, tempered glass & EVA
4. Weatherproof aluminum alloyed frames for outdoor environment; artistic design with solid quality to install. Unique technology to prevent slash inside the frame which may cause freezing water or frame deformation.
5. DC 24V system
6. Output : weatherproof connectors

**ELECTRICAL CHARACTERISTICS**

| | 220W | 230W | 235W |
|---------------------------------|------------------------------|---------|---------|
| Maximum power (Pmax) | 220W | 230W | 235W |
| Voltage @ Pmax (Vpm) | 29.03V | 29.44V | 29.68V |
| Current @ Pmax (Ipm) | 7.58A | 7.81A | 7.92A |
| Open circuit voltage (Voc) | 37.12V | 37.26V | 37.33V |
| Short circuit current (Isc) | 8.28A | 8.43A | 8.51A |
| Output tolerance | ± 3% | | |
| Maximum system voltage | 1000 Vdc | | |
| Series fuse rating | 12A | | |
| Application | DC 24V system | | |
| system Cell | 6" Multi-crystalline silicon | | |
| No. of cells and connections | 60 PCS in series (6 x 10) | | |
| Efficiency of module | 13.54 % | 14.16 % | 14.47 % |
| Temperature coefficient of Pmax | -0.37 %/°C | | |
| Temperature coefficient of Voc | -0.32 %/°C | | |
| Temperature coefficient of Isc | +0.038 %/°C | | |

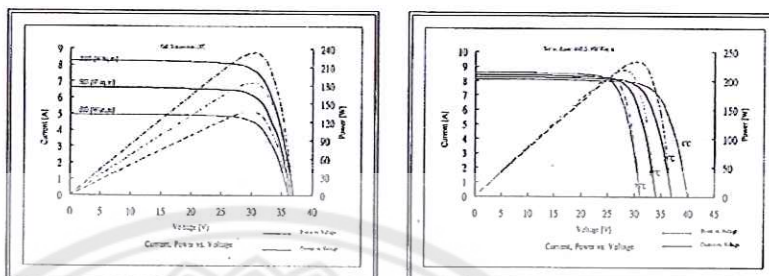
* Measured at STC (Standard Test Condition;
1000W/m² Irradiance, AM 1.5 and 25°C)

ABSOLUTE MAXIMUM RATINGS

| | |
|-----------------------|--------------|
| Operating temperature | -40 to +85°C |
| Storage temperature | -40 to +85°C |

MECHANICAL CHARACTERISTICS

| | |
|-------------------------------------|--|
| Dimension (WxLxH) | 1632 x 995 x 50 mm |
| Weight | Approximately 20.43Kg |
| Packing configuration | Horizontal |
| Size of carton | 1689 x 1071 x 955 mm |
| Pallet quantity | 18 PCS / Pallet |
| Loading capacity (20 ft. container) | 12 Pallet / container |
| Loading capacity (40 ft. container) | 28 Pallet / container |
| Construction | Front : high transmission low-iron tempered glass, 3.2mm Back : PET Encapsulates : EVA |
| Junction box | IP65, waterproof |
| Bypass diodes | 3 diodes to avoid power decreasing by shade |
| Output cable | 4mm ² cable with polarized waterproof connectors Negative 900mm, Positive 900mm |
| Frame | Clear anodized aluminum, AL6063-T5 |

PPV-220M6 / 230M6 / 235M6**I-V CURVES****QUALITY**

ISO 9001: 2000 certified.

IEC/EN 61215 and IEC/EN 61730 are certified by TÜV.

Warranty : 10 years limited warranty of 90% power output
and 25 years limited warranty of 80% power output.

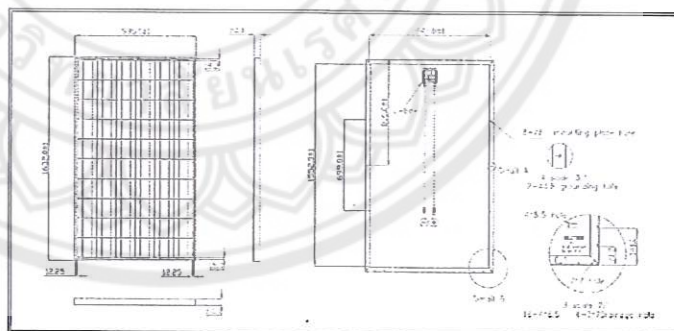
**INSTALL AND SAFETY GUIDE**

DO NOT damage or scratch the rear surface of the module

DO NOT handle or install modules when they are wet.

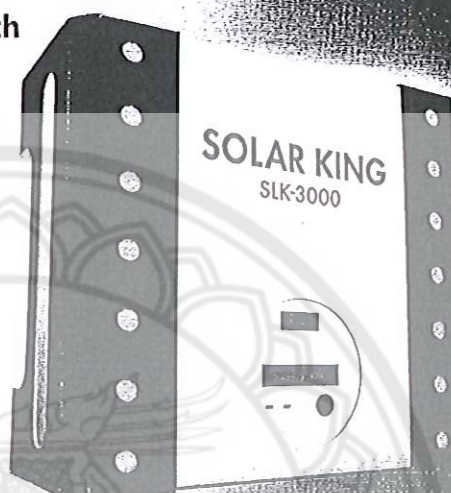
ONLY qualified personnel should install or perform maintenance.

BE AWARE of dangerous high DC voltage.

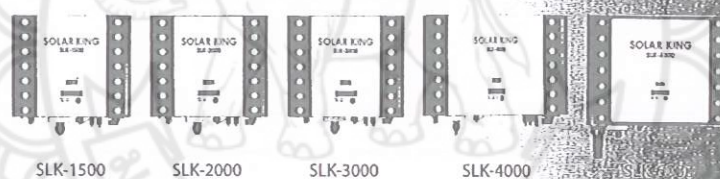
MODULE DIMENSIONS

** This document summarizes product specifications which are subject to change without prior notice.

**Power up your world with
Solar King Inverters!**



Europe and APAC Version



Features & Benefits

| | | |
|-----------------------|--|--|
| Optimum Yields | - High efficiency | - Transformerless design |
| | - 99% MPPT tracking efficiency | |
| Safe | - Internal DC switch | - Ground Fault Current Interrupter (GFCI) |
| | - Stainless steel case IP65 | |
| User Friendly | - Easy-to-use LCD panel | - Advanced fanless design for quieter operation |
| | - Clear LED indicators | - Compact and light |
| Reliable | - Accessory: (Wireless) RS485 card, Wireless module, SNMP card, GSM / GPRS module, USB | - Global certificates: Italy(DK5940), Germany(VDE0126-1-1), Spain(RD1663/2000), UK(G83/1), USA(UL1741), Australia(AS4777), CSA22.1(Canada), CGC(China) |

Inverter

23

Solar King 1500~6000

| Model | SLK-1500 | SLK-2000 | SLK-3000 | SLK-4000 | SLK-6000 |
|---|---|----------|---------------------------|---------------------------|------------------------------|
| Input Data | | | | | |
| Maximum input power | 1750W | 2340W | 3510W | 4700W | 6400W |
| Max. DC voltage | 500VDC | | | | 600VDC |
| Nominal DC voltage | 360V ~ 400V | | | | |
| MPPT voltage range | 200V ~ 400V $\pm 5\%$ | | | | 150V ~ 600V $\pm 5\%$ |
| Working voltage | 100V $\pm 5\%$ ~ 500V -5%+0% | | | | 100V $\pm 5\%$ ~ 600V -5%+0% |
| Full rating working range | 200V ~ 500V | | | 250V ~ 500V | 250V ~ 600V |
| Min. DC voltage | 100V $\pm 5\%$ | | | | |
| Start feeding voltage | 150V $\pm 5\%$ | | | | |
| Max. input current | 10ADC | 11ADC | 17.6ADC | 18.8ADC | 25.6ADC |
| DC voltage ripple | $<10\%$ | | | | |
| DC insulation resistance | $>8\text{M ohm}$ | | | | |
| DC switch (integrated/optional) | e/o | | | | |
| DC connector | Tyco or MC4 | | | | |
| Number of MPPT tracker/string | 1/1 | | | 1/3 | |
| Output Data | | | | | |
| Nominal output power | 1500W | 2000W | 3000W | 4000W | 6000W |
| Maximum output power | 1650W | 2200W | 3300W | 4400W | 6000W |
| Operational voltage range | 180V, minimum 280V, maximum *According to local requirement | | | | |
| Operational frequency range | 50/60Hz, auto selection 47 $\leq f_{50} \leq 53$ for 50Hz 57 $\leq f_{60} \leq 63$ for 60Hz *According to local requirement | | | | |
| Nominal output current | 6.5A | 8.7A | 13.0A | 17.4A | 26.1A |
| O/P current distortion | THD $<4\%$, each harmonics $<3\%$ | | | | |
| Power factor | >0.99 | | | | |
| General Data | | | | | |
| Maximum conversion efficiency (DC/AC) | $>94\%$ | $>95\%$ | $>95\%$ | $>96\%$ | $>96\%$ |
| European efficiency | $>93\%$ | $>94\%$ | $>94\%$ | $>95\%$ | $>95\%$ |
| All night power consumption | $<0.1\text{W}$ | | | | |
| Operation temperature | $-20 \sim 55^{\circ}\text{C}$ | | | | |
| Humidity | 0 ~ 95%, non-condensing | | | | |
| Mechanical Data | | | | | |
| Display | LCD 1" 16 characters | | | | |
| Heat dissipation | Convection | | | | |
| Acoustic noise level | $<38\text{dB}$, A-weighted, frequency up to 20kHz | | | | |
| Phase conductors | Single phase | | | | |
| Case (Stainless/SECC) | e/o | e/o | e/o | e/o | e/o |
| Protection degree | IP 65 | | | | |
| Physical/Shipping: WxDxH (mm) | 352x300x133 / 460x460x265 | | 352x300x143 / 460x460x265 | 550x300x133 / 660x460x265 | 550x420x143 / 660x580x265 |
| Physical/Shipping: Weight (kg) | 14/16 | | | 21/23 | 27/31 |
| AC connector | e/o | e/o | e/o | e/o | e/o |
| Certification | CE/VDE126-1-1/DK5940/AS4777/G83/RD1663 | | | | |
| Interfaces: RS232/USB/Communication slot (SNMP and RS485) | e/o | e/o | e/o | e/o | e/o |
| Data logger | Solar ECO NAVI, Solar-Log™ | | | | |

e/o Standard/Optional

เลขที่ รป. 280/2555



หนังสือรับประกันคุณภาพ

หม้อแปลงไฟฟ้า ถิรไทย

หนังสือสำคัญฉบับนี้ออกให้สำหรับหม้อแปลงไฟฟ้า ขนาด

TR 1000kVA 3Ph 50Hz 22000 - 400 V

ผู้ซื้อ บริษัท อินฟิไนท์ กรีน จำกัด หมายเลขเครื่อง 5512886 - 88

บริษัท รับประกันคุณภาพ -2- ปี

นับจากวันที่ 21 ธันวาคม 2555 ถึงวันที่ 20 ธันวาคม 2557

ข้อยกเว้น

สาเหตุอื่นเนื่องมาจากความผิดพลาดของผู้ใช้, ใช้งานผิดเงื่อนไขกำหนด, กรณีฟ้าผ่า หรือจากการซ่อมแซม, แก้ไข, คัดแปลง จากบุคคลที่ไม่ได้รับมอบหมายจากบริษัทฯ

บริษัท ถิรไทย จำกัด (มหาชน)

ผู้มีอำนาจลงนาม

Authorized Signature

516/1 M.4 Bangpoo Industrial Estate Samutprakarn 10280 Tel. 769-7699, Fax.323-0910, 709-3236, 709-3887
e-mail address : marketing@tirathai.co.th , www.tirathai.co.th

เลขที่ รป. 282/2555



หนังสือรับประกันคุณภาพ

หม้อแปลงไฟฟ้า ทิราไทย

หนังสือสำคัญฉบับนี้ออกให้สำหรับหม้อแปลงไฟฟ้า ขนาด

TR 1500kVA 3Ph 50Hz 22000 - 400 V

ผู้ซื้อ บริษัท อินทิท กรีน จำกัด หมายเลขเครื่อง 5512890

บริษัทฯ รับประกันคุณภาพ -2- ปี

นับจากวันที่ 21 ธันวาคม 2555 ถึงสิ้นสุดวันที่ 20 ธันวาคม 2557

ข้อยกเว้น

สาเหตุอันเนื่องมาจากความผิดพลาดของผู้ใช้, ใช้งานผิดเงื่อนไขกำหนด, กรณีสืบค้น หรือจากการซ่อมแซม, แก้ไข, คัดแปลง จากบุคคลที่ไม่ได้รับมอบหมายจากบริษัทฯ

บริษัท ทิราไทย จำกัด (มหาชน)

ผู้มีอำนาจลงนาม

Authorized Signature

516/1 M.4 Bangpoo Industrial Estate Samutprakarn 10280 Tel. 769-7699, Fax.323-0910, 709-3236, 709-3887
 e-mail address : marketing@tirathai.co.th, www.tirathai.co.th

Solar Module

PPV-220M6 / 230M6 / 235M6

220/230/235Wp Multicrystalline silicon photovoltaic module

1. Assembled by 60 pcs of 6" multicrystalline solar cell with average efficiency rate 13.54% - 14.47%
2. Bypass diode on the module minimized the efficiency dropping ratio caused by shades
3. Modules are constructed of high quality clear anodized aluminum frames and high transparency, low-iron, tempered glass & EVA
4. Weatherproof aluminum alloyed frames for outdoor environment; artistic design with solid quality to install. Unique technology to prevent slash inside the frame which may cause freezing water or frame deformation.
5. DC 24V system
6. Output : weatherproof connectors



ELECTRICAL CHARACTERISTICS

| | 220W | 230W | 235W |
|---------------------------------|------------------------------|---------|---------|
| Maximum power (Pmax) | 220W | 230W | 235W |
| Voltage @ Pmax (Vpm) | 29.03V | 29.44V | 29.68V |
| Current @ Pmax (Ipm) | 7.58A | 7.81A | 7.92A |
| Open circuit voltage (Voc) | 37.12V | 37.26V | 37.33V |
| Short circuit current (Isc) | 8.28A | 8.43A | 8.51A |
| Output tolerance | ± 3% | | |
| Maximum system voltage | 1000 Vdc | | |
| Series fuse rating | 12A | | |
| Application | DC 24V system | | |
| system Cell | 6" Multi-crystalline silicon | | |
| No. of cells and connections | 60 PCS in series (6 x 10) | | |
| Efficiency of module | 13.54 % | 14.16 % | 14.47 % |
| Temperature coefficient of Pmax | -0.37 %/°C | | |
| Temperature coefficient of Voc | -0.32 %/°C | | |
| Temperature coefficient of Isc | +0.038 %/°C | | |

* Measured at STC (Standard Test Condition;
1000W/m² Irradiance, AM 1.5 and 25°C)

ABSOLUTE MAXIMUM RATINGS

| | |
|-----------------------|--------------|
| Operating temperature | -40 to +85°C |
| Storage temperature | -40 to +85°C |

MECHANICAL CHARACTERISTICS

| | |
|-------------------------------------|--|
| Dimension (WxLxH) | 1632 x 995 x 50 mm |
| Weight | Approximately 20.43Kg |
| Packing configuration | Horizontal |
| Size of carton | 1689 x 1071 x 955 mm |
| Pallet quantity | 18 PCS / Pallet |
| Loading capacity (20 ft. container) | 12 Pallet / container |
| Loading capacity (40 ft. container) | 28 Pallet / container |
| Construction | Front : high transmission low-iron tempered glass, 3.2mm Back : PET Encapsulates : EVA |
| Junction box | IP65, waterproof |
| Bypass diodes | 3 diodes to avoid power decreasing by shade |
| Output cable | 4mm ² cable with polarized waterproof connectors Negative 900mm, Positive 900mm |
| Frame | Clear anodized aluminum, AL6063-T5 |



Smart Pyranometers

The more intelligent way to measure solar irradiance

Enhanced performance by digital signal processing
 RS-485 serial data interface with Modbus® protocol
 0 to 1 V voltage output
 4 to 20 mA current output
 Extremely low power

Introduction

Solar radiation drives almost every dynamic process on the Earth's surface and above, from ocean current circulation to the weather, and life itself. Precise long-term measurements of the radiation budget at the surface are fundamental to understanding the Earth's climate system and weather forecasting, and are important in agriculture, hydrology and ecology. Accurate solar radiation data has also become crucial information in solar energy and other industrial applications.

Kipp & Zonen has been manufacturing pyranometers for over 80 years. These instruments are designed for measuring the total (global) irradiance from the sun and sky falling on a plane surface in the wavelength range from 300 nm (nanometers) to 3000 nm. We produce models at all price and performance points, up to the very best available, designed for a long operating life in all environments, from deserts to the Antarctic.

Our pyranometers meet, or exceed, the requirements of ISO 9060:1990 and IEC 60904 and are fully traceable to the World Radiometric Reference (WRR) in Davos, Switzerland, where Kipp & Zonen instruments form part of the World Standard Group.

Now, Kipp & Zonen makes the link between our class-leading instruments and industry standard interfaces to bring you something completely new, the SMP series of smart pyranometers.

Building on the proven CMP Series design and technology that is used around the world, the new SMP pyranometers add digital

signal processing and interfaces optimised for industrial data acquisition and control systems. Kipp & Zonen has developed a smart interface that features Modbus® data communication for connection to programmable logic controllers (PLC's), inverters, digital control equipment and the latest generation of data loggers. Amplified Voltage or Current outputs are also included for devices that have high level analogue inputs or current loop interfaces.

The smart interface not only provides versatile outputs. An integrated temperature sensor and digital polynomial functions provide correction for the temperature sensitivity of the detector. The response time has been improved and the output ranges are standardised, making it easy to interchange instruments for recalibration. Using Modbus® a range of instrument status and configuration information is available, with user-selectable options.

SMP pyranometers have extremely low power consumption so that internal heating does not affect the detector performance. They operate from a wide range of supply voltages, making them ideal for power-critical applications.

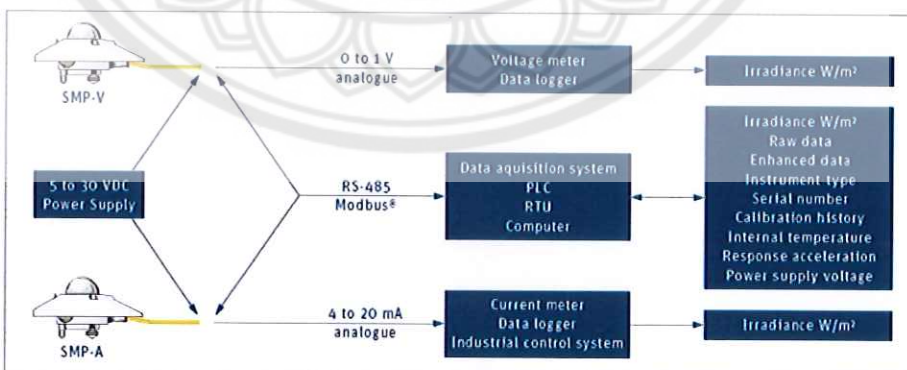
Interfacing

SMP Series pyranometers are equipped with a smart interface. There are two versions, one has an analogue output of 0 to 1 V, the other is 4 to 20 mA. Both have a 2-wire RS-485 interface with Modbus® (RTU) protocol. All the outputs are protected against short-circuits, and reversed polarity.

The analog outputs allow easy connection to virtually any data logger or without the need for sensitive mV inputs. Modbus® interfaces directly to RTU's, PLC's, SCADA systems, industrial networks and controllers. Not only measurement data is available, the user can access the pyranometer type and serial number, instrument settings, calibration history, status information, and more. A recalibrated instrument

keeps the same analog and digital measurement ranges, so saving time by eliminating re-scaling of data collection equipment.

SMP Series pyranometers can operate from a power supply in the range from 5 VDC to 30 VDC and have both reverse polarity and over-voltage protection.



Choice of Pyranometer

To achieve the required spectral and directional characteristics SMP Series pyranometers use thermopile detectors and glass domes. SMP3, SMP10 and SMP11 both have built-in bubble levels and adjustable levelling feet. Snap-on sun shields reduce solar heating of the housings. The waterproof connectors have gold-plated contacts and are fitted with 10 m of high quality signal cable as standard.

SMP3, SMP10 and SMP11 come in two versions; 'V' with a 0 to 1 V analogue output, and 'A' with 4 to 20 mA. Both versions have the Modbus® interface, very low power requirements and are supplied with comprehensive, traceable, calibration certificates. The most appropriate model for an application largely depends on the desired accuracy and performance.

SMP3 is smaller and lighter than the SMP11 pyranometer. It has a robust 4 mm thick glass dome to protect the thermopile detector from external influences. The small size and sealed construction make this instrument the ideal choice for monitoring solar energy installations, agriculture, horticulture, hydrology and industrial applications. With its digital temperature compensation it is the fastest and best performing ISO 9060:1990 Second Class pyranometer available.



SMP10 is the secondary standard pyranometer with the best price quality performance ratio on the market. With the same specifications and detector as SMP11, SMP10 extends this quality to applications where maintenance is difficult and/or forms a major part of the cost of ownership.



The SMP10 has internal desiccant that lasts for at least 10 years. This minimizes maintenance significantly. The interval for dome cleaning can be extended, and the quality of measurements maximized, by adding the CVF4 ventilation unit.

SMP11 has a dual dome construction of higher quality glass and increased thermal mass. It uses a more sophisticated detector design than the SMP3 and is a significant step up in performance. SMP11 comfortably exceeds the requirements for ISO Secondary Standard pyranometers and is the ideal choice for site prospecting, technology research and high quality solar radiation monitoring in solar energy applications. It is also particularly suitable for upgrading meteorological networks and for use in sun tracker based solar monitoring stations.

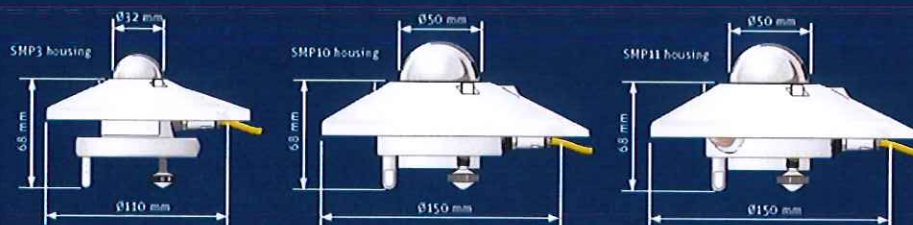


Building a System

The system capabilities of Kipp & Zonen pyranometers can be extended with our wide range of compatible products and accessories, including; mountings, ventilation unit, adjustable tilt mounting kit, shadow ring, sun trackers and data loggers.



Please refer to our website www.kippzonen.com for more information on the above products and other accessories available.



| Specifications | SMP3 | SMP10 & SMP11 |
|--|--|---|
| Classification to ISO 9060:1990 | Second Class | Secondary Standard |
| Spectral range (50% point) | 300 to 2800 nm | 285 to 2800 nm |
| Analogue output - V version | 0 to 1 V | 0 to 1 V |
| Analogue output range | 200 to 2000 W/m ² | 200 to 2000 W/m ² |
| Analogue output - A version | 4 to 20 mA | 4 to 20 mA |
| Analogue output range | 0 to 1600 W/m ² | 0 to 1600 W/m ² |
| Serial output | RS 485 Modbus® | RS 485 Modbus® |
| Serial output range | 400 to 2000 W/m ² | 400 to 4000 W/m ² |
| Response time (63%) | <1.5 s | <0.7 s |
| Response time (55%) | <12 s | <2 s |
| Zero offsets | | |
| (a) thermal radiation (at 200 W/m ²) | <15 W/m ² | <7 W/m ² |
| (b) temperature change (5 °C) | <5 W/m ² | <2 W/m ² |
| Non-stability (range/year) | <1% | <0.5% |
| Non-linearity (100 to 1000 W/m ²) | <1.5% | <0.2% |
| Directional response | <20 W/m ² | <10 W/m ² |
| (up to 80 W/m ² 1000 W/m ² beam) | | |
| Spectral selectivity (350 to 1300 nm) | <3% | <3% |
| Temperature response | <3% (-20 °C to +50 °C) <5% (-40 °C to +70 °C) | <1% (-20 °C to +50 °C) <2% (-40 °C to +70 °C) |
| Tilt response (0° to 90° at 1000 W/m ²) | <1% | <0.2% |
| Field of view | 180° | 180° |
| Accuracy of bubble level | <0.2° | <0.1° |
| Supply voltage | 5 to 30 VDC | 5 to 30 VDC |
| Power consumption (112 VDC) | V version: 55 mW A version: 100 mW | V version: 55 mW A version: 100 mW |
| Detector type | Thermopile | Thermopile |
| Software, Windows™ | Smart Sensor Explorer Software, for configuration, test and data logging | Smart Sensor Explorer Software, for configuration, test and data logging |
| Operating temperature range | 40 °C to +80 °C | 40 °C to +80 °C |
| Storage temperature range | 40 °C to +80 °C | 40 °C to +80 °C |
| Humidity range | 0 to 100% non-condensing | 0 to 100% non-condensing |
| Ingress Protection (IP) rating | 67 | 67 |
| Recommended applications | Technical solutions for efficiency and maintenance monitoring of PV power installations, routine measurements in weather stations, agriculture, horticulture and hydrology | High performance for PV panel and thermal collector testing, solar energy research, solar prospecting, materials testing, advanced meteorology and climate networks |



Go to www.kippzonen.com for your local distributor

HEAD OFFICE

Kipp & Zonen B.V.
Defttechpark 36, 2626 XT Delft
P.O. Box 507, 2600 AM Delft
The Netherlands
+31 (0) 15 2755 210
info@kippzonen.com
www.kippzonen.com

Kipp & Zonen B.V. reserve the right to alter specifications of the equipment described in this documentation without prior notice

4414 333-V1411



DuPont Apollo C Series photovoltaic modules are designed and manufactured using the cutting-edge amorphous / microcrystalline silicon (a-Si/ μ c-Si) thin film technology. With unique product features and capabilities, they are able to provide ideal solution for rooftop solar projects.

Key Product Advantages:

- **Better Return on Investment (ROI)**

High Efficiency

DuPont Apollo C Series thin film modules can generate high energy power resulted from their improved cell conversion efficiency.

Light-Weight Feature

With its light-weight feature (12.8kg/sqm), DuPont Apollo C Series modules provide an ideal choice for light rooftop applications. This feature minimizes the overall BOS (Balance-of-System) cost through simplifying supporting structure, and thus lowering the system installation cost.

Stable Performance Under High Temperature and Weak Light Conditions

DuPont Apollo C Series modules provide stable performance under high temperature and weak light conditions (e.g. reflective, indirect and diffusive light) and the shadowing environment. This feature enables greater flexibility for adjusting the mounting angle to meet special rooftop requirement in the system design.

- **Suitable for Green Building with Aesthetic Design**

The aesthetic design of DuPont Apollo C Series modules is a preferable option for green building design and can blend with the original building appearance. Its white backsheet design can reduce the rate of heat absorption of PV modules and thus improve the overall power performance.

- **Quality and Reliability**

DuPont Apollo C Series modules are manufactured in an ISO 9001 certified facility, and the modules have received the internationally recognized IEC 61646, IEC 61730 and UL 1703 certifications.

- **Green Product Commitment**

DuPont Apollo is committed to environmental responsibility and our hazardous substance process management in product design, development and manufacturing has obtained the internationally recognized IECQ QC 080000 qualification.



General Enquiry : +852 3664 3000 | enquiry.apollo@hkg.dupont.com
 Customer Service : +852 3664 3018 | cs@hkg.dupont.com
www.apollo.dupont.com



The miracles of science™

DuPont Apollo C Series Thin Film Modules



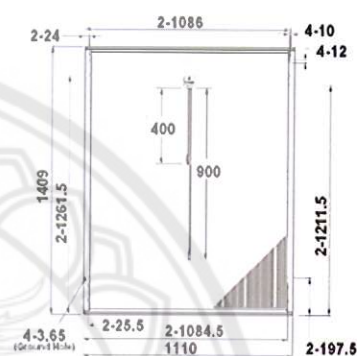
The miracles of science™

- ☒ High Energy Yields
 ☒ Stable Power Output
 ☒ Robust Encapsulation
 ☒ Easy Mounting
☒ Low Cable Power Loss

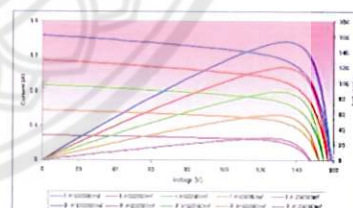
Product Specification

| Model | DA142 | DA145 | DA148 | DA151 | DA154 |
|---|--|--------|--------|--------|--------|
| Technology | Amorphous/ Microcrystalline Silicon (Tandem Junction) | | | | |
| Mechanical characteristics | | | | | |
| Dimensions | L 1409 x W 1110 x T 35 mm | | | | |
| Weight | 20 kg | | | | |
| Front Cover | 4.0 mm TCO Glass | | | | |
| Encapsulant | EVA | | | | |
| Back Cover | Backsheet | | | | |
| Frame | Aluminium | | | | |
| Electrical Characteristics | | | | | |
| At Standard Test Conditions (STC) | | | | | |
| Nominal power output (Pmpp) | 142W | 145W | 148W | 151W | 154W |
| Voltage at Pm point (Vmpp) | 119 V | 121 V | 122 V | 123 V | 124 V |
| Current at Pm point (Impp) | 1.19A | 1.20A | 1.22A | 1.23A | 1.24A |
| Open circuit voltage (Voc) | 157 V | 157 V | 158 V | 158 V | 159 V |
| Short circuit current (Isc) | 1.42A | 1.43A | 1.43A | 1.44A | 1.44A |
| Open circuit voltage, Initial (Voc, initial) | 161 V | 161 V | 162 V | 162 V | 163 V |
| Short circuit current, Initial (Isc, initial) | 1.44 A | 1.45 A | 1.45 A | 1.46 A | 1.46 A |
| At Nominal Operating Cell Temperature (NOCT) | | | | | |
| Nominal power output (Pmpp) | 105W | 107W | 110W | 112W | 114W |
| Voltage at Pm point (Vmpp) | 110 V | 111 V | 112 V | 114 V | 115 V |
| Current at Pm point (Impp) | 0.96 A | 0.97 A | 0.98 A | 0.98 A | 0.99 A |
| Open circuit voltage (Voc) | 145 V | 145 V | 146 V | 146 V | 146 V |
| Short circuit current (Isc) | 1.15 A | 1.15 A | 1.16 A | 1.16 A | 1.17 A |
| Temperature Characteristics at 1000W/m², AM 1.5 | | | | | |
| α Temperature coefficient of Isc | + 0.09% / °C | | | | |
| β Temperature coefficient of Voc | - 0.35% / °C | | | | |
| γ Temperature coefficient of Pmpp | - 0.30% / °C | | | | |
| Operating Conditions | | | | | |
| Operating temperature | -40 ~ +85 °C | | | | |
| Maximum mechanical load (front/back) | 2400 / 2400 N/m² | | | | |
| Maximum system voltage | 1000 V (IEC) / 600 V (UL) | | | | |
| Maximum reverse current overload | 2 A | | | | |
| Connector | MC4 Compatible | | | | |
| Cable size | 2.5 mm² | | | | |
| Cable length | 400 mm, 900 mm | | | | |
| Standard Guarantees and Certifications | | | | | |
| Product Warranty | 6 years | | | | |
| Performance Warranty | 90% of nominal power for 10 years 80% of nominal power for 25 years | | | | |
| Certifications | IEC 61646 / IEC 61730 / UL1703 / ULC1703 | | | | |
| Packaging Details | | | | | |
| Packaging unit | 29 modules per pallet | | | | |
| Dimensions (L x W x H) | L 1436 x W 1117 x H 1275 mm | | | | |
| Storage | 928 modules (32 pallets) in 40' HQ container | | | | |

Module Outline



Electrical Characteristics for DA154 at 25°C



Above electrical data represents stabilized module performance, unless specified otherwise.

P_{mpp} at STC is subject to tolerance of ±5%.

Initial P_{mpp} is approximately 12-16% higher than stabilized P_{mpp}.

STC: 1000 W/m², AM 1.5, cell temperature 25 °C.

NOCT: 43.4 ± 0.2 °C, 600 W/m², AM 1.5, ambient temperature 20 °C, wind speed 1 m/s.

All data may be subject to change without prior notice. Please consult with your sales representative for the exact product specifications of the actual shipment.

Copyright © 2011 DuPont Apollo Limited. All Rights Reserved. The DuPont Oval logo and "The miracles of science" are trademarks of E.I. du Pont de Nemours and Company or its affiliates. DuPont Apollo is a wholly owned subsidiary of DuPont specializing in silicon based thin film photovoltaic modules. Please visit us at www.apollo.dupont.com

LEONICS®

APOLLO GTC-HE series

THREE PHASE GRID CONNECTED CENTRAL INVERTER WITH CONTAINER



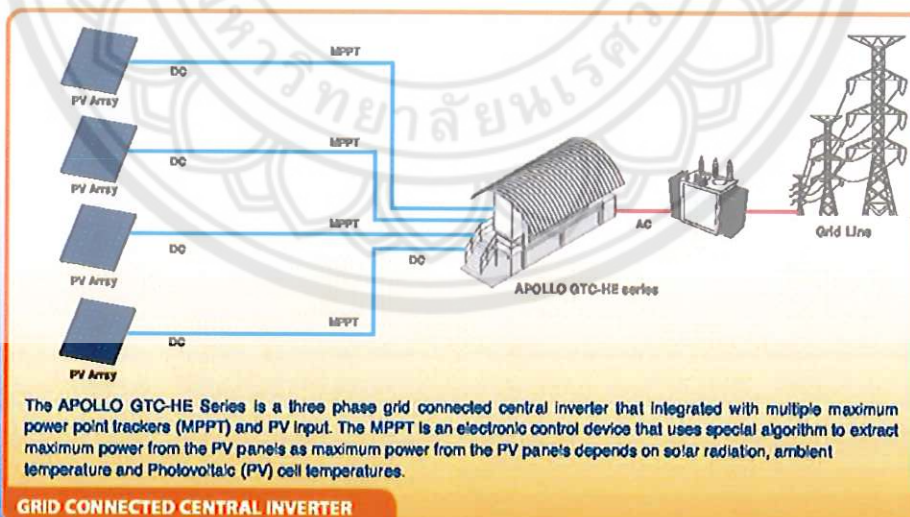
Note: Preparing foundation and building concrete base are customer's responsibility.



OPTION

- Solar-powered weather station
- Irradiation sensor
- PV module temperature sensor

- Three phase grid connected inverter with built-in output transformer
- Peak efficiency > 97.3% (CEC > 97.0% and Euro > 96.88%)
- Total Harmonic Distortion THDI < 3% (VSP requirement)
- 2-6 parallel redundant inverters
- Integrate with 2-6 MPPT inputs
- Over and under voltage and frequency protections
- Over current protection phase to N, G
- Automatic Synchronize with utility grid line
- Islanding protections during failure of utility grid power supply
- Automatic start and shutdown during over heating
- Superior user protection with galvanic isolation
- Display LCD unit for voltage, current, watts, energy, and accumulated energy at inverter for each phase and 3 phases
- Fully automatic self-START in the morning and STOP in the evening
- Installation in container cabinet with door sensors, smoke detector and in-container ambient temperature sensor
- ISO 9001:2008 and ISO 14001 certified factory



GRID CONNECTED CENTRAL INVERTER

LEONICS®

APOLLO GTC-HE series THREE PHASE GRID CONNECTED CENTRAL INVERTER



SPECIFICATIONS

| MODEL | | GTC-500HE | GTC-750HE | GTC-1000HE | GTC-1250HE | GTC-1500HE |
|------------------------|---|---|---------------------|----------------------|----------------------|----------------------|
| RATED POWER | PV Input (max) | 550 kW _p | 825 kW _p | 1100 kW _p | 1375 kW _p | 1650 kW _p |
| | Output | 500 kW | 750 kW | 1000 kW | 1250 kW | 1500 kW |
| SYSTEM | Number of MPPT | 2 | 3 | 4 | 5 | 6 |
| PV INPUT | Configuration | Multi-Inverter, Multi-PV with MPPT | | | | |
| | Technology | High frequency switching, IGBT technology | | | | |
| | MPPT tracking voltage range (V _{mp} of PV string) | 400 to 700 V _{dc} (calculate by using V _{mp}) | | | | |
| | Maximum open circuit voltage (V _{oc} of PV string) | 850 V _{dc} (calculate by using V _{oc}) | | | | |
| AC OUTPUT TO GRID LINE | Grid line voltage | 380 / 400 / 415 Volt (L-L), 220 / 230 / 240 Volt (L-N) (-15%, +10%) | | | | |
| | Phase | Three phase four wires | | | | |
| | Frequency | 50 / 60 Hz ± 0.5 Hz (± 0.2 Hz to ± 5 Hz adjustable) | | | | |
| | Power factor | > 0.98 | | | | |
| | Total harmonic distortion | THDI < 3% | | | | |
| | Power limiting | 110% | | | | |
| ISOLATION | Galvanic isolation | yes | | | | |
| EFFICIENCY | | Peak > 97.3% (CEC > 97.0%, Euro > 96.88%) | | | | |
| PROTECTION | Input / Output | Over voltage / Under voltage (AC & DC), Frequency (AC) | | | | |
| | Islanding operation | Active and passive anti-islanding | | | | |
| | Over heat | Automatic shutdown and restart | | | | |
| | Surge dissipation | 20 kA category C1 for AC (separate supply) | | | | |
| INDICATOR | LED | Mains, Operating, Synchronize, PV, Over Temp., Alarm | | | | |
| | LCD | Voltage, Current, Watt, Energy Today, Accumulated kWh (LCD for each phase and one remote LCD display for 3 phase data) | | | | |
| POWER CONSUMPTION | | less than 40 Watt / number of MPPT (standby mode) 0 Watt (sleep mode) | | | | |
| AUDIABLE ALARM | | Main failure, Inverter fault | | | | |
| ACOUSTIC NOISE | At 1 metre | less than 50 dB (when fan does not run) | | | | |
| COOLING | | Force fan cooling | | | | |
| ENVIRONMENT | Temperature | 0 - 45°C | | | | |
| | Relative humidity | 0 - 95 % (Non - condensing) | | | | |
| DESIGN | Standard | IEC 61727, IEC 62116, IEC 60335-1, AS 3100, AS 4777 | | | | |
| | Enclosure | IP 54 | | | | |
| DIMENSION | W x H x D (approx. in metre) | 2.44x2.64x3.66 | 2.44x2.64x4.86 | 2.44 x2.64x6.06 | 2.44x2.64x7.26 | 2.44x2.64x8.46 |
| WEIGHT | Approximate in ton | 5 | 7.5 | 10 | 12.5 | 15 |

Continuous product development is our commitment. In that manner, the above specifications may be changed without prior notice.

Authorized Distributor
LEONICS ESCO CO., LTD.
 29 Soi Bangna-Trad Rd 34, Bangna, Bangkok 10260 THAILAND
 Phone: 0-2746-9500, 0-2746-8708 Fax: 0-2746-8712 e-mail: esco@leonics.com
 * www.leonics.com *

Authorized Dealer:

M LEN 890 INV 871 Rev 1 009212

Specification of MV transformer For Saraburi Project

| Description | Unit | Detail |
|---------------------------------|-------|---------------------|
| Rating | kVA | 1250 |
| Standard | | IEC60076 |
| Frequency | Hz | 50 |
| No. of Phase | | 3 |
| Type | | Hermetically sealed |
| Cooling | | ONAN |
| Rated voltage | | |
| HV side | kV | 22 |
| LV side | V | 400 |
| Tap voltage on HV side | % | +/-2 x 2.5 |
| Connection | | Delta – wye |
| Vector diagram | | Dyn 11 |
| Characteristics based on ONAN | | |
| Impedance voltage at 75 Deg. C. | % | 6 |
| No load loss | kW | 1.8 – 1.9 |
| Load loss | kW | 10.6 – 10.7 |
| Efficiency at P.F. = 1.0 | | |
| 100% load | % | > 99 |
| 75% load | % | |
| 50% load | % | |
| 25% load | % | |
| Total mass | kg | 4350 – 4420 |
| Oil in tank | Liter | 1130 – 1200 |
| Dimension | | |
| H (mm.) | | 1850 – 1910 |
| L (mm.) | | 1970 – 2130 |
| W (mm.) | | 1130 – 1330 |
| Warranty | Years | 2 |

Remark Specification is subjected to change without prior notice.



Pyranometers

For the Accurate Measurement of Solar Irradiance

Installed around the world by national networks
 Specifications to ISO 9060:1990 and IEC 60904 standards
 Widely used within World Meteorological Organisation scientific programmes
 The broadest range of pyranometers and accessories available

Introduction

Solar radiation drives almost every dynamic process on the Earth's surface and above, from ocean current circulation to the weather, and life itself. Precise long-term measurements of the radiation budget at the surface are fundamental to understanding the Earth's climate system. Rising fossil fuel costs and the need to reduce Carbon footprints has produced a rapid growth in the market for 'green' energy, in which the fastest growing sector is solar power.

Scientists, researchers and commercial companies in renewable energy, climatology, weather, agriculture, water resources and environment all require accurate and reliable measurements of solar radiation. The measurement is made by pyranometers, which are radiometers designed for measuring the total (global) irradiance on a plane surface resulting from radiant fluxes in the wavelength range from 300 nanometers (nm), or less, to 3000 nm.

Kipp & Zonen has been manufacturing pyranometers for over 85 years. We produce models at all price and performance points, up to the very best available. All comply with the

requirements of ISO 9060:1990 and are fully traceable to the World Radiometric Reference (WRR) in Davos, Switzerland, where Kipp & Zonen Instruments form part of the World Standard Group.

Our top level pyranometers have exceptional levelling accuracy, built-in temperature sensors and a test certificate with individually measured directional and temperature responses. These important features ensure the highest accuracy measurements. Kipp & Zonen pyranometers are designed for a long operating life with simple maintenance and a wide range of accessories is available.

Applications

Kipp & Zonen pyranometers have been developed to be suitable for use in all environments, from the Antarctic to deserts. They are installed around the world for meteorology, hydrology, climate research, solar energy, environmental and materials testing, greenhouse control, building automation and many other applications.

The CMP10 is specially designed for applications where regular visits and maintenance is difficult. A dedicated brochure is available for the CM 4, for use in climate chambers up to 150°C.

CMP 3 is smaller and lighter than the other CMP Series pyranometers. It has a robust 4 mm thick glass dome to protect the thermopile from external influences. The small size and sealed construction make this instrument the ideal choice for horticulture, monitoring solar energy installations, industrial applications, and it can be used underwater. A screw-in mounting rod is available for easy installation.

CMP 6 has a similar detector to CMP 3, but has improved performance due to the increased thermal mass and the double glass dome construction. It is recommended for cost-effective, good quality, measurements in meteorological and hydrological networks and agriculture.

CMP10 is the secondary standard pyranometer with the best price-quality-performance ratio on the market. With the same specifications and detector as CMP 11, CMP10 extends this quality to applications where maintenance is difficult and/or forms a major part of the cost of ownership.

The CMP10 has internal desiccant that lasts for at least 10 years. This minimizes maintenance significantly. The interval for dome cleaning can be extended, and the quality of measurements maximized, by adding the CVE4 ventilation unit.

Kipp & Zonen provides every CMP10 with a 5 year warranty as standard. This warranty applies provided that the CMP10 is used only under atmospheric conditions, that the housing is not opened and that the Kipp & Zonen cable and connector is correctly fitted. The internal desiccant is changed with every factory re calibration.

CMP 11 uses a temperature compensated detector. It is a step up in performance from CMP 6 and particularly suitable for upgrading meteorological networks. The faster response time meets the requirements for solar energy research and development applications. CMP 11 is also ideal for use in sun tracker based solar monitoring stations.

Choice of Pyranometer

To achieve the required spectral and directional characteristics CMP Series pyranometers use thermopile detectors and glass or quartz domes. All models have built-in bubble levels and adjustable levelling feet. The waterproof connectors have gold plated contacts and are fitted with 10 m of high quality signal cable as standard. The instruments do not require power and are supplied with comprehensive calibration certificates.

The most appropriate model for an application largely depends on the desired accuracy and performance.





CMP 21 is similar to **CMP 11** but has individually optimised temperature compensation. A standard thermistor sensor is fitted to monitor the housing temperature. Each instrument is supplied with its own temperature and directional (cosine) response data. It is the choice for scientific use and in top level solar radiation monitoring networks such as the Baseline Surface Radiation Network (BSRN) of the World Meteorological Organisation.

CMP 22 has all the features of **CMP 21** but uses very high quality quartz domes for a wider spectral range, improved directional response, and reduced thermal offsets. Because of the high optical quality of these domes the directional error is reduced below 0.5% up to 80° solar zenith angle. Kipp & Zonen is confident that **CMP 22** is the best pyranometer currently available.

Building a System

The system capabilities of Kipp & Zonen pyranometers can be extended with our wide range of compatible products and accessories. Please refer to our website www.kippzonen.com for more information on the following products.

Albedometer

To calculate Albedo the incoming global radiation is measured by a pyranometer facing upward and the radiation reflected by the ground is measured by a pyranometer facing downward. **CMA 6** and **CMA 11** are integrated Albedometer versions of **CMP 6** and **CMP 11**. Details can be found in our dedicated Albedometer brochure.

Ventilation Unit

CVF4 ventilation unit is designed for use with all **CMP Series** pyranometers (**CMP 3** fits but ventilation is less effective). Ventilation helps to keep the dome clean and reduces infrared thermal offsets by stabilization of the dome temperature. The two levels of heating can be used to remove raindrops, dew, frost and snow.

Sun Tracker

SOLYS 2 and **ZAP** sun trackers are all-weather reliable instruments used to accurately point a pyranometer at the sun for direct radiation measurements. When fitted with an optional shading assembly and a pyranometer they measure diffuse radiation with no need for periodic manual adjustments. Adding a second pyranometer for the global radiation makes a high quality solar monitoring station.



Shadow Ring

The combination of a pyranometer and a **CM 121** shadow ring offers a simple solution for measuring diffuse radiation from the sky. The ring only requires simple adjustment every few days to ensure that the shadow covers the pyranometer dome completely as the sun moves across the sky.

Amplification

Pyranometers have low output signals in the mV range. **AMPBOX** converts this to the industrial standard 4 to 20 mA current loop signal and provides a defined output range in W/m^2 . Amplification is advised for noisy environments, use with data acquisition equipment with high level inputs, and for very long cables (> 100 m). For pyranometers with amplified analog and digital outputs, see our **SMP** series.

Data loggers

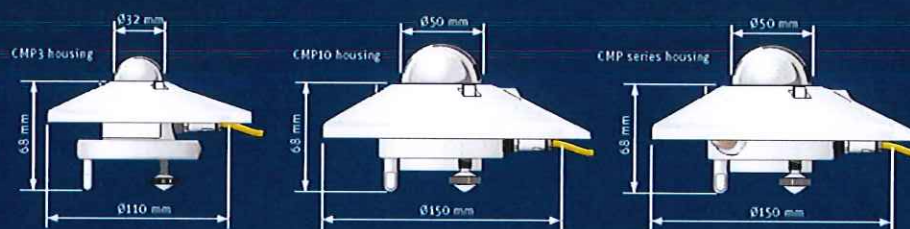
Kipp & Zonen has a range of high performance data logging and display products for use with **CMP series** pyranometers and our other solar radiometers.

Mounting

Kipp & Zonen offers mounting fixtures for horizontal, tilted and down looking pyranometers. **CMF 1** is a small round plate with integral rod for mounting upward and/or downward facing pyranometers. **CMB 1** is a mounting bracket for mounting a 12-20 mm rod to a mast, 22-60 mm pole or wall. The adjustable tilt **CMP** mounting kit allows for tilted mounting of the pyranometer with a 0° to 90° graduated scale for the zenith angle.

Glare Screen Kit

A downward facing pyranometer should not see any radiation coming from the hemisphere above or from the first 5° below the horizon. To prevent this, a glare screen kit is available for use with all **CMP series** pyranometers (except the **CMP 3**).



| Specifications | CMP 3 | CMP 6 | CMP10 & CMP 11 | CMP 21 | CMP 22 |
|--|--|--|--|--|---|
| Classification to ISO 9060:1990 | Second Class | First Class | Secondary Standard | Secondary Standard | Secondary Standard |
| Spectral range (50% points) | 300 to 2800 nm | 285 to 2800 nm | 285 to 2800 nm | 285 to 2800 nm | 200 to 3600 nm |
| Sensitivity | 5 to 20 $\mu\text{V}/\text{W}/\text{m}^2$ | 5 to 20 $\mu\text{V}/\text{W}/\text{m}^2$ | 7 to 14 $\mu\text{V}/\text{W}/\text{m}^2$ | 7 to 14 $\mu\text{V}/\text{W}/\text{m}^2$ | 7 to 14 $\mu\text{V}/\text{W}/\text{m}^2$ |
| Impedance | 20 to 2000 Ω | 20 to 2000 Ω | 10 to 1000 Ω | 10 to 1000 Ω | 10 to 1000 Ω |
| Expected output range (0 to 1000 W/m^2) | 0 to 30 mV | 0 to 30 mV | 0 to 20 mV | 0 to 20 mV | 0 to 20 mV |
| Maximum operational irradiance | 2000 W/m^2 | 2000 W/m^2 | 4000 W/m^2 | 4000 W/m^2 | 4000 W/m^2 |
| Response time (5%) | <6 s | <6 s | <1.7 s | <1.7 s | <1.7 s |
| Response time (95%) | <18 s | <18 s | <5 s | <5 s | <5 s |
| Zero offsets | | | | | |
| (a) thermal radiation (at 200 W/m^2) | <15 W/m^2 | <12 W/m^2 | <7 W/m^2 | <7 W/m^2 | <3 W/m^2 |
| (b) temperature change (5 K) | <5 W/m^2 | <4 W/m^2 | <2 W/m^2 | <2 W/m^2 | <1 W/m^2 |
| Non-stability (change/year) | <1% | <1% | <0.5% | <0.5% | <0.5% |
| Non-linearity (1000-10000 W/m^2) | <1.5% | <1% | <0.2% | <0.2% | <0.2% |
| Directional response (up to 60° with 1000 W/m^2 at 24°C) | <20 W/m^2 | <20 W/m^2 | <10 W/m^2 | <10 W/m^2 | <5 W/m^2 |
| Spectral selectivity (350 to 1500 nm) | <3% | <3% | <3% | <3% | <3% |
| Temperature response | <5% (10°C to +60°C) | <4% (10°C to +60°C) | <1% (10°C to +60°C) | <1% (10°C to +60°C) | <0.5% (10°C to +60°C) |
| Tilt response (at 1000 W/m^2) | <1% | <1% | <0.2% | <0.2% | <0.2% |
| Field of view | 180° | 180° | 180° | 180° | 180° |
| Accuracy of bubble level | <0.2° | <0.1° | <0.1° | <0.1° | <0.1° |
| Temperature sensor output | | | | 10K Thermistor (optional Pt 100) | 10K Thermistor (optional Pt 100) |
| Detector type | Thermopile | Thermopile | Thermopile | Thermopile | Thermopile |
| Operational temperature range | 40°C to +80°C | 40°C to +80°C | 40°C to +80°C | 40°C to +80°C | 40°C to +80°C |
| Storage temperature range | 40°C to +80°C | 40°C to +80°C | 40°C to +80°C | 40°C to +80°C | 40°C to +80°C |
| Humidity range | 0 to 100% non-condensing | 0 to 100% non-condensing | 0 to 100% non-condensing | 0 to 100% non-condensing | 0 to 100% non-condensing |
| Ingress Protection (IP) rating | 67 | 67 | 67 | 67 | 67 |
| Recommended applications | Diagnostic solutions for routine measurements in weather stations, field testing | Good quality measurements for hydrology networks, greenhouse climate control | Meteorological networks, PV panel and thermal collector testing, materials testing | Meteorological networks, reference measurements in extreme climates, polar or arid | Scientific research requiring the highest level of measurement accuracy and reliability |

Notes: 1. For the maximum specifications, please refer to the data sheet for each model.

2. Standard Pt 100 thermistor or optional Pt 1000 thermistor can be used with CMP 21 and CMP 22.

3. Non-linearity is the maximum deviation from linearity, measured with CMP 21 and CMP 22.



Go to www.kippzonen.com for your local distributor

HEAD OFFICE

Kipp & Zonen B.V.
 Delltechpark 36, 2628 XH Delft
 P.O. Box 507, 2600 AM Delft
 The Netherlands
 T +31 (0) 15 2755 210
 F +31 (0) 15 2620 351
info@kippzonen.com

Kipp & Zonen B.V. reserve the right to alter specifications of the equipment described in this documentation without prior notice

4424470-V1311